

UNIVERSITÀ DELLA CALABRIA



UNIVERSITA' DELLA CALABRIA

Dipartimento di Farmacia e Scienze della Salute e della Nutrizione

Dottorato di Ricerca in
Medicina Traslazionale

CICLO
XXX

TITOLO TESI

**Preclinical and Mechanistic Studies of Small-Molecule Drugs
Targeting Stat3**

Settore Scientifico Disciplinare CHM/108


Coordinatore:

Ch.mo Prof. Sebastiano Andò

Firma 

Supervisore/Tutor:

Ch.mo Prof. Antonio Garofalo

Firma 

Ch.mo Dr. Francesca Aiello

Firma 

Dottorando: Dott.ssa Mariateresa Badolato

Firma Mariateresa Badolato

INDEX

Abbreviation.....1

Abstract.....4

CHAPTER 1: STAT proteins family and signaling pathway

1.1 Signaling circuits and regulatory networks.....20

1.2 The STAT proteins family.....21

1.3 STAT3 signal transduction: the canonical and the non-canonical pathways.....24

1.4 STAT3-regulated transcription in normal and cancer cells.....27

1.5 STAT3 as a novel molecular target for cancer prevention and treatment.....30

CHAPTER 2: STAT3 inhibitors for cancer prevention and therapy

2.1 Inhibition of STAT3 signaling pathway in cancer cells.....32

2.2 Oligonucleotides and peptides.....34

2.3 Small molecule inhibitors.....34

 2.3.1 *Natural inhibitors of STAT3 signaling pathway*.....35

 2.3.2 *Synthetic agents inhibiting STAT3 signal*.....35

 2.3.3 *Other small molecule inhibitors of STAT3 signaling pathway*.....37

 2.3.4 *Inhibitors of JAK and Src kinases*.....39

 2.3.5 *Small molecule inhibitors of STAT3 under clinical trial studies*.....40

2.4 Prospect of STAT3 inhibitors.....41

2.5 Identification of new scaffolds for the development of new small molecules targeting STAT3 signaling pathway for cancer therapy.....42

CHAPTER 3: Design, synthesis, and biological evaluation of [1,2,4]triazolo[1,5-a]pyrimidinium salts

3.1 Design and synthesis of TZC derivatives.....48

3.2 Chemistry.....48

3.3 Biological evaluation.....51

 3.3.1 *Antiproliferative activity of TZC derivatives*.....51

 3.3.2 *Evaluation of the direct inhibition of STAT3*.....55

 3.3.3 *Western blot analysis of compound **TZC10***.....56

 3.3.4 *Induction of ROS generation and combination study*.....56

3.4 Conclusion.....58

3.5 Experimental section.....58

Chemistry

 3.5.1 *General experimental methods*.....58

 3.5.2 *Synthesis*.....59

Biology

3.5.3 Cell culture.....	67
3.5.4 Growth inhibition assay.....	67
3.5.5 Colony formation assay.....	68
3.5.6 Wound healing (scratch) assay.....	68
3.5.7 Fluorescence polarization assay.....	68
3.5.8 Western blot.....	69
3.5.9 ROS detection assay.....	69
3.5.10 Combination assay.....	70

CHAPTER 4: Design, synthesis, and experimental validation of 4-methyl substituted 2,6-di-*tert*-butylphenol derivatives

4.1 Design and synthesis of DTP derivatives.....	72
4.2 Chemistry.....	72
4.3 Biological evaluation.....	73
4.3.1 Antiproliferative activity of DTP derivatives.....	73
4.3.2 Direct inhibition of STAT3 signal.....	75
4.3.3 Inhibition of the reductase activity of PDI.....	76
4.4 Conclusion.....	78
4.5 Experimental section.....	79
<i>Chemistry</i>	
4.5.1 General experimental methods.....	79
4.5.2 Synthesis.....	80
<i>Biology</i>	
4.5.3 Insulin turbidimetry assay.....	82

CHAPTER 5: Design and synthesis of novel 2,3-dihydroquinazolin-4(1*H*)-one derivatives with remarkable antiproliferative activity

5.1 Design and synthesis of DHP, QZ and DHQ derivatives.....	85
5.2 Chemistry.....	85
5.3 Cytotoxic profile of the new DHQ derivatives.....	88
5.3.1 The benzene ring of DHQs is necessary for their cytotoxicity.....	88
5.3.2 The oxidized form of DHQ has a lower cytotoxicity against cancer cell lines..	89
5.3.3 The cytotoxicity of 2-aryl DHQs depends on the feature and the position of different substitutions of the phenyl ring.....	90
5.3.4 2-Indole substituted DHQs are selectively cytotoxic against pancreatic cancer cells but not against normal ones.....	91
5.3.5 Direct inhibition of STAT3.....	93
5.3.6 Western blot analysis of compounds DHQ27-28 and DHQ30-31	94
5.4 Conclusion.....	94
5.5 Experimental section.....	95
<i>Chemistry</i>	
5.5.1 General experimental methods.....	95

5.5.2 Synthesis of 2-substituted 2,3-dihydropyridopyrimidin-4-(1H)-one derivatives (DHP1-11)	96
5.5.3 Synthesis of 2-substituted 2,3-dihydropyridopyrimidin-4-(1H)-one derivatives (DHP12-15)	98
5.5.4 Synthesis of 2-substituted quinazolin-4(3H)-one derivatives (QZ1-15)	100
5.5.5 Synthesis of 2-aryl substituted 2,3-dihydroquinazolin-4(1H)-one derivatives (DHQ1-14)	103
5.5.6 Synthesis of 2-indole substituted 2,3-dihydroquinazolin-4(1H)-one derivatives (DHQ15-35)	106
References	111

Abbreviations

5-FU: 5-fluorouracil

CBP: Creb-binding protein

CDK5: cyclin-dependent kinase 5

CGHC: Cys-Gly-His-Cys motif

DFO: deferoxamine

DHP: 2,3-dihydropyridopyrimidin-4(1*H*)-one

DHQ: 2,3-dihydroquinazolin-4(1*H*)-one

DNMT1: DNA methyltransferase 1

DPBS: Dulbecco's phosphate-buffered saline

DTP: 4-methyl substituted 2,6-di-*tert*-butylphenol

DTT: dithiothreitol

E₂: estrogen

FDA: Food and Drug Administration

FP: fluorescence polarization

GC-MS: gas chromatography coupled mass spectrometry

gp130: glycoprotein 130

H₂O₂: hydrogen peroxide

IC₅₀: median inhibition concentration

IFN- α : interferon alpha

IFN- γ : interferon gamma

IL-6: interleukin-6

IL6R: IL-6 receptor subunit

JAK: Janus Kinase

JNK: Jun nuclear kinase

KO: knock-out

MAPK: mitogen-activated protein kinase

MLSD: multiple ligand simultaneous docking

mRNA: messenger RNA

MTD: maximum tolerated dose

MTT: 3-(4,5-dimethylthiazol-2-yl)-2,5-diphenyltetrazolium bromide

NCI: National Cancer Institute

Necrostatin-1: 5-(1*H*-Indol-3-ylmethyl)-3-methyl-2-sulfanylideneimidazolidin-4-one

NLS: nuclear localization signal

NMR: nuclear magnetic resonance

PACMA: propionic acid carbamoyl methyl amide

PDI: protein disulfide isomerase

PIAS3: protein inhibitor of activated STAT3

PKC: protein kinase C

QZ: quinazolin-4(1*H*)-one

ROS: reactive oxygen species

RPMI-1640: Roswell Park Memorial Institute medium

SAR: structure-activity relationship

SH2: Src homology 2

siRNA: small interfering RNA

SOCS3: suppressor of cytokine signaling 3

STATs: Signal transducers and activators of transcription

TAD: transcriptional activation domain

TZC: [1,2,4]triazolo[1,5-*a*]pyrimidine nucleus

WT: wild-type

z-VAD: methyl (3*S*)-5-fluoro-3-[[[(2*S*)-2-[[[(2*S*)-3-methyl-2-(phenylmethoxycarbonyl amino)butanoyl]amino]propanoyl]amino]-4-oxopentanoate

Abstract

Nowadays, cancer is one of the primary cause of death in the world. The term “cancer” does not mean a single and precise disease, but it represents a collection of various related diseases, in which abnormal cells grow without control and can invade different tissues and organs. Generally, the initiation of cancer has no symptoms, so it’s difficult to detect it in an early stage and often there are no proper treatments when diagnosed. There are many types of cancer, developed by various signals which involve many molecules and molecular mechanisms. So, specific therapeutic strategies are required to fight cancers and combination of drugs may be needed.

According to the cancer statistics from National Cancer Institute (NCI), the United States is the country with the largest number of diagnosed cancer. In particular, pancreatic cancer is the third leading cause of cancer death in the United States. It is more commonly diagnosed in men than in women, and in increasing age (people aged 65-74). Pancreatic cancer is often associated to high mortality rate and the average survival time for this type of cancer is low and only 8% of patients survive for 5 years. Treatments for this deadly cancer include surgery, radiation therapy and chemotherapy, but they depend on the type and the stage of cancer and most of time they are not completely successful. The Food and Drug Administration (FDA) organization approved several drugs for the treatment of pancreatic cancer, like 5-fluorouracil (5-FU) and gemcitabine, but chemoresistance make it completely non-effective. Drug combinations, especially with cisplatin and oxaliplatin, are widely used to combat this disease. (<http://seer.cancer.gov/>) Taken together, these statistics show how urgent is the discovery of new drugs to treat pancreatic cancer. Recently, the rates of recovery and 5-years relative survival after diagnosis increased for both genders. This is merit of the continuous research by Translational Medicine, in particular Oncology, which today represents the most modern and important approach for

the treatment of cancer. It allows to move from the discoveries of new molecular and cancer mechanisms in the laboratory directly to the clinical management of the patient, relatively quickly, suggesting innovative therapies for the treatment of this disease.

Signal transducers and activators of transcription (STATs) comprise a family of cytoplasmic transcription factors that mediate intracellular signaling usually generated at cell surface receptors and thereby transmit it to the nucleus. Among them, STAT3 was initially recognized as a transcription factor, which mediates the nuclear action of many different cytokines and growth factors. In addition to its role in normal cell function, STAT3 is over-expressed in brain and central nervous system, head and neck, and gastric cancers. In particular, the constitutive activation of STAT3 in a wide range of cancers, especially pancreatic, colorectal, and ovarian ones, has attracted the attention of researchers and has led to consider STAT3 as a drug target for the development of potential anticancer agents. Increasing evidences suggest that aberrant STAT3 signaling promotes the development and progression of human cancers by either inhibiting apoptosis or inducing cell proliferation and survival, angiogenesis, and metastasis. Inhibition of STAT3 signaling pathway suppresses cancer growth and induces apoptosis of cancer cells. Although many natural products and synthetic small molecules have been found to directly or indirectly inhibit STAT3 activation, they present some limits and currently there are no FDA-approved inhibitors of STAT3 for the cancer treatment. Therefore, the identification and the development of novel agents that can effectively target STAT3 remains an important scientific and clinical challenge.

The present work was conducted in collaboration with the Department of Medicinal Chemistry, College of Pharmacy of the University of Michigan (USA), which has long been actively involved in a "Translational Oncology Program". Here, a group of researchers led by Professor Nouri Neamati, initially identified two promising scaffolds

for the development of STAT3 inhibitors, the [1,2,4]triazolo[1,5-*a*]pyrimidine nucleus (TZC) and the 4-methyl substituted phenyl scaffold (DTP) (Figure I).

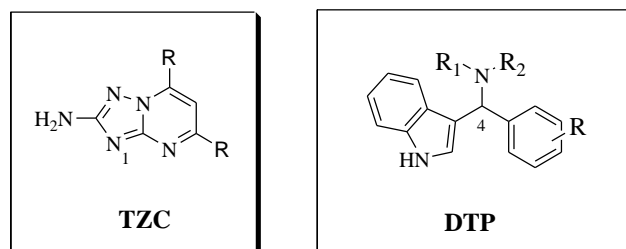


Figure I. Chemical representation of the new identified scaffolds.

They performed a medium-throughput screening of a highly diverse library of 20 000 molecules, representing over one million compounds, in the pancreatic cancer cell line Mia PaCa-2. The most potent compounds, showing median inhibition concentration (IC₅₀) less than 10 μ M, were then tested for STAT3 inhibition in a fluorescence polarization (FP) assay. The two scaffolds demonstrated a significant inhibition of STAT3 (IC₅₀ < 50 μ M). They also performed the rational design of new derivatives of both scaffolds, which may show better activity of the identified lead compounds (Data not shown).

During my first year of the Doctoral School in Translational Medicine at the Department of Pharmacy, Health and Nutritional Sciences under the supervision of Dr. Francesca Aiello and Professor Antonio Garofalo, I synthesized a small library of derivatives for both scaffolds, fully characterized by ¹H-NMR, ¹³C-NMR and GC-MS, and started a structure-activity relationship (SAR) study.

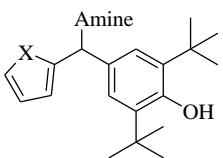
In particular, the modifications related to the TZC nucleus included the introduction of electron-donating groups on the hanging phenyl rings; the substitution of the free amino group on C2 with alkyl and acyl groups; and the functionalization of the heterocyclic N1 with variously decorated bromo-acetophenone, leading to the formation of TZC salts

(Table I). The DTP scaffold was decorated with heterocycles such as thiophene, pyrrole and furan, and various aliphatic cyclic amine, like piperidine, morpholine and pyrrolidine (Table II).

Table I. Small library of TZC derivatives.

Compound	R	R ₁	R ₂
TZC1	H	H	H
TZC2	H	methyl	methyl
TZC3	H	acetyl	H
TZC6	methoxy	H	H
TZC4	H	H	H
TZC5	H	H	acetyl
TZC7	methoxy	H	H
TZC8	methoxy	F	H
TZC9	methoxy	Cl	H
TZC10	methoxy	methyl	H
TZC11	methoxy	H	acetyl
TZC12	H	H	benzoyl
TZC13	methoxy	H	benzoyl
TZC14	H	H	<i>o</i> -OCH ₃ -benzyl
TZC15	methoxy	H	<i>o</i> -OCH ₃ -benzyl
TZC16	H	H	<i>m</i> -Cl-benzyl
TZC17	methoxy	H	<i>m</i> -Cl-benzyl
TZC18	H	H	acetophenone
TZC19	methoxy	H	acetophenone
TZC20	H	methyl	<i>p</i> -methyl-acetophenone
TZC21	methoxy	methyl	<i>p</i> -methyl-acetophenone

Table II. Small library of DTP derivatives.

Compound	X	Amine
		
DTP1	S	piperidine
DTP2	S	morpholine
DTP3	S	pyrrolidine
DTP4	NH	piperidine
DTP5	NH	morpholine
DTP6	O	piperidine

Then, I joined the “Translational Oncology Program” at the University of Michigan, for 13 months, under the supervision of Professor Nouri Neamati. In the USA, I had the opportunity to conduct research in both chemistry and biology fields. Firstly, I worked on the characterization of the biological profile and the mechanism of action of the new TZC and DTP derivatives. The antiproliferative activity of all the synthesized compounds was determined in a panel of human cancer cell lines, and the IC_{50} values of the most active compounds were calculated. Some TZC salts (**TZC7** and **TZC10**) and DTP derivatives (**DTP1-3**) significantly inhibited the growth of cancer cells, in particular the pancreatic cancer cell line Mia PaCa-2 (IC_{50} **TZC7** = 2.1 μ M; IC_{50} **TZC10** = 1.2 μ M; IC_{50} **DTP1** = 5.0 μ M). The ability of the active compounds to inhibit the colony formation and migration of pancreatic cancer cells was also evaluated. The inhibition of STAT3 was determined through FP assay using the protein previously purified in the biology laboratory; then, the levels of phospho-STAT3 in the cells were evaluated by Western blot analysis. While **TZC10** showed to inhibit STAT3 similarly to the control Stattic, well-known STAT3 inhibitor, and to reduce phospho-STAT3 levels in a dose-dependent manner, DTP derivatives moderately inhibited the protein. Successively, the possible mechanism of

action of both classes of compounds was investigated using a set of biological assays. TZC salts may stimulate production of reactive oxygen species (ROS) and induce apoptosis in Mia Paca-2 cancer cell line. Because of the structural similarity of DTP derivatives with known modulators of the protein disulfide isomerase (PDI), such as estradiol (E_2) and propionic acid carbamoyl methyl amide-31 (PACMA-31) (Figure II), the inhibition of the reductase activity of PDI by DTP derivatives was also assessed by an insulin turbidimetry assay.

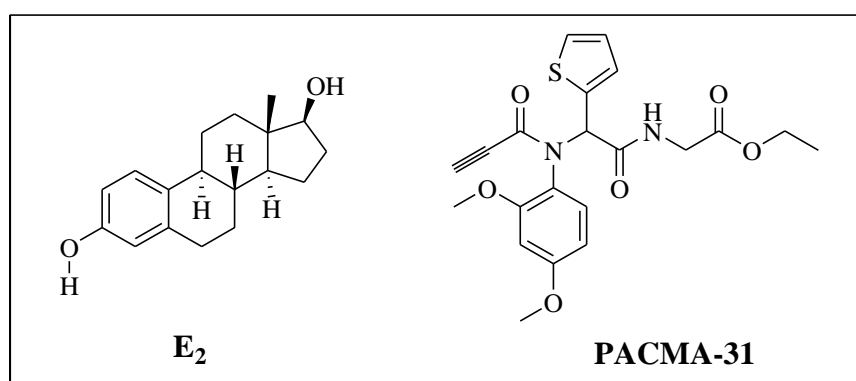


Figure II. Chemical representation of know PDI modulators.

DTP1-3 derivatives significantly inhibited PDI with IC_{50} values in the low micromolar range ($IC_{50}^{DTP1} = 1.51 \mu M$; $IC_{50}^{DTP2} = 1.69 \mu M$; $IC_{50}^{DTP3} = 4.17 \mu M$). These results make them potential multi-target anticancer agents.

In the last months of my permanence in the USA and during my third years of PhD I was working on a third scaffold, the 2,3-dihydroquinazolin-4(1*H*)-one (DHQ) (Figure III), identified as scaffold for the development of potential anticancer agents, similarly to TZC and DTP scaffolds, after medium-throughput screening. Series of 2,3-dihydropyridopyrimidin-4(1*H*)-ones (DHPs), quinazolin-4(1*H*)-ones (QZs) and DHQs were synthesized and lead optimization campaigns were undertaken to improve upon their potency and start a SAR study (Table III). Then, the biological profile as well as the mechanism of action of the new DHQ derivatives was intensely investigated.

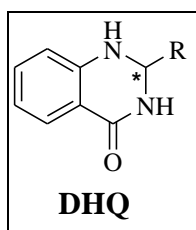


Figure III. Molecular structure of the DHQ framework.

Table III. Small library of DHP derivatives.

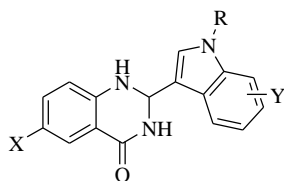
Compound	R
DHP1	Phenyl
DHP2	4-(piperidin-1-yl)phenyl
DHP3	2-fluoro-5-(trifluoromethyl)phenyl
DHP4	4-(4-methylpiperazin-1-yl)phenyl
DHP5	1-methyl-1 <i>H</i> -indol-3-yl
DHP6	2-hydroxy-5-methylphenyl
DHP7	4-morpholinophenyl
DHP8	1,7-dimethyl-1 <i>H</i> -indol-3-yl
DHP9	1-ethyl-1 <i>H</i> -indol-3-yl
DHP10	4-(diethylamino)phenyl
DHP11	4-(dimethylamino)phenyl
DHP12	4-(trifluoromethyl)phenyl
DHP13	4-(piperidin-1-yl)phenyl
DHP14	4-(diethylamino)phenyl
DHP15	4-(piperidin-1-yl)phenyl

Table III. Small library of QZ and DHQ derivatives.

Compound	R	X	Y
QZ1	4-(4-methylpiperazin-1-yl)phenyl	H	N
QZ2	2-hydroxy-5-methylphenyl	H	N
QZ3	4-(diethylamino)phenyl	H	N
QZ4	1-methyl-1 <i>H</i> -indol-3-yl	H	H
QZ5	4-(diethylamino)phenyl	H	H
QZ6	6-fluoro-1-propyl-1 <i>H</i> -indol-3-yl	H	H
QZ7	1-isopropyl-7-methyl-1 <i>H</i> -indol-3-yl	F	H
QZ8	1-cyclopropyl-7-methyl-1 <i>H</i> -indol-3-yl	F	H
QZ9	6-fluoro-1-cyclopropyl-1 <i>H</i> -indol-3-yl	F	H
QZ10	1-cyclopropyl-7-chloro-1 <i>H</i> -indol-3-yl	F	H
QZ11	1-ethyl-6-fluoro-1 <i>H</i> -indol-3-yl	F	H
QZ12	1-methyl-1 <i>H</i> -indol-3-yl	F	H
QZ13	1-ethyl-1 <i>H</i> -indol-3-yl	F	H
QZ14	1-cyclopropyl-6-fluoro-1 <i>H</i> -indol-3-yl	F	H
QZ15	7-chloro-1-cyclopropyl-1 <i>H</i> -indol-3-yl	F	H

DHQ1	4-(diethylamino)phenyl	H	-
DHQ2	phenyl	F	-
DHQ3	4-(piperidin-1-yl)phenyl	F	-
DHQ4	4-(4-methylpiperazin-1-yl)phenyl	F	-
DHQ5	4-morpholinophenyl	F	-
DHQ6	4-(diethylamino)phenyl	F	-
DHQ7	4-(dimethylamino)phenyl	F	-
DHQ8	4-(1 <i>H</i> -pyrrol-1-yl)phenyl	F	-
DHQ9	4-(pyrimidin-5-yl)phenyl	F	-
DHQ10	3-fluorophenyl	F	-
DHQ11	2-fluoro-5-(trifluoromethyl)phenyl	F	-
DHQ12	2-hydroxy-5-methylphenyl	F	-
DHQ13	benzo[d][1,3]dioxol-5-yl	F	-
DHQ14	4-(imidazo[1,2-a]pyridin-3-yl)phenyl	F	-

Compound	R	X	Y
----------	---	---	---



DHQ15	methyl	H	H
DHQ16	methyl	H	7-methyl
DHQ17	ethyl	H	H
DHQ18	benzyl	H	7-methyl
DHQ19	propyl	H	7-methyl
DHQ20	propyl	H	7-chloro
DHQ21	ethyl	H	7-chloro
DHQ22	ethyl	H	7-methyl
DHQ23	H	H	7-methyl
DHQ24	benzyl	H	6-fluoro
DHQ25	methyl	H	H
DHQ26	methyl	F	7-methyl
DHQ27	ethyl	F	H
DHQ28	propyl	F	7-methyl
DHQ29	propyl	F	7-chloro
DHQ30	ethyl	F	7-chloro
DHQ31	ethyl	F	7-methyl
DHQ32	H	F	7-methyl
DHQ33	benzyl	F	6-fluoro
DHQ34	propyl	F	6-fluoro
DHQ35	ethyl	F	6-fluoro

During my three years PhD program, I worked hard to define my profile of young medicinal chemist. The support of my supervisors was indispensable and helpful. I am grateful and honored of their teachings, which allowed me to greatly improve my competence in the field of Medicinal Chemistry. Therefore, I had the opportunity to participate to many National and International Congresses, showing my progresses in research through both poster and oral presentations. I attended the 19^o “Course of Mass Spectrometry”, held at Certosa di Pontignano (SI) in 2015. I was also winner of a fellowship offered by the Pharmaceutical Chemistry Division of the Italian Chemical

Society to attend the European School of Medicinal Chemistry 2017 in Urbino. Furthermore, this PhD experience allowed me to advance my English understanding. I got a B1 Preliminary Cambridge English Qualification (PET) in 2014 and a C1 qualification through the Test of English as a Foreign Language (TOEFL) in 2015. I also contributed to the scientific field through the publication of my progresses in research. Moreover, during my third year of PhD program, I was tutor of the laboratory teaching activities for the course “Analysis of Medicines” SSD CHIM/08. Finally, I am a member of the team of the project “RYGoldZip”, led by Dr. Francesca Aiello, and we won the “Clinic Center Life Sciences” award and the “Start Cap Calabria 2017” for the discovery and formulation of a topical product with wound healing properties for diabetic ulcers.

Attendance to Congresses:

[Merck Young Chemists Symposium – Milano Marittima \(November, 13th-15th, 2017\)](#)

Badolato Mariateresa – **Speaker**

“Glycyrrhiza glabra L. leaves: from agrochemical waste to new potential therapeutic agents”

Badolato M., Tundis R., Cappello A., Carullo G., Polerà N., Aiello F.

Glycyrrhiza glabra L. leaves: from agrochemical waste to new potential therapeutic agents

Department of Pharmacy and Health Sciences and Nutrition, University of Calabria, Ed. Polifunzionale, 87036 - Arcavacata Rende (Cs), Italy.

Carullo G.,^a Restuccia D.,^a Spizzirri U. G.,^a Giorgi G.,^b Badolato M.,^a Aiello F.^a

After wine: typical white Calabrian grape pomaces as useful source of functional food

^a Department of Pharmacy and Health Sciences and Nutrition, University of Calabria, Ed. Polifunzionale, 87036 – Arcavacata di Rende (Cs), Italy. ^b Department of Biotechnologies, Chemistry and Pharmacy, University of Siena, Polo Scientifico S. Miniato, Via A. Moro 2, 53100 Siena, Italy.

XXVI Congresso Nazionale della Società Chimica Italiana – Paestum (September, 10th-14th, 2017)

Badolato M.,^{a,b} Carullo G.,^a Polerà N.,^a Garofalo A.,^a Neamati N.,^b Aiello F.^a

Design, synthesis and biological evaluation of triazolopyrimidinium salts as novel antiproliferative agents

^aDepartment of Pharmacy and Health Sciences and Nutrition, University of Calabria, Ed. Polifunzionale, 87036 – Arcavacata di Rende (Cs), Italy. ^bDepartment of Medicinal Chemistry, College of Pharmacy and Translational Oncology Program, University of Michigan, North Campus Research Complex, 2800 Plymouth Road, Building 520, Ann Arbor, MI 48109, USA.

Carullo G., Trotta F., Sirianni R., Polerà N., Badolato M., Aiello F.

A multi-component one-pot synthesis of 3-amino alkylated indoles, new interesting antiproliferative agents against breast cancer cells

Department of Pharmacy and Health Sciences and Nutrition, University of Calabria, Ed. Polifunzionale, 87036 - Arcavacata Rende (Cs), Italy.

European School of Medicinal Chemistry – Urbino (July, 2nd-6th, 2017)

Fellowship winner

Badolato M.,^{a,b} Aiello F.,^a Garofalo A.,^a Neamati N.,^b

Discovery of novel DHQ derivatives with remarkable cytotoxicity profile.

^aDepartment of Pharmacy and Health Sciences and Nutrition, University of Calabria, Ed. Polifunzionale, 87036 – Arcavacata di Rende (Cs), Italy. ^bDepartment of Medicinal Chemistry, College of Pharmacy and Translational Oncology Program, University of Michigan, North Campus Research Complex, 2800 Plymouth Road, Building 520, Ann Arbor, MI 48109, USA.

XXIV National Meeting in Medicinal Chemistry & 10th Young Medicinal Chemists Symposium – Perugia (September, 11th-14th, 2016)

Carullo G.,^a Aiello F.,^a Badolato M.,^a Ligresti A.,^b Allarà M.,^b Schiano Moriello A.,^b De Petrocellis L.,^b Di Marzo V.,^c Corelli F.,^c Brizzi A.,^c

Synthesis and Biological evaluation of small molecules acting as TRPV1 ligands and/or FAAH inhibitors.

^aDipartimento di Farmacia e Scienze della Salute e della Nutrizione, Università della Calabria, 87036, Arcavacata di Rende (Cs), Italy. ^bIstituto di Chimica Biomolecolare, Endocannabinoid Research Group, Consiglio Nazionale delle Ricerche, 80078, Pozzuoli (Na), Italy. ^cDipartimento di Biotecnologie, Chimica e Farmacia, Università degli Studi di Siena, Polo Scientifico S. Miniato, Via A. Moro 2, 53100 Siena, Italy.

Convegno congiunto delle sezioni Calabria e Sicilia – Società Chimica Italiana (December, 3rd-4th, 2015)

Badolato Mariateresa - **Speaker**

“Progettazione e sintesi di nuovi probes GPER-selettivi”

Dipartimento di Farmacia e Scienze della Salute e della Nutrizione, Università della Calabria, 87036, Arcavacata di Rende (Cs), Italy.

XXIII National Meeting in Medicinal Chemistry & 9th Young Medicinal Chemists Symposium – Salerno (September, 6th-9th, 2015)

Brizzi A.,^a Aiello F.,^b Badolato M.,^b Garogalo A.,^b Frosini M.,^c Maestrini V.,^c Pessina F.,^d Sticozzi C.,^e Valacchi G.,^e De Petrocellis L.,^f Luongo L.,^f Maione S.,^g Ligresti A.,^h Di Marzo V.,^h

Synthesis and biological evaluation of small molecule TRPV1 ligands.

^a University of Siena, Via A. Moro 2, 53100 – Siena, Italy. ^b Department of Pharmacy and Health and Nutrition Sciences, University of Calabria, Edificio Polifunzionale, 87036 - Arcavacata di Rende (Cs), Italy. ^c Department of Life Sciences, University of Siena, 53100, Siena, Italy. ^d Department of Molecular and Development Medicine, University of Siena, 53100 – Siena, Italy. ^e Department of Life Sciences and Biotechnology, University of Ferrara, Italy. ^f Endocannabinoid Research Group, Institute of Cybernetics, National Research Council, Via Campi Flegrei 34, 80078 - Pozzuoli (Na), Italy. ^g Department of Experimental Medicine, Pharmacology Section “L. Donatelli”, Second University of Napoli, Via Costantinopoli 16, 80138 – Napoli, Italy. ^h Endocannabinoid Research Group, Institute of Biomolecular Chemistry, National Research Council, 80078 – Pozzuoli (Na), Italy.

Convegno SIF: “Advances in pain research: pathophysiology and new therapeutics strategies”- Napoli (June, 18th-19th, 2015)

Aiello F.,^a Ligresti A.,^b Badolato M.,^a Maestrini V.,^c Luongo L.,^d Frosini M.,^c Pessina F.,^e Sticozzi C.,^f De Petrocellis L.,^g Valacchi G.,^f Maione S.,^d Garogalo A.,^a Corelli F.,^h Di Marzo V.,^b Brizzi A.,^h

Targeting the Transient Receptor Potential Vanilloid Type-1 channel: pharmacological characterization and analgesic properties of a novel family of TRPV1 ligands.

^a Dipartimento di Farmacia e Scienze della Salute e della Nutrizione, Università della Calabria, 87036, Arcavacata di Rende (Cs), Italy. ^b Endocannabinoid Research Group, Istituto di Chimica Biomolecolare, Consiglio Nazionale delle Ricerche, 80078, Pozzuoli (Na), Italy. ^c Dipartimento di Scienze della Vita, Università degli Studi di Siena, Via A. Moro 2, 53100 Siena, Italy. ^d Dipartimento di Medicina Sperimentale, Sezione di Farmacologia “L. Donatelli”, Seconda Università di Napoli, Via Costantinopoli 16, 80138 Napoli, Italy. ^e Dipartimento di Medicina Molecolare e dello Sviluppo, Università degli Studi di Siena, Italy. ^f Dipartimento di Scienze della Vita e Biotecnologie, Università degli Studi di Ferrara, Italy. ^g Endocannabinoid Research Group, Istituto di Cibernetica,

Consiglio Nazionale delle Ricerche, Via Campi Flegrei 34, 80078 Pozzuoli, Napoli, Italy. ^h Dipartimento di Biotecnologie, Chimica e Farmacia, Università degli Studi di Siena, Via A. Moro 2, 53100 Siena, Italy.

XXV Congresso Nazionale della Società Chimica Italiana – Università della Calabria (September, 7th-12th, 2014)

Badolato M., Aiello F., Grande F., Barone I.^a, Brancale A., Catalano S., Garogalo A., Andò S.,

Design and synthesis of CXCR4 antagonists with anti-proliferative activity.

Dipartimento di Farmacia e Scienze della Salute e della Nutrizione, Università della Calabria, Edificio Polifunzionale, 87036 - Arcavacata di Rende (Cs), Italy. ^aSchool of Pharmacy and Pharmaceutical Sciences, Cardiff University, King Edward VII Avenue, Cardiff, CF10 3NB, UK.

Grande F.^a, Avino S.^a, Santolla M. F.^a, Aiello F.^a, Perri M. G.^a, Rosano C.^b, Badolato M.^a, Vigliatore F.^a, Garofalo A.^a, Maggiolini M.^a,

Identification of two novel berzo[b]pyrrolo[1,2-*d*][1,4]oxazin-4-one derivatives acting as GPER antagonists.

^a Department of Pharmacy, Health and Nutritional Sciences, University of Calabria, Rende (Cs), Italy. ^b U.O.S. Biopolymers and Proteomics - Irccs AOU San Martino, IST-National Institute for Cancer Research, Genova, Italy.

Cellular Environmental Stressors in Biology and Medicine: Focus on Redox Reactions - Third International Conference – Università di Ferrara (June, 25th-27th, 2014)

Pessina F.^a, Aiello F.^b, Brizzi A.^c, Sticozzi C.^d, Badolato M.^b, De Petrocellis L.^e, Corelli F.^c, Garofalo A.^b, Valacchi G.^d, Di Marzo V.^f,

Small-molecules TRPV1 modulators: design, synthesis and pharmacological characterization of new 4-(thiopen-2-yl)butanoic acid amides.

^aDipartimento di Medicina Molecolare e dello Sviluppo, Università degli Studi di Siena, Italy. ^bDipartimento di Farmacia e Scienze della Salute e della Nutrizione, Università della Calabria, Arcavacata di Rende, Cosenza, Italy. ^c Dipartimento di Biotecnologie, Chimica e Farmacia, Università degli Studi di Siena, Italy. ^d Dipartimento di Scienze della vita e biotecnologie, Università degli Studi di Ferrara, Italy. ^e Istituto di Cibernetica, Consiglio Nazionale delle Ricerche, Endocannabinoid Research Group Pozzuoli, Italy ^fIstituto di Chimica Biomolecolare, Consiglio Nazionale delle Ricerche, Endocannabinoid Research Group, Pozzuoli, Italy.

XVI Congresso Nazionale dei Chimici – Palazzo Campanella – Reggio Calabria (May, 29th-31st, 2014)

Grande F., Aiello F., Badolato M., Vigliatore F., Garofalo A.,

Combination of hormones and nutrients for the development of hybrid nutraceuticals.

Department of Pharmacy, Health and Nutritional Sciences, University of Calabria, Rende (CS), Italy.

Scientific publications:

Mariateresa Badolato, Francesca Aiello, and Nouri Neamati. **2,3-Dihydroquinazolin-4(1H)-one as a Privileged Scaffold in Drug Design**. Submitted to *RSC Advance* (2018).

Rosa Tundis, Luca Frattaruolo, Gabriele Carullo, Biagio Armentano, Mariateresa Badolato, Monica Rosa Loizzo, Francesca Aiello, and Anna Rita Cappello, **An ancient remedial repurposing: synthesis of new pinocembrin fatty acid acyl derivatives as potential antimicrobial/anti-inflammatory agents**, *Natural Products Research*, *accepted manuscript* (2017).

Nicoletta Polerà, Mariateresa Badolato, Filomena Perri, Gabriele Carullo, and Francesca Aiello, **Quercetin and its Natural Sources in Wound Healing Management**, *Current Medicinal Chemistry*, *accepted manuscript* (2017).

Mariateresa Badolato, Gabriele Carullo, Mariarita Perri, Erika Cione, Fabrizio Manetti, Maria Luisa Di Gioia, Antonella Brizzi, Mariacristina Caroleo, and Francesca Aiello, **Quercetin/Oleic Acid-Based G-protein-coupled receptor 40 (GPR40) Ligands as New Insulin Secretion Modulators**, *Future Medicinal Chemistry* 9 (16), 1873-1885 (2017).

Mariateresa Badolato, Gabriele Carullo, Erika Cione, Maria Cristina Caroleo, and Francesca Aiello. **From the hive: Honey, a novel weapon against cancer**. *European Journal of Medicinal Chemistry* 142, 290-299 (2017).

Mariateresa Badolato, Gabriele Carullo, Francesca Aiello, and Antonio Garofalo. **Synthesis and Experimental Validation of New PDI Inhibitors with Antiproliferative Activity**, *Journal of Chemistry* 2017, 2370359 (2017).

Mariateresa Badolato, Gabriele Carullo, Biagio Armentano, Salvatore Panza, Rocco Malivindi, and Francesca Aiello. **Design, synthesis and biological evaluation of a small library of 5H-pyrrole [1,2-a] [3,1] benzoxazin-5-one derivatives as anti-estrogenic agents**, *Bioorganic & Medicinal Chemistry Letters* 27, 3092-3095 (2017).

Gabriele Carullo, Anna Rita Cappello, Luca Frattaruolo, Mariateresa Badolato, Biagio Armentano, and Francesca Aiello. **Quercetin and derivatives: useful tools in inflammation and pain management**. *Future Medicinal Chemistry* 9 (1), 79-93 (2017).

Yoshinari Miyata, Mariateresa Badolato, and Nouri Neamati. **HSPA5**. *Choi S. (eds) Encyclopedia of Signaling Molecules. Springer, New York, NY (2016).*
<https://doi.org/10.1007/978-1-4614-6438-9>

Francesca Aiello, Gabriele Carullo, Mariateresa Badolato, and Antonella Brizzi. **TRPV1–FAAH–COX: The Couples Game in Pain Treatment**. *ChemMedChem* 11, 1686-1694 (2016).

Francesca Aiello, Mariateresa Badolato, Federica Pessina, Claudia Sticozzi, Vanessa Maestrini, Carlo Aldirucci, Livio Luongo, Francesca Guida, Alessia Ligresti, Anna Artese, Marco Allarà, Giosuè Costa, Maria Frosini, Aniello Schiano Moriello, Luciano De Petrocellis, Giuseppe Valacchi, Stefano Alcaro, Sabatino Maione, Vincenzo Di Marzo, Federico Corelli, Antonella Brizzi. **Design and Synthesis of New Transient Receptor Potential Vanilloid Type-1 (TRPV1) Channel Modulators: Identification, Molecular Modeling Analysis, and Pharmacological Characterization of the N-(4-Hydroxy-3-methoxybenzyl)-4-(thiophen-2-yl)butanamide, a Small Molecule Endowed with Agonist TRPV1 Activity and Protective Effects against Oxidative Stress**. *ACS Chemical Neurosci* 7 (6), 737-748 (2016).

Fedora Grande, Ines Barone, Francesca Aiello, Andrea Brancale, Michela Cancellieri, Mariateresa Badolato, Francesca Chemi, Cinzia Giordano, Valentino Viricillo, Daniela Bonofiglio, Antonio Garofalo, Sebastiano Andò, Stefania Catalano. **Identification of novel 2-(1*H*-indol-1-yl)-benzohydrazides CXCR4 ligands impairing breast cancer growth and motility**. *Future Medicinal Chemistry* 8 (2), 93-106 (2016).

Awards:

First place in the category “Clinic Center Life Sciences” (€ 25.000,00) “Premio Nazionale Innovazione 2017” with the project RYGoldZip, preparation for topical use based on a new molecular hybrid able to promote the wound healing oh chronic ulcers.

First place in “Start Cup Calabria 2017” (€ 5.000,00) with the project RYGoldZip, preparation for topical use based on a new molecular hybrid able to promote the wound healing oh chronic ulcers.

CHAPTER 1:
STAT proteins family and signaling pathway

1.1 Signaling circuits and regulatory networks

In general, the tendency to maintain a stable, relatively constant internal environment is called homeostasis and is actually a dynamic equilibrium. Biological systems require a carefully controlled homeostasis, which involves a great communication between sensors and effectors, through tightly regulatory networks. This communication is sustained by cell-cell interactions, secreted factors and extracellular matrix components, and tends to reach a balance that resists outside forces of changes. Maintenance of homeostasis depends on negative feedback loops, which act to oppose the stimulus that triggers them. Anything that interferes with the feedback mechanisms can disrupt homeostasis and, in the case of the human body, leads to diseases when the balance is not restored (Figure 1).

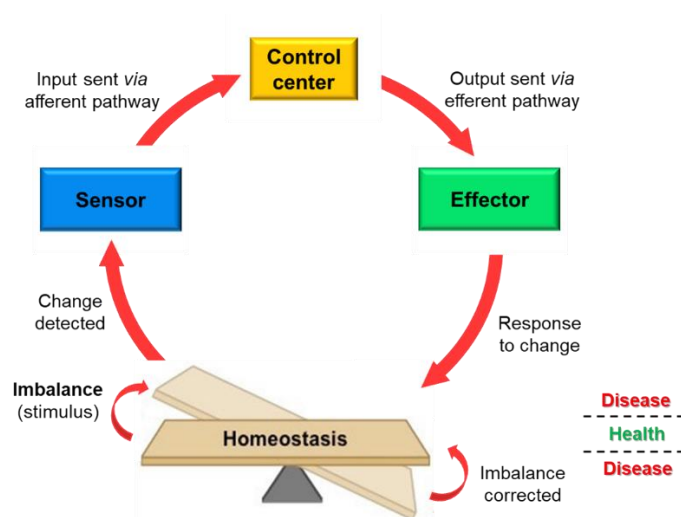


Figure 1. Homeostatic control mechanisms.

Any change will be detected by sensors, usually receptors, and relayed to a regulatory control center in the brain. It will process the information and activate the effector whose function is to oppose the stimulus by bringing the balance back.

In the human body, a constant number of cells and a proper organ function is preserved since cells can respond to exogenous signals with proliferation, differentiation or cell death. Several intracellular signaling molecules transduce mitogenic signals from the environment and cell surface to the nucleus, regulating the normal function of cells. The

alteration or loss of such components cause continued signal transduction, even when an activating signal is absent. Consequently, cells escape from their signaling circuits and inappropriately proliferate, resist apoptosis, induce angiogenesis and invade distant organs. Many evidences demonstrate how cancer results from mutational events that interfere with the usual cooperative behavior of the cells, deregulating various cell signaling pathways that control cell function. (*Beerenwinkel et al. 2007*)

Knowing the signaling components and their integration in signaling networks might be a potential therapeutic strategy. (*Bild et al. 2006*)

STAT proteins have emerged as important transcription factors, which can also transduce signals. In particular, STAT3 has been found to play key roles in carcinogenesis and can be considered a potential target in developing strategies to prevent or treat cancer. (*Xiong et al. 2014*)

1.2 The STAT proteins family

STAT proteins owe their name to their double function as signal transducer and activator of transcription. They were first identified by *Darnell et al.* in 1994 through the study of transcriptional activation in response to interferon alpha (IFN- α) and gamma (IFN- γ). The STAT family comprises seven members, namely STAT1, STAT2, STAT3, STAT4, STAT5a, STAT5b and STAT6 (Figure 2). Ranging in size from 750 to 850 amino acid residues (90-155 kDa), all STAT proteins share structurally and functionally conserved domains. The N-terminus contains an oligomerization domain and mediates the oligomerization of STAT dimers to tetramers. STAT tetramers contribute to stabilize the STAT-DNA binding and then increase the transcriptional activity. The region between residues 130 and 315 is a four-stranded helical coiled-coil domain that mediates the interaction of STAT with other helical proteins. The DNA-binding domain interacts with

specific DNA elements within STAT-sensitive promoter, ensuring the DNA-binding specificity of each STAT protein. The Src homology 2 (SH2) domain, preceded by the linker region, mediates the interaction of STATs with the receptor and Janus Kinases (JAKs), other than the formation of STAT dimers. The C-terminus containing a transcriptional activation domain (TAD) is the least conserved domain and provides functional specificity, interacting with co-activators and co-repressors. All STAT proteins have a critical tyrosine residue (Y) approximately at position 700 in the TAD. It is target of phosphorylation and essential for STAT activation and function. Phosphorylated STATs can dimerize, translocate in the nucleus and bind to DNA, allowing the transcription of their target genes. Except for STAT2 and STAT6, all STATs contain a critical serine residue (S); if phosphorylated it can improve the transcriptional activity.

Inactive non-phosphorylated STATs are present in the cytoplasm of healthy cells and can be divided into two groups, depending on their different activation and function. STAT2, STAT4 and STAT6, activated through a small number of cytokines, play an important role in the development of T-cells and IFN- γ signaling. On the other hand, STAT1, STAT3 and STAT5 are activated in several tissue types through many ligands and are implicated in IFN- γ signaling, development of mammary glands and embryogenesis. Playing a key role in cell cycle progression and apoptosis, STAT3 and STAT5 are also involved in oncogenesis. (*Lim and Cao, 2006; Lavecchia et al. 2011*)

STAT proteins are all encoded by separate genes. In the human genome, they are organized in 3 different chromosomes: STAT1 and STAT4 are grouped on chromosome 2, whereas STAT2 and STAT6 on chromosome 12. STAT3, STAT5a and STAT5b are clustered on chromosome 17. (*Copeland et al. 1995*)

In particular, STAT3 gene is located on chromosome 17q21.31. (*Choi et al. 1996*)

Among all STAT proteins, STAT3 is the most studied member, due to its role in the

development of carcinogenesis, other than its involvement in different pathological conditions, including inflammation. (Lin and Karin, 2007)

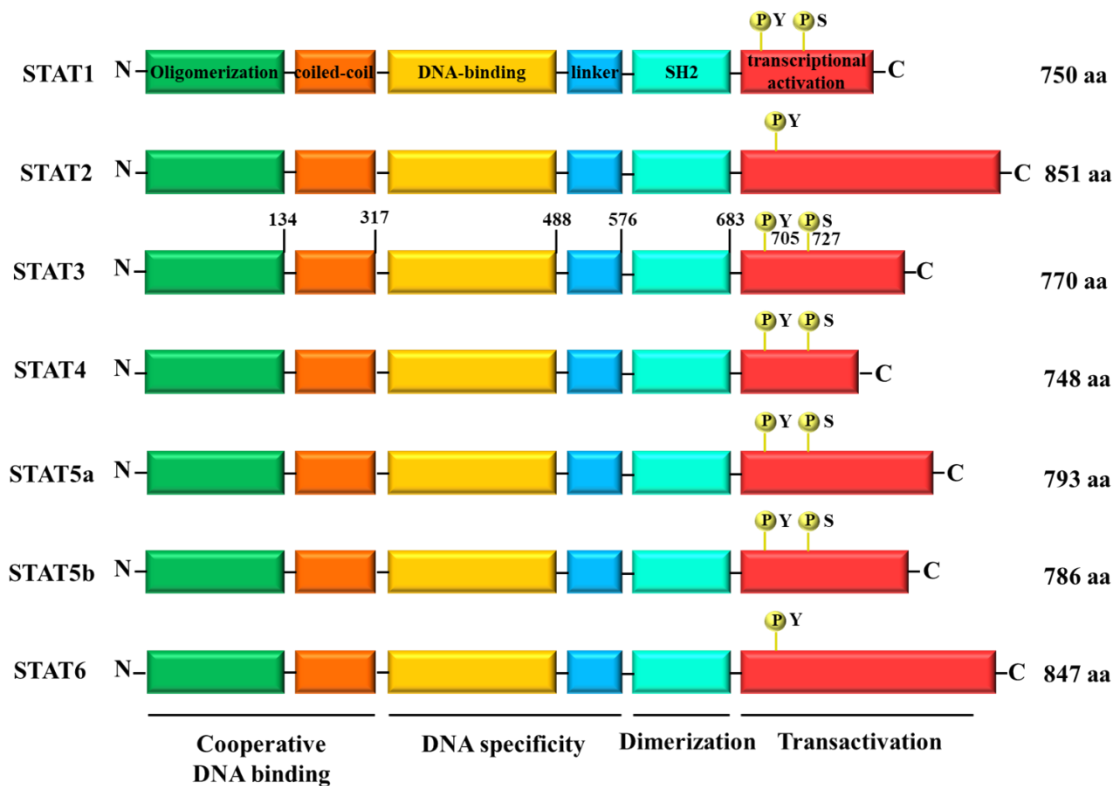


Figure 2. The STAT family members.

The N-terminal domain of STATs contains an oligomerization domain, followed by the coiled-coil domain and a central DNA-binding domain with a sequence specificity for a palindromic IFN- γ -activated sequence (GAS) element. The DNA-binding domain is connected to the SH2 domain by a linker region. The C-terminal domain has transactivation activity and presents conserved tyrosine and serine residues.

STAT3 is a 92 kDa protein, composed of 770 amino acids. Its TAD contains two important phosphorylation sites: the residue Y705, that promotes STAT3 activation and dimerization; and the residue S727, phosphorylated after tyrosine phosphorylation, that ensures the maximal transcriptional activity. (Wen *et al.* 1995)

Furthermore, STAT3 dimerization is regulated by reversible acetylation of single lysine residue (K685). (Yuan *et al.* 2005)

In 1998, *Becker et al.* first reported X-ray crystal structure of STAT3 homodimer bound to DNA (Figure 3).

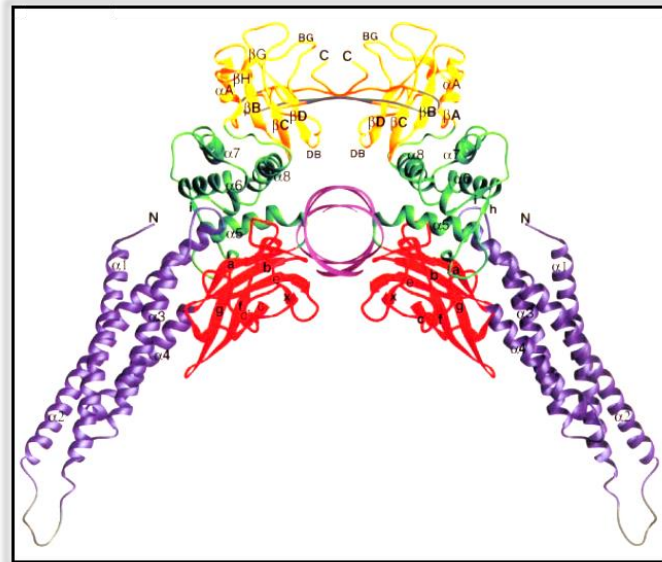


Figure 3. Three-dimensional structure of STAT3 homodimer-DNA complex. The N-terminal domain is shown in purple, the β -barrel domain in red, the linker region in green, and the SH2 domain and phosphotyrosine-containing region in yellow. Regions between helices $\alpha 1$ and $\alpha 2$, and residues from 689 to 701 are shown in grey. The figure represents the view along the DNA axis, with the dyad of the complex running vertically. (Figure by *Becker et al.* 1998)

1.3 STAT3 signal transduction: the canonical and the non-canonical pathways

STAT3 activation can be triggered in different ways, through the tyrosine phosphorylation pathway (Figure 4). Receptor-associated JAKs are activated upon cytokine receptor binding (e.g. interleukin-6, IL-6) by cross-phosphorylation. The receptor of IL-6 is a complex containing IL-6 receptor subunit (IL6R) and IL-6 signal transducer glycoprotein 130 (gp130). JAKs are cytoplasmic tyrosine kinases that are inactive in unstimulated cells. The interaction of IL-6 with its receptor results in dimerization of gp130 in the cytoplasm and subsequent recruitment of JAKs. The aggregation of JAKs leads to self-activation by either auto- or trans-phosphorylation.

Consequently, the activated JAKs phosphorylate tyrosine residues on the cytoplasmic domain of the IL-6 receptor, which become docking elements for the SH2 domain of cytoplasmic STAT3 proteins. Being close to JAKs, STAT3 is phosphorylated at specific tyrosine residue (Y705) in the C-terminal portion and activated. The activation of STAT3 can be also initiated by the binding of cytokines and growth factors to their receptors, which have intrinsic tyrosine kinase activity. After ligand binding, the receptors dimerize, autophosphorylate each other and may directly activate STAT3 without JAKs recruitment. Furthermore, STAT3 can be phosphorylated and activated by constitutively active non-receptor tyrosine kinases, such as Src and Abl. Upon activation, STAT3 proteins form homo- or hetero-dimers through reciprocal interaction between the phosphotyrosine of one monomer and the SH2 domain on the partnering STAT3 protein. Then, STAT3 dimers translocate into the nucleus, where they bind to specific promoter elements of target genes and regulate gene expression. (*Rane and Reddy, 2000; Levy and Darnell, 2002*)

The dynamic shuttling of STAT3 dimers between cytoplasmic and nuclear compartments is facilitated by importin- α /importin- β 1/Ran complex and presence of nuclear localization signal (NLS). (*Cimica et al. 2011*) Although phosphorylation of STAT3 is important for its function as transcription factor, the translocation of STAT3 into the nucleus may be independent of its phosphorylation status. (*Liu et al. 2005*)

Among all STAT proteins, STAT3 plays a central role in several normal biological functions and carcinogenesis, since it critically regulates the transcription of a number of key genes involved in cell proliferation and survival, other than differentiation, apoptosis, angiogenesis, invasion and metastases. The upstream signals that triggers activation of STAT3 signaling *via* phosphorylation of conserved Y705 residue is known as canonical pathway of activation.

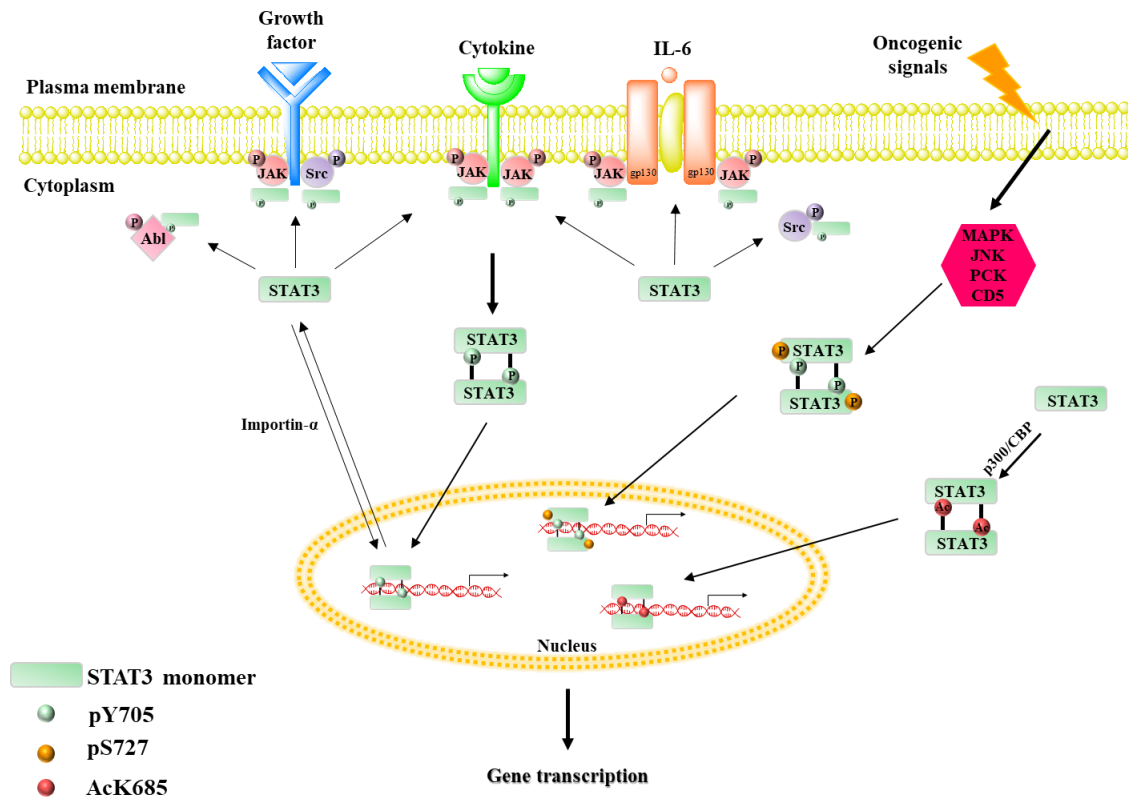


Figure 4. The classical canonical and non-canonical pathways of STAT3 activation.

The canonical pathway of STAT3 activation depend on the phosphorylation of Y705 residue of STAT3, by both receptor-associated JAKs and receptors with intrinsic tyrosine kinase activity, upon binding of their specific ligands, as well as by non-receptor tyrosine kinases. The activated STAT3 dimerizes and translocates into the nucleus, where regulates the expression of target genes. The phosphorylation of S727 by various upstream kinases represent the non-canonical pathway of STAT3 activation. Apart from phosphorylation of Y705 and S727, STAT3 also undergoes acetylation at K685 residue, inducing STAT3 dimerization even in the absence of pY705 and pS727.

The non-canonical pathway of STAT3 signaling is independent of classical Y705 phosphorylation. STAT3 can be phosphorylated at another crucial residue, S727. Different converging kinases, such as MAPK, JNK, PKC family and CDK5, are responsible for phosphorylating STAT3 at S727. Several reports highlighted the independent role of pS727 and pY705 in regulating STAT3 function in cancer. Phosphorylated S727 either alone or together with pY705 activates the transcription of genes involved in cell proliferation, survival, DNA repair, drug resistance and some unknown genes.

STAT3 also undergoes acetylation at K685, induced by interaction of p300/CBP histone acetyl transferase protein with the C-terminus of STAT3. Upon K685 acetylation, STAT3 showed increased nuclear localization, DNA binding and enhanced transactivation activity. The acetylated STAT3 dimers interact with DNMT1 and methylate the promoter of tumor suppressor genes to inhibit its expression. (*Dimri et al. 2017*)

1.4 STAT3-regulated transcription in normal and cancer cells

STATs were originally considered as latent cytoplasmic molecules, activated through phosphorylation and acting as transcription factors with specific DNA binding activity in the nucleus. In particular, STAT3 dynamically translocates from the cytoplasm to the nucleus, maintaining a prominent nuclear presence. In normal cells, STAT3 activation and transcription are tightly regulated and transient. STAT3 was first discovered and characterized as critical mediators in the immune system. In fact, it was originally found to induce the expression of a limited set of target genes in response to IL-6 released during inflammation, interacting with the acute-phase response factor. (*Lütticken et al. 1994; Raz et al. 1994*)

STAT3 is ubiquitously expressed in most tissues; therefore, its function was then widely studied in cell culture systems, showing the central role of STAT3 in a variety of signaling systems and responses. Several studies suggested that STAT3 is the main signal transducer downstream of gp130-like receptors, since it could stimulate the proliferation of B lymphocytes, activate terminal differentiation and growth arrest in monocytes, and maintain the pluripotency of embryonic stem cells. (*Heinrich et al. 1998; Niwa et al. 1998; Raz et al. 1999; Matsuda et al. 1999*)

STAT3 is also essential for the differentiation of helper T cells, implicated in a variety of autoimmune disease. (*Yang et al. 2007*)

Furthermore, IL-6-mediated activation of STAT3 is required for the maturation of dendritic cells. (*Park et al. 2004*)

Unlike all other members of the STAT gene family, the disruption of STAT3 gene causes embryonic lethality. (*Takeda et al. 1997*)

Despite STAT3 plays a crucial role in the early developmental process, the ablation of STAT3 in adult tissues causes unexpectedly mild phenotypes. Depending on the target tissue, STAT3 can modulate cell proliferation and survival, or apoptosis. (*Levy and Lee, 2002; Gao et al. 2017*)

For this reason, STAT3 is often correlated to carcinogenesis and it is considered as an oncogene (Figure 5).

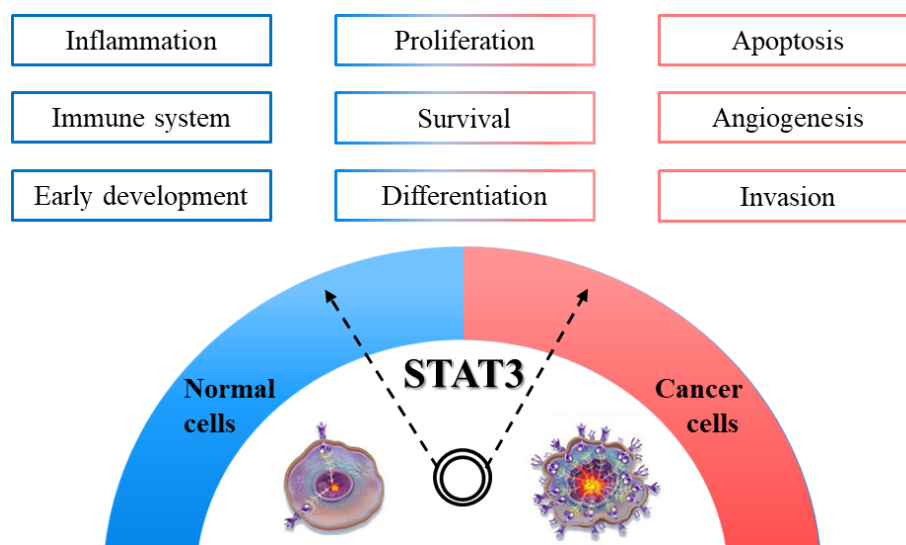


Figure 5. STAT3-regulated transcription in normal and cancer cells.

Once in the nucleus, STAT3 dimers bind to specific DNA regions and mediate the expression of a variety of genes, in response to different stimuli in multiple cell types. The expression of these downstream genes regulates several processes both in normal and cancer cells, in which STAT3 signaling pathway is no longer transient but persistent.

If STAT3 activation is transient in normal cells, its persistent and aberrant activation was reported in malignant transformation and carcinogenesis (Figure 6).

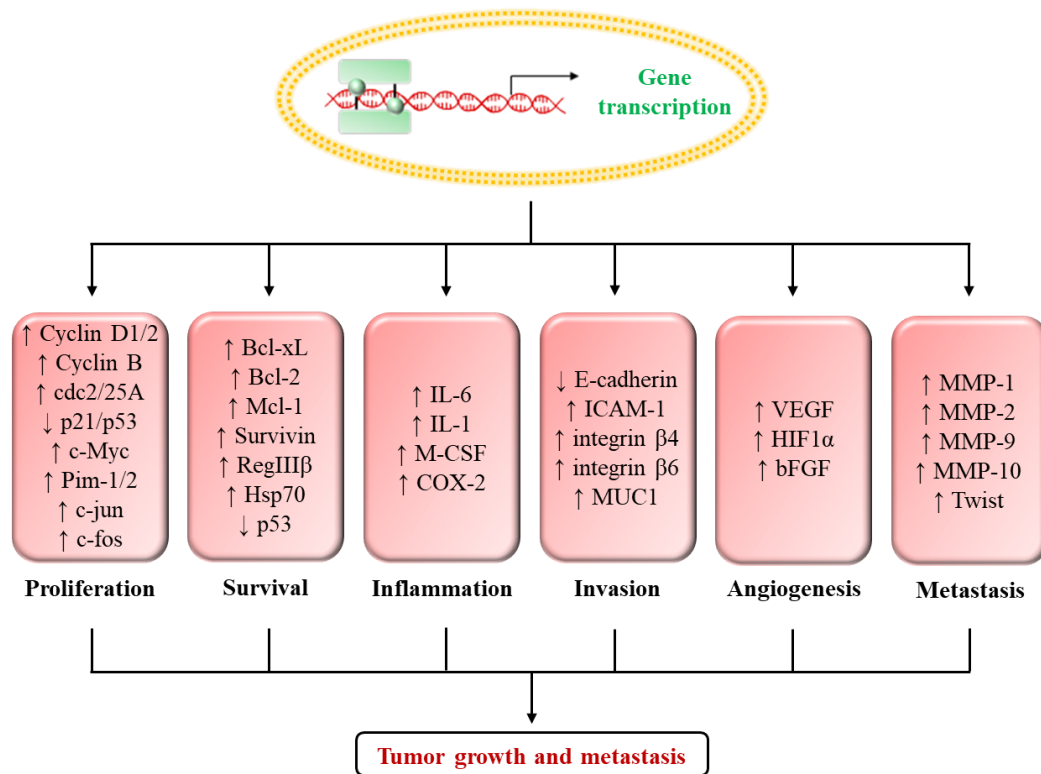


Figure 6. STAT3 contribution to tumor growth and metastasis.

STAT3 promotes cell proliferation primarily by modulating the expression of key genes, correlated to tumor growth and involved in the regulation of the cell cycle. STAT3 contributes to malignancy by preventing apoptosis, through upregulation of several anti-apoptotic proteins. STAT3 signaling is implicated in cancer inflammation. STAT3 plays an important role in cell migration and contributes to angiogenesis. Persistent activation of STAT3 is often correlated to tumor invasion and metastasis.

The increased level of phosphorylated STAT3 is due mostly to the excess of growth factors and/or cytokines within the tumor microenvironment that activate STAT3 in a paracrine way. Activation of oncogenes and inactivation of tumor-suppressor genes, as well as deregulation of multiple potential upstream inputs and genetic events in neoplastic cells directly activate STAT3 or release inflammatory mediators in an autocrine manner. Through regulation of its target genes, constitutive activated STAT3 contributes to carcinogenesis mainly by triggering pro-proliferative and pro-survival signaling. STAT3 signaling is also involved in the prevention of apoptotic pathway and tumor inflammation. Furthermore, some STAT3 target genes contribute to tumor invasion, angiogenesis and

metastasis. Activated STAT3 is finally involved in the maintenance of cancer stem cells, also known as tumor initiating cells, able to generate diverse tumor cells and contribute to tumor heterogeneity. (Siveen *et al.* 2014; Xiong *et al.* 2014)

Due to its ability to regulate the expression of various genes involved in cell proliferation and differentiation, apoptosis, immune and inflammatory responses, angiogenesis, tumor invasion and metastasis, maintenance of cancer stem cells, STAT3 is integrally involved in carcinogenesis.

1.5 STAT3 as a novel molecular target for cancer prevention and treatment

Increasing evidences confirm that STAT3 plays a critical role in the development and progression of multiple cancer types. Because it is constitutively activated during the growth and the invasiveness of a variety of cancers, STAT3 has emerged as an attracting novel target for cancer prevention and for the design and the development of new drugs potentially effective as chemotherapeutic agents.

The inhibition of STAT3 signaling provides a rational strategy to block carcinogenesis at early stage of tumor development. The discovery of STAT3 inhibitors is currently demanded for both cancer prevention and treatment. STAT3 was originally considered as non-targetable or undruggable and the development of STAT3 inhibitors was delayed, contributing to the lack of FDA-approved STAT3 inhibitors. Recent advances in cancer biology and drug discovery efforts has motivated researchers to develop STAT3 inhibitors as a novel generation of antitumor drugs.

CHAPTER 2:
STAT3 inhibitors for cancer prevention and therapy

2.1 Inhibition of STAT3 signaling pathway in cancer cells

Increasing evidences have shown STAT3 as a key cell signaling molecule in the proliferation and survival of cancer cells.

Since STAT3 is constitutively activated in several malignances, it is a promising drug target and the inhibition of its signaling pathway could be a potential strategy to prevent or treat cancer (Figure 7).

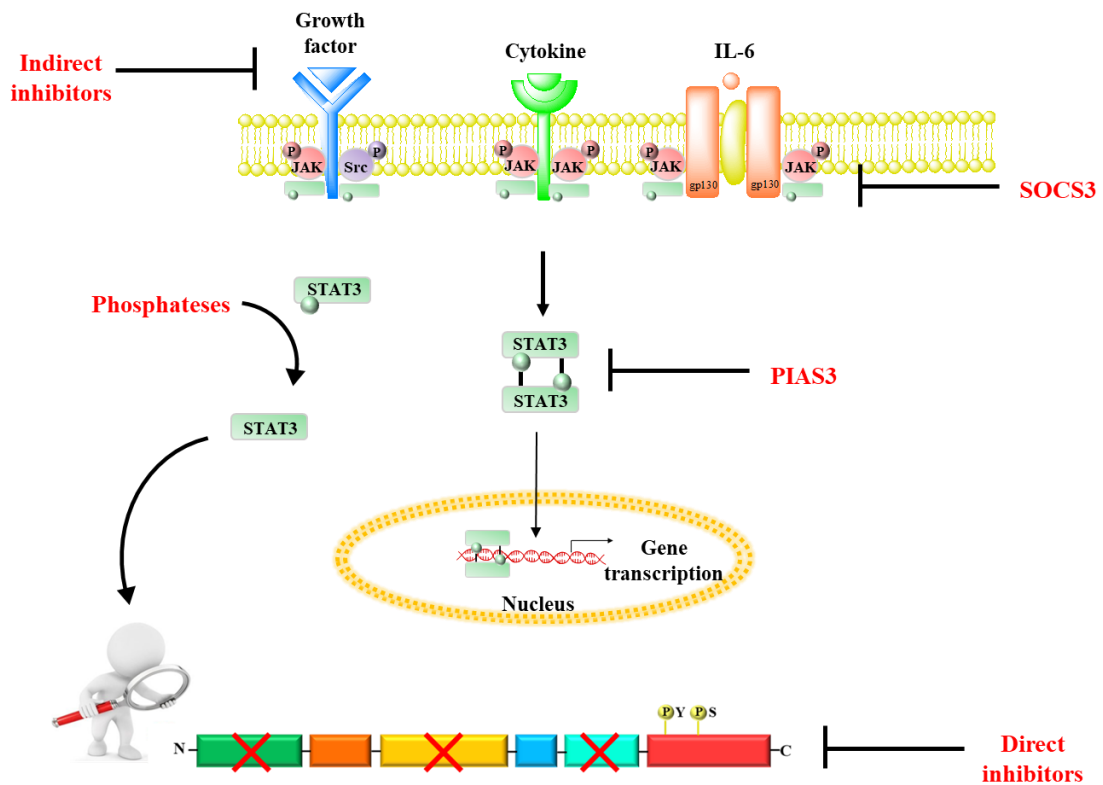


Figure 7. Endogenous and exogenous STAT3 inhibitors.

The endogenous inhibitors keep STAT3-mediated proliferation in equilibrium under normal conditions. The direct and indirect inhibition of STAT3 signaling pathway is a potential strategy for cancer prevention and treatment.

As already mentioned, in normal cells STAT3 activation and transcription is tightly controlled by an equilibrium between stimulation and inhibition.

If tyrosine kinase-mediated phosphorylation activates STAT3 monomers, in contrast, some phosphatases, such as cytoplasmic and nuclear phosphatase, downregulate its

activity. They repress JAK-STAT signaling through dephosphorylation of STAT3. Initially, the persistent activation of STAT3 automatically triggers regulatory feedback loops. For example, the expression of suppressor of cytokine signaling 3 (SOCS3) is induced by activated STAT3. It serves as a feedback inhibitor, preventing the persistent activation of STAT3 signaling pathway. (*Munoz et al. 2014*)

Furthermore, the protein inhibitor of activated STAT3 (PIAS3) deregulates cell proliferation by modulation of DNA binding transcription factors and their oncogenic activity. (*Munoz et al. 2014*)

Although there are not FDA-approved STAT3 inhibitors available for use to date, many molecules were found to be able to interfere with STAT3 signaling. The crucial role of STAT3 in cancer initiation, progression and metastasis has motivated many groups to design and develop approaches to inhibit STAT3 signaling. Two main strategies can be exploited to inhibit STAT3 signaling pathway:

- **indirect inhibition:** blocking the upstream regulators of the pathway, such as growth factors and cytokines, as well as kinases, involved in STAT3 phosphorylation, then in its activation;
- **direct inhibition of STAT3 protein:** with small molecule inhibitors targeting one of the STAT3 structural domains, such as SH2, DNA-binding and N-terminal domains. Interacting directly with STAT3, they inhibit phosphorylation, dimerization, nuclear translocation, DNA binding and transcription of target genes.

Many different classes of molecules have been investigated, including antisense oligonucleotides, small interfering RNA (siRNA), peptides and small molecule inhibitors. Results show a decrease in cell proliferation and invasiveness, as well as an increase in apoptosis.

2.2 Oligonucleotides and peptides

Antisense RNA and siRNA have been used to inhibit STAT3 gene expression by binding mRNA, resulting in subsequent degradation. Furthermore, decoy oligodeoxynucleotides can mimic the consensus STAT DNA binding sequence and it is used to compete for STAT3 DNA binding. The result is a downregulation of STAT3-dependent gene transcription. Most *in vitro* and *in vivo* studies using oligonucleotides and siRNA as STAT3 inhibitors are consistent and show the suppression of tumor cell growth and the induction of apoptosis. Phase 0, Phase 1, and Phase 1/2 trial studies of oligonucleotide inhibitors are still ongoing. (Groner *et al.* 2008; Munoz *et al.* 2014)

Peptides have been used to block reciprocal docking between SH2 domain of one STAT3 monomer and the pY705 motif on the partnering STAT3 monomer, preventing protein-protein dimerization. The isolated SH2 domain of STAT3, a short peptide of six amino acids, reduces the DNA binding of STAT3, while peptide aptamers, designed on the base of crystallography and structural analysis, interact with upstream receptors and functionally important domains of STAT3, preventing phosphorylation, dimerization and DNA binding. The use of pure peptide is limited by low biological activity, poor membrane permeability, modest stability, and relative non-specificity for STAT3, then peptidomimetic and nonpeptide approaches can overcome these limitations. (Groner *et al.* 2008; Munoz *et al.* 2014)

2.3 Small molecule inhibitors

Small molecule inhibitors of STAT3 is the largest class of compounds used to prevent and treat cancer. They can act in both direct and indirect ways, inhibiting STAT3 phosphorylation, dimerization, nuclear translocation, and/or DNA binding. Multiple methods including high-throughput screening of large chemical libraries, virtual

screening and rational design based on peptides and peptidomimetic inhibitors, fragment-based drug design, and multiple ligand simultaneous docking (MLSD) were used to identify novel small molecule inhibitors of STAT3.

Many natural and synthetic agents showed significant inhibition of STAT3 activation and thereby suppression of tumor growth and metastasis. Unfortunately, a comparison across different classes of inhibitors is difficult since there is no uniformity in terms of assay systems used to evaluate their potency. (*Debnath et al. 2012*)

2.3.1 Natural inhibitors of STAT3 signaling pathway

A selection of natural products inhibiting STAT3 signal is shown in Figure 8. Mostly they inhibit the constitutive activation of STAT3 in a dose- and time-dependent manner, by inhibiting IL-6 and JAK-induced phosphorylation of STAT3, inducing ROS generation that blocks STAT3 signaling, blocking STAT3 translocation into the nucleus, and inhibiting the expression of STAT3 target genes.

Although natural products have the advantage to be generally well tolerated, many limitations hamper their application as effective chemopreventive and chemotherapeutic agents. In fact, they present non-specific effects on targeting STAT3, off-target effects, variable bioavailability and moderate efficacy. (*Debnath et al. 2012; Siveen et al. 2014*)

2.3.2 Synthetic agents inhibiting STAT3 signal

Rational structural modification in natural products might give novel drug candidates for cancer prevention and therapy (Figure 9). STA-21 is a natural STAT3 inhibitor discovered through virtual screening. It inhibits dimerization, nuclear translocation, DNA binding, and the expression of STAT3-regulated target genes in cancer cells with constitutively active STAT3. Several analogs of STA-21, with hydroxyl, acetyl and

sulfamidic groups, bind to the SH2 domain of STAT3. In particular, LLL-12 is more potent than the lead compound. (Debnath et al. 2012; Siveen et al. 2014)

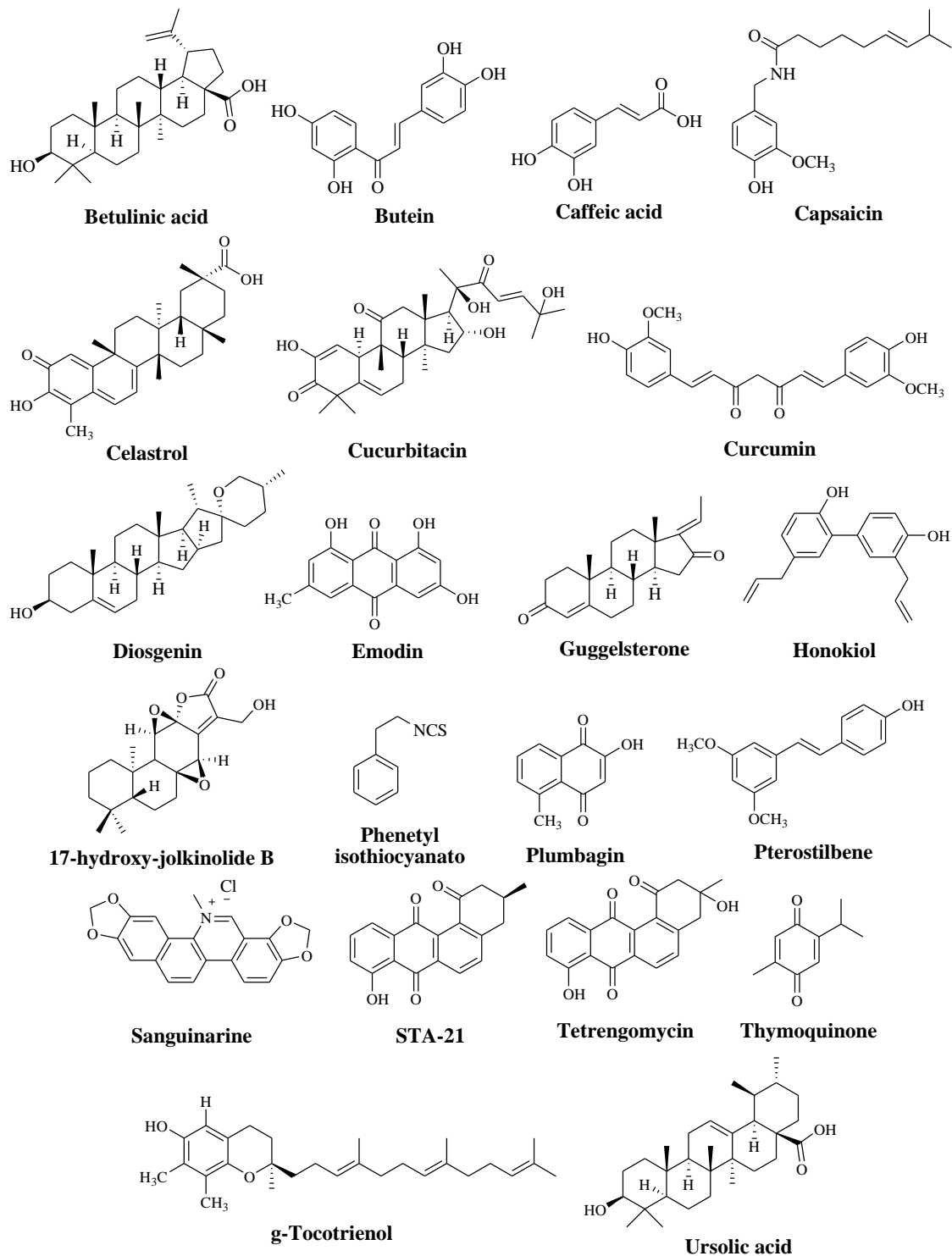
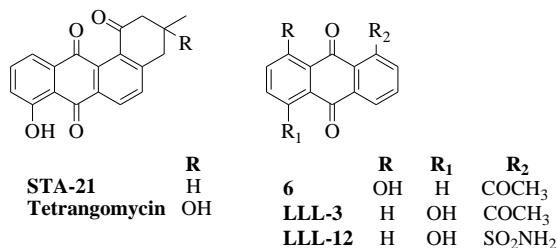


Figure 8. Chemical structures of selected natural inhibitors of STAT3 signal.

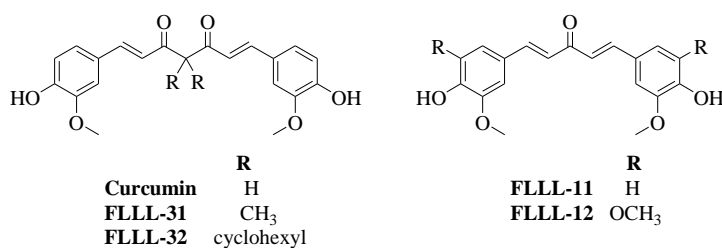
Curcumin inhibits IL-6-induced STAT3 phosphorylation and nuclear translocation. Some analogs have been designed based on its structure. They also decrease phosphorylated STAT3 levels and induce apoptosis in a dose-dependent manner in several cancer cell lines. (Debnath *et al.* 2012)

Several quinolinones have been reported as JAK/STAT3 pathway inhibitors. These analogs inhibit STAT3 phosphorylation at Y705. The carboxylic analog is less potent than esters, whereas the introduction of a cyano group significantly increases the potency of quinolinones analogs. (Debnath *et al.* 2012)

Analogs of STA-21



Analogs of Curcumin



Analogs of quinolinones

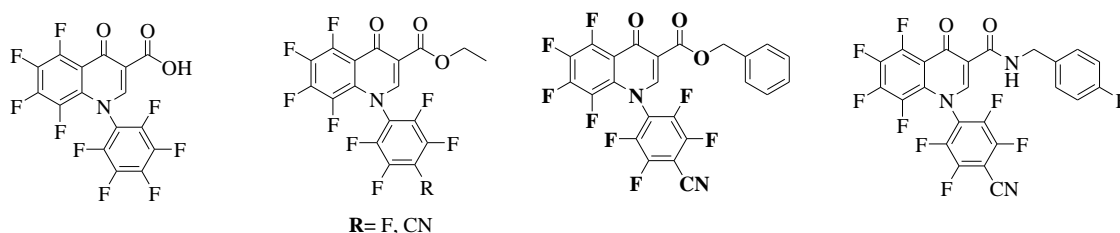


Figure 9. Synthetic analogs of natural STAT3 inhibitors.

2.3.3 Other small molecule inhibitors of STAT3 signaling pathway

Another small molecule, Stattic, has been identified *via* high-throughput screening of a

diverse chemical library as a STAT3 inhibitor, binding its SH2 domain, and inhibiting the proliferation of cancer cells. Stattic may lack target selectivity because of its simple chemical structure. Some analogs of Stattic have been synthesized in order to optimize the lead compound (Figure 10). Unfortunately, the attempt was unsuccessful, suggesting the importance of both nitro group and unsaturated five-membered ring for the inhibitory activity of Stattic. (Debnath et al. 2012; Siveen et al. 2014)

On the other hand, S 31-201 has been identified as STAT3 inhibitor through structural-based virtual screening of chemical libraries from NCI. It preferentially inhibits the DNA binding ability of STAT3 dimers, showing antiproliferative activity both *in vitro* and *in vivo* studies. In an attempt to optimize compound S 31-201, structure-based modeling resulted in several analogs with improved potency (Figure 10). (Debnath et al. 2012)

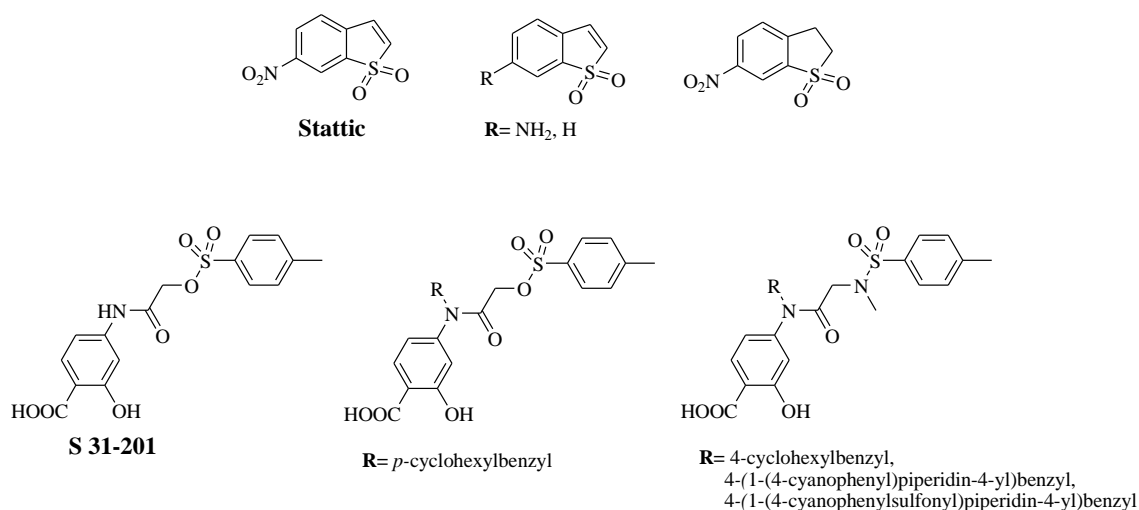


Figure 10. Chemical structures of Stattic, S 31-201 and their analogs.

Using high-throughput and virtual screening, several drugs and additional compounds have been found to interfere directly and/or indirectly with STAT3 signaling pathway (Figure 11).

All these identified compounds need further characterization in order to elucidate their

actual molecular targets. Therefore, it is too early to classify them as STAT3 inhibitors.

(Debnath et al. 2012)

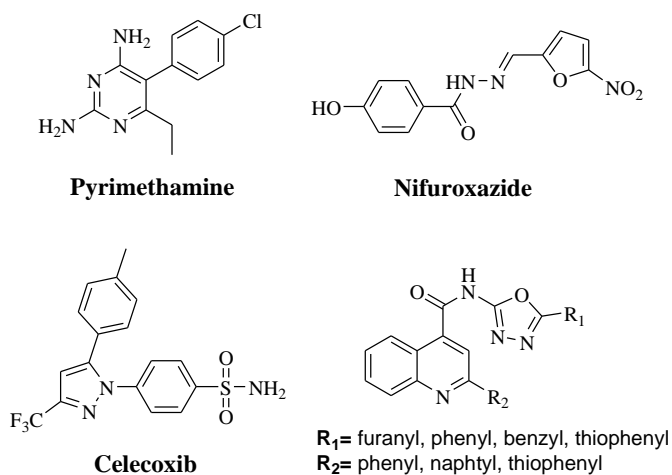


Figure 11. Additional compounds identified from high-throughput and virtual screening.

2.3.4 Inhibitors of JAK and Src kinases

STAT3 phosphorylation is essential for its activation and then for its signaling pathway. Inhibiting the upstream kinases such as JAK and Src, which phosphorylate STAT3 is a rational approach to inhibit STAT3 signal and have a chemopreventive and/or chemotherapeutic effect. Both JAK and Src inhibitors decrease phosphorylated STAT3 levels, causing suppression of tumor growth, induction of apoptosis, and inhibition of metastasis. New developed compounds show antiproliferative activity by inhibiting synergistically multiple cytoplasmic kinases. (Xiong et al. 2014)

Few kinase inhibitors are shown in Figure 12.

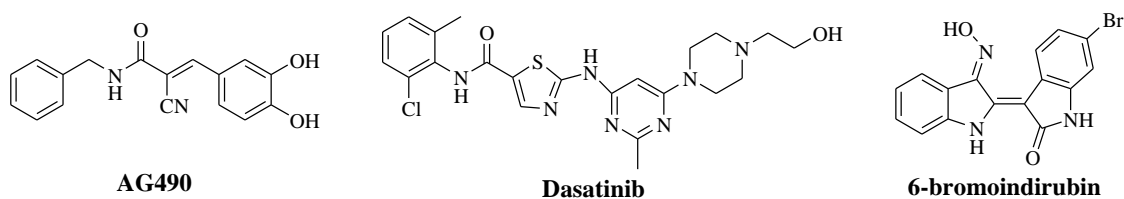


Figure 12. Inhibitors of JAK and Src kinases.

2.3.5 Small molecule inhibitors of STAT3 under clinical trial studies

STAT3 inhibitors have important features that certainly need further investigations, but the preliminary results are promising. Nowadays, few inhibitors are under evaluation in a number of early phase trials, in gastric cancer. (Cafferkey *et al.*, 2016)

First, Kim *et al.* identified compound OPB-31121 (structure not disclosed) as STAT3 inhibitor by suppressing both constitutively activated and IL-6-mediated JAK/STAT signaling pathways. It reduces cell proliferation, induces apoptosis, and downregulates the expression of antiapoptotic proteins both *in vitro* and *in vivo* studies. OPB-31121 also has synergistic effect with known antitumor drugs, such as 5-FU and cisplatin. It binds to the SH2 domain of STAT3 in a unique way, compared to other inhibitors, as shown by computational docking and molecular dynamics simulation. (Brambilla *et al.*, 2015)

Currently, OPB-31121 is under the first experimental phase of clinical trials, to evaluate the safety and tolerability. Its administration is associated with mild side effects, including grade 1 to 2 nausea, vomiting, diarrhea, and fatigue. (Bendell *et al.*, 2014)

Compound OPB-51602 (structure not disclosed) is also an oral direct inhibitor of STAT3. Wong *et al.* investigated the maximum tolerated dose (MTD), safety, and pharmacokinetics of OPB-51602 in a phase 1 study. It inhibits tyrosine and serine phosphorylation of STAT3 *in vitro*. The phase 1 clinical study confirms the safety of OPB-51602 in terms of toxicity. The most common adverse effects observed are again nausea, vomiting, diarrhea, anorexia, peripheral neuropathy, and fatigue. (Ogura *et al.*, 2015)

Compound BBI608, also known as napabucasin, inhibits STAT3-regulated transcription (Figure 13). In preclinical studies, napabucasin exhibits its effect in various ways, including a dose-dependent decrease of antiapoptotic protein levels and suppression of genes important for cancer stemness. (Li *et al.*, 2015)

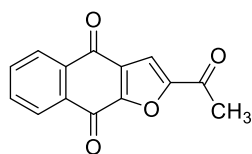


Figure 13. Chemical structure of napabucasin.

A phase 1 clinical study confirms napabucasin as a safe drug; the MTD was not reached. Its administration is associated with moderate side effects, including grade 1 to 2 nausea, diarrhea, anorexia and fatigue. (*Langleben et al. 2013*)

Further Phase 1b and 2 studies combining napabucasin with well-known antitumor drugs, such as paclitaxel, bevacizumab and gemcitabine, were conducted in patients with advanced cancer. Treatment with both drugs causes regression or suppression of tumor growth. (*Hitron et al. 2014; Becerra et al. 2015; Shitara et al. 2015*)

Due to its promising results, the last clinical phase study of napabucasin is ongoing, in patients with pretreated advanced gastric and GEJ adenocarcinoma. (*Shah et al. 2015*)

2.4 Prospect of STAT3 inhibitors

Although STAT3 is constitutively activated in several malignances, the inhibition of STAT3 signaling pathway is not such a simple approach to exploit for cancer prevention and therapy. If activation of either enzymes or cell surface receptors efficiently amplify cell signaling, STAT3 molecules are signal transducers themselves. Currently, approved drugs are mostly inhibitors of enzymes and receptors and this inhibition, even if partial, results in the suppression of cell signaling. On the other hand, the complete inhibition of STAT3 signaling pathway is difficult to achieve. The promise of STAT3 as a drug target is currently limited by its functional properties. STAT3 does not exhibit enzymatic activity and does not have any low molecular weight binding ligands. Although there are

no clinically approved drugs targeting STAT3 and some researchers still consider it as an undruggable target, many different classes of molecules have been identified as interfering the STAT3 signaling pathway. Mostly they present some limits and the development of highly efficient STAT3 inhibitors is still challenging, other than strongly demanded.

2.5 Identification of new scaffolds for the development of new small molecules targeting STAT3 signaling pathway for cancer therapy

Nitrogen-containing heterocycles are quite common fragments in drugs and bioactive compounds. (*Leeson and Springthorpe; 2007*)

Several small molecules directly and indirectly interfering with STAT3 signal, as well as FDA-approved therapeutic kinase inhibitors for cancer therapy, contain heterocyclic moiety in their chemical structure. (*Zhang et al. 2009; Thoma et al. 2014; Wu et al. 2015*)

To identify potential STAT3 inhibitors, the research group led by professor Neamati screened a highly diverse library of 20 000 molecules, representing over one million compounds, in the pancreatic cancer cell line Mia PaCa-2. From the initial screen, they identified over 400 cytotoxic compounds with $IC_{50} < 10 \mu M$. The most potent compounds were then tested for STAT3 inhibition in a FP assay. The N-containing TZC and DTP scaffolds, showing a significant inhibition of STAT3 ($IC_{50} < 50 \mu M$), were selected for further analysis and optimization (Figure 14). Each scaffold was suitable for optimization by introducing various specific moieties, able to interact directly with STAT3 or with one of the upstream kinases involved in its activation, obtaining specific modulators of the STAT3 signaling pathway. The functionalization with various chemical groups was performed to better define the SAR. A series of TZC salts was designed also in order to eventually improve the solubility and the efficacy of these heterocycles.

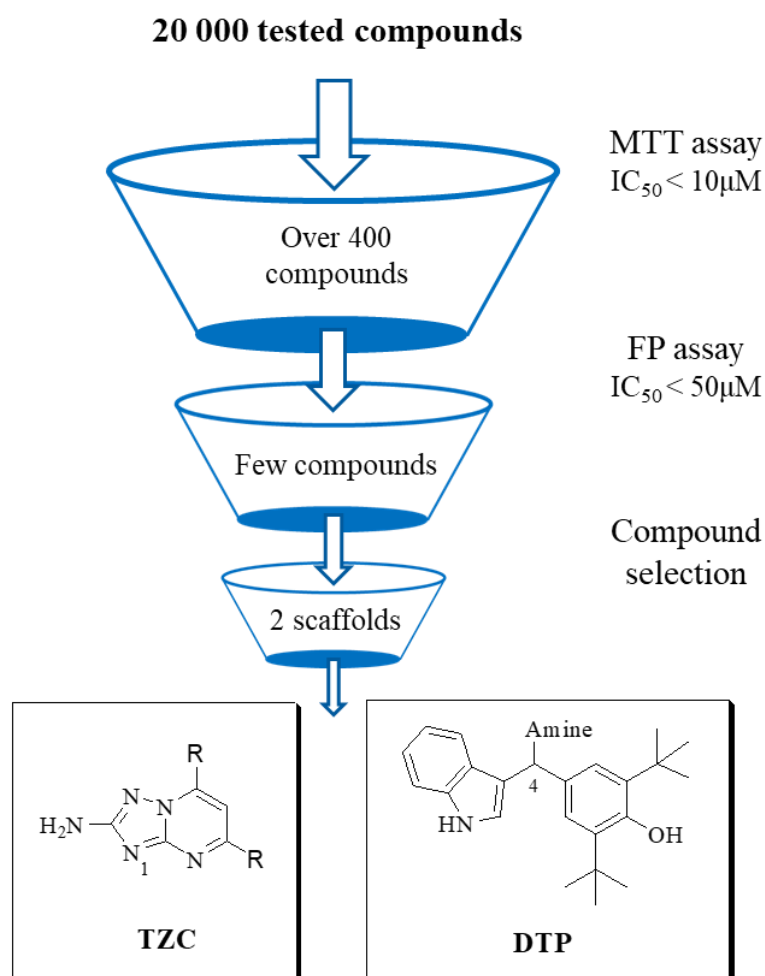


Figure 14. Identification of two potential scaffold for the development of STAT3 inhibitors.

As already mentioned, whereas the activation of STAT3 in normal cells is transient, the overexpression and/or persistent activation of STAT3 has been reported in most human cancers, including pancreatic ones. Pancreatic cancer afflicts people all around the world. It is associated to a very high mortality rate. Although a lot of research is focused on finding better treatments for this lethal disease, statistics still confirm how urgent is the discovery of new drugs to properly treat pancreatic cancer.

Continuously to the interest of prof. Neamati's research in the discovery and development of promising drugs to treat pancreatic cancer, in his laboratory I performed a medium-throughput screening of in-house compounds (Figure 15).

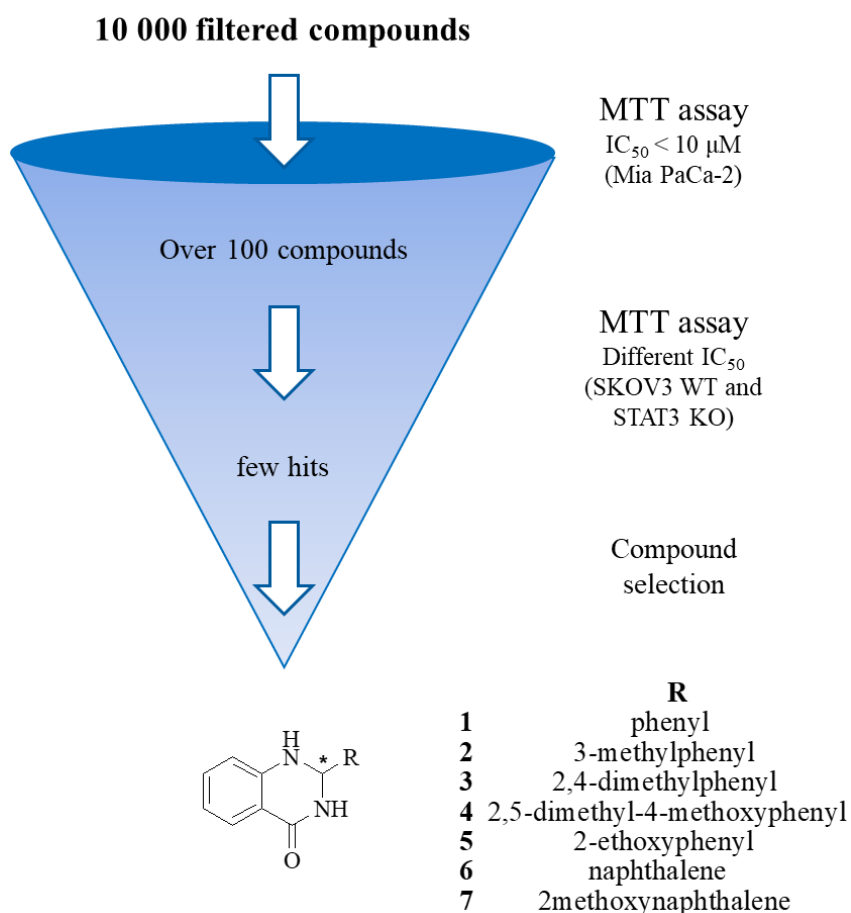


Figure 15. Identification of DHQ scaffold for the development of potential anticancer agents.

Some DHQ derivatives were found to be very cytotoxic against Mia PaCa-2 cell lines. Furthermore, few of them showed different cytotoxicity against ovarian cancer cell lines, SKOV3 wild-type (WT) and the engineered SKOV3 STAT3 knock-out (KO), suggesting that these compounds might interfere with STAT3 signaling pathway (Table 1).

Since DHQ moiety showed diverse biological activities, it has long been an attracting scaffold for developing new drugs and was selected as a potential lead compound.

In the last half century, numerous compounds bearing variously decorated DHQ core structure showed a wide spectrum of biological activities and medicinal properties, including anticancer one.

Table 1. Cytotoxicity of in-house DHQ derivatives against pancreatic and ovarian cancer cell lines.

Compound	IC ₅₀ (μM) ^a		
	Mia PaCa-2	SKOV3 WT	SKOV3 STAT3 KO
1	1.3	9.8	9.0
2	3.7	16.3	14.1
3	0.6	8.9	8.4
4	0.7	1.6	6.2
5	0.5	3.5	2.7
6	0.1	8.9	9.1
7	2.9	9.6	8.9

^aIC₅₀ values were determined by MTT assay after 72 h treatment. The data are shown as the mean ± standard deviation (SD), n=3.

DHQ derivatives and its oxidized form QZ, part of several natural and synthetic bioactive compounds, also found a few clinical applications as diuretic and sedative. Regarding the antitumor effect of DHQ derivatives, the first evidence of their cytotoxicity against cancer cell lines has been reported almost 50 years ago, but through this time, efforts to determine the mechanism of action of DHQs were unsuccessful. (*Yale and Kalkstein, 1967*)

Few compounds with DHQ skeleton have been found acting as tubulin inhibitors and similarly to the antimitotic colchicine, able to inhibit the proliferation of cancer cells. (*Hamel et al. 1996; Hour et al. 2000*)

Since many study have suggested that the interaction between colchicine and tubulin is stereoselective, pure (*S*)-enantiomers of DHQ may are necessary for the interaction with tubulin. (*Chinigo et al. 2008*)

Although tubulin has been suggested as possible target of DHQ compounds, it probably is not the main target and further investigations are needed to better understand the mechanism of action and to explain the antitumor activity of DHQ derivatives.

The aim of my PhD work was to synthesize small libraries of each identified scaffold and determine the biological profile of the new compounds. Then, series of TZC and DTP derivatives, as well as new DHPs, QZs and DHQs were synthesized and lead optimization campaigns were undertaken to improve upon their potency.

A set of biological assays was performed to evaluate the antiproliferative activity of all synthesized derivatives, in a panel of different human cancer cell lines, including pancreatic, colorectal and ovarian ones. The inhibition of STAT3 was also determined and their mechanism of action was deeply investigated.

The promising results *in vitro* suggest a potential clinical relevance and application of these new derivatives as anticancer agents, then preclinical studies are still ongoing.

CHAPTER 3:
Design, synthesis, and biological evaluation of
[1,2,4]triazolo[1,5-*a*]pyrimidinium salts

3.1 Design and synthesis of TZC derivatives

The design of the new TZC derivatives is shown in Figure 16. The TZC nucleus was selected as scaffold for the development of potential STAT3 inhibitors. Then, the synthetic strategies included the synthesis of the TZC nucleus and structural modifications at the free amino group and the heterocyclic N1, which lead to TZC salts.

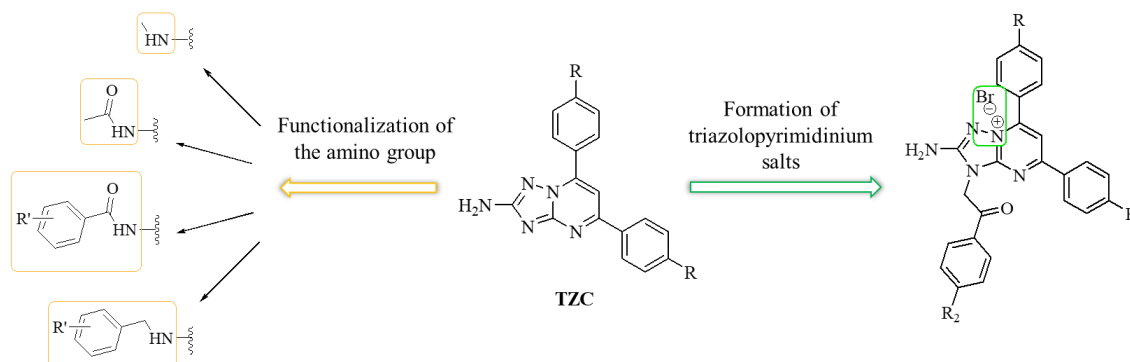
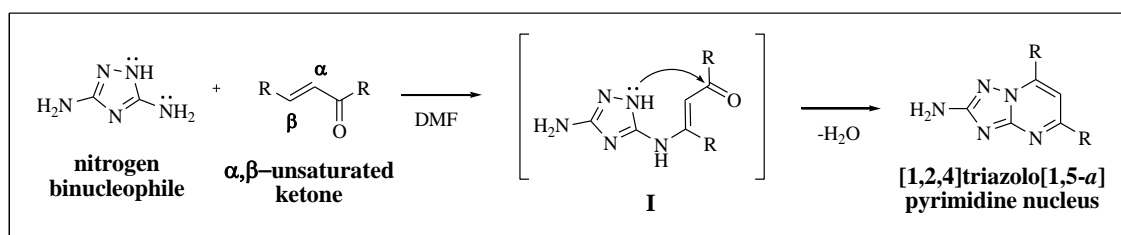


Figure 16. Design strategies for TZC derivatives.

3.2 Chemistry

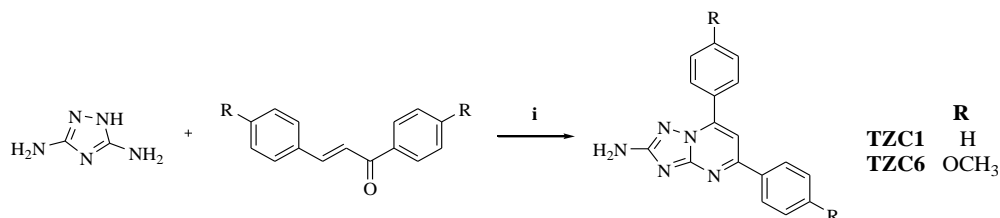
The TZC nucleus can be obtained through cyclocondensation of nitrogen binucleophiles with α,β -unsaturated ketones, according to the mechanism showed in Box 1.



Box 1. Mechanism of cyclocondensation of nitrogen binucleophiles with α,β -unsaturated ketones.

After the formation of the intermediate β -aminovinyl ketone (**I**), the cyclization occurs at the N1 center, which being included in the hydrazine fragment of the triazole ring is very nucleophilic. The resulting [1,2,4]triazolo[1,5-*a*]pyrimidine system is thermodynamically stable. (*Desenko et al. 1990*)

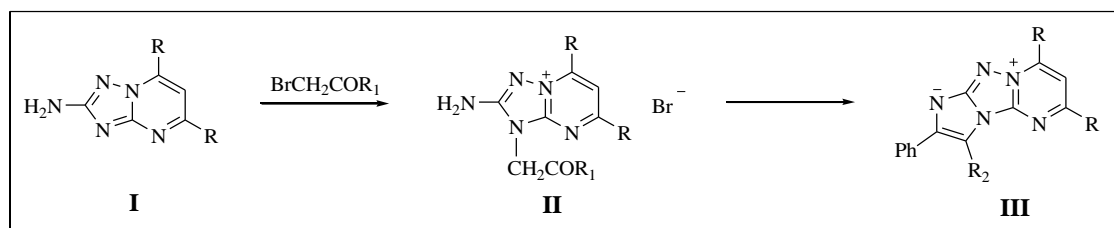
TZC1 and **TZC6** were initially prepared as first intermediates, suitable for functionalization. In particular, they were obtained from cyclocondensation between 3,5-diamino-1,2,4-triazole with *trans*-chalcone and 4,4'-dimethoxychalcone respectively (Scheme 1).



Scheme 1. Reagents and conditions.

i) 3,5-diamino-1,2,4-triazole (1 eq.), chalcones (0.96 eq.), DMF, 150-160°C.

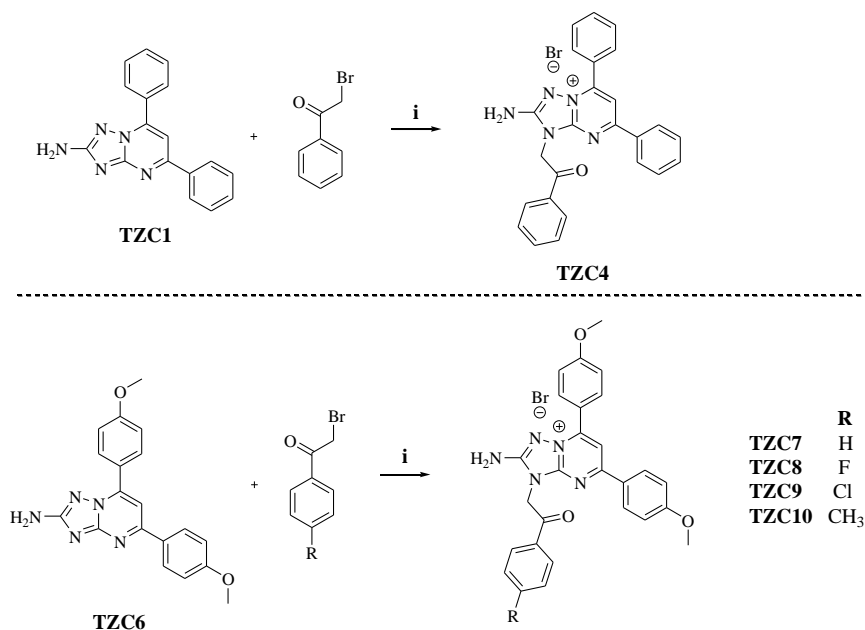
In 1986, *Maidannik et al.* reported for the first time the alkylation of 2-amino-[1,2,4]triazolo[1,5-*a*]pyrimidines by α -bromoketone and the formation of the resulting salts, as intermediates in the synthesis of mesoionic tricyclic systems (Box 2).



Box 2. Formation of TZC salts.

In the resulting salts, the electron density is delocalized in the [1,2,4]triazolo[1,5-*a*]pyrimidine system; the nitrogen of the free amino group has planar trigonal coordination, indicating a strong conjugation between the π -system of the bicycle and its unshared electron pair. (*Maidannik et al.* 1986)

The TZC salts (**TZC4**, **TZC7**, **TZC8**, **TZC9**, and **TZC10**) were then obtained by reaction of **TZC1** or **TZC6** with variously substituted 2-bromo-acetophenones, as depicted in Scheme 2. (*Bishop et al.* 1999; *Kolos et al.* 1999)

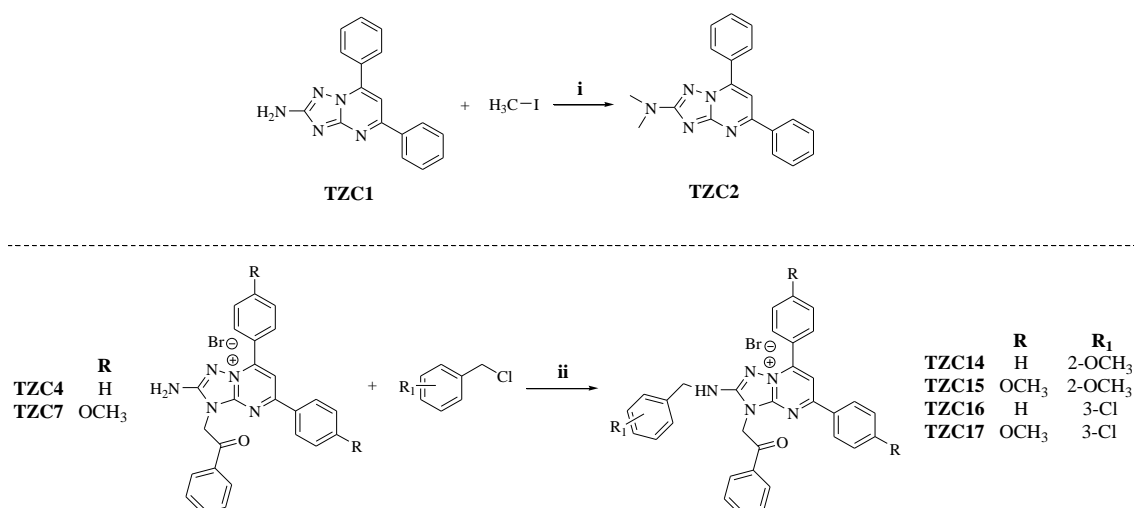


Scheme 2. Reagents and conditions.

i) **TzC1** or **TzC6** (1 eq.), substituted 2-bromo-acetophenones (1.2 eq.), DMF, 120°C.

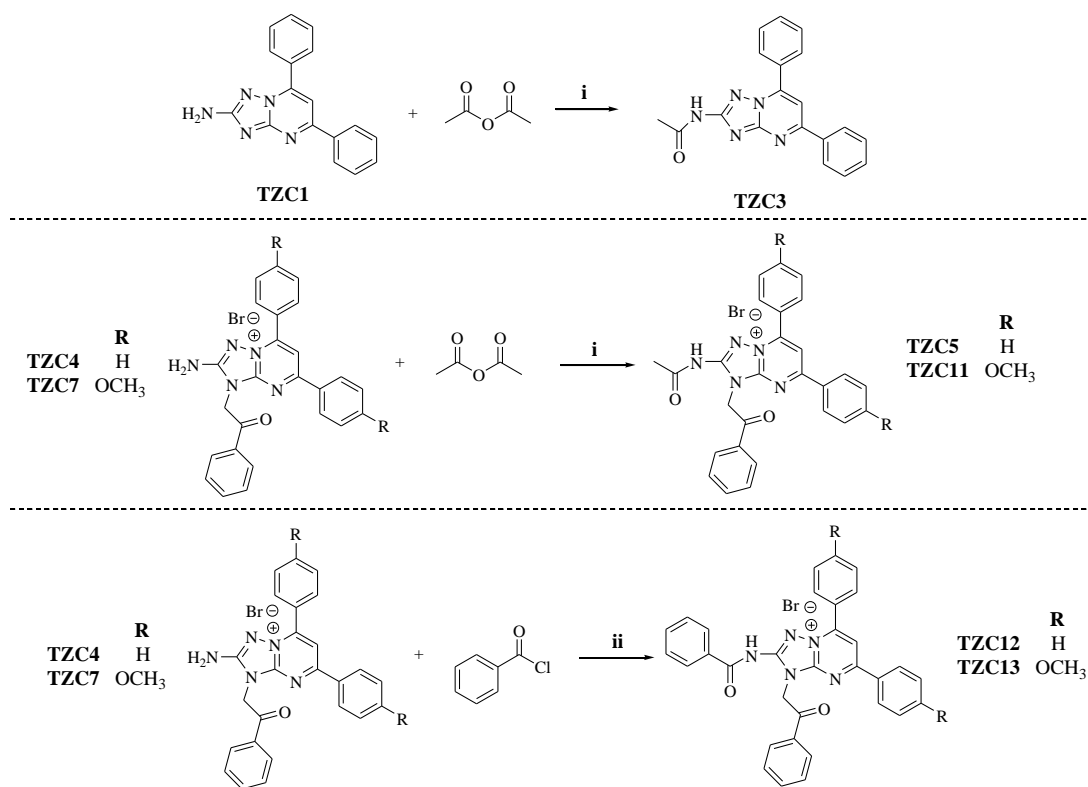
The free amino group of both TzC intermediates and salts underwent alkylation and acylation reaction, as shown in Scheme 3a and 3b.

Finally, Scheme 4 shows the synthesis of triazolopyrimidinium derivatives (**TzC18**-**TzC21**) obtained with an excess of the respective substituted 2-bromo-acetophenone.



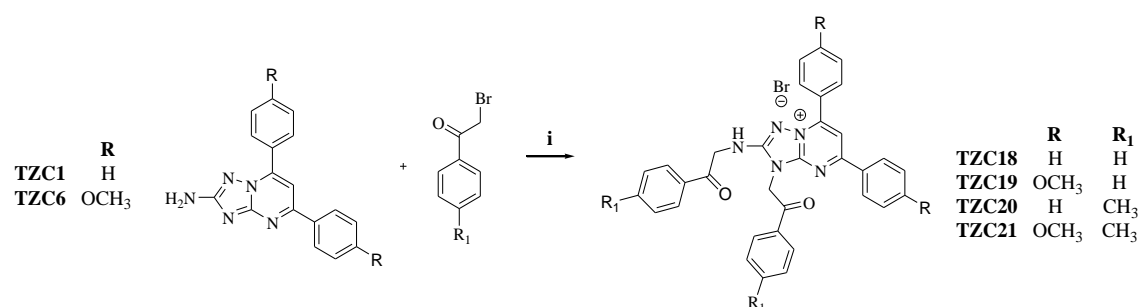
Scheme 3a. Reagents and conditions.

i) **TzC1** (1 eq.), methyl iodide (1 eq.), K₂CO₃ (0.9 eq.), THF, rt. ii) **TzC4** or **TzC7** (1 eq.), substituted benzyl chloride (1 eq.), KOtBu (1 eq.), THF, rt.



Scheme 3b. Reagents and conditions.

i) **TZC1** or **TZC4** or **TZC7** (1 eq.), acetic anhydride, 140°C. ii) **TZC4** or **TZC7** (1 eq.), benzoyl chloride (0.83 eq.), Et₃N (1.7 eq.), THF, rt.



Scheme 4. Reagents and conditions.

i) **ZC1** or **TZC6** (1 eq.), substituted 2-bromoacetophenones (2.5 eq.), DMF, 120°C.

3.3 Biological evaluation

3.3.1 Antiproliferative activity of TZC derivatives

The *in vitro* inhibition of cell proliferation induced by the new synthesized TZC derivatives was evaluated against a panel of human cancer cell lines, including pancreatic

(Mia PaCa-2), breast (MDA-MB-231), brain (U87G), and colorectal (HCT116 p53^{+/+}) cancers, by MTT (3-(4,5-dimethylthiazol-2-yl)-2,5-diphenyltetrazolium bromide) assay, using gemcitabine as positive control. Based on the MTT results, a SAR study was built but not computationally confirmed yet (Figure 17).

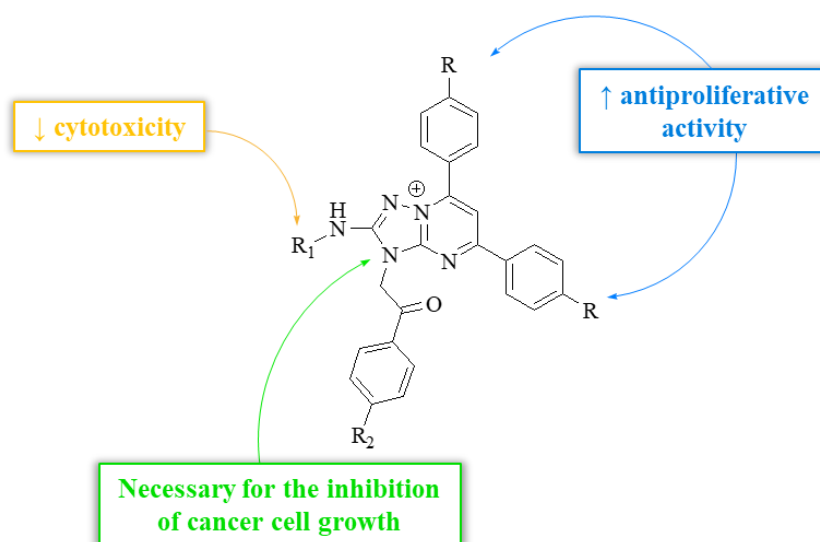


Figure 17. Structure-activity relationship for TzC derivatives.

Results suggest that, in general, the neutral TzC compounds (**TzC1-TzC3**, **TzC6**) exhibited no cytotoxic effect against cancer cells ($IC_{50} > 30\mu M$). On the contrary, TzC salts showed antiproliferative activity, in function of the chemical nature of the substituent on the amino group. Acyl derivatives inhibited the proliferation of cancer cells better than alkyl derivatives. All the TzC salts with free amino group, and in particular **TzC7** and **TzC10**, exhibited the best inhibition of cancer cell growth (IC_{50} values in low micromolar range, see Table 2), even better than the drug gemcitabine. Furthermore, the presence of electron-donor groups in *para* on the hanging rings improve the antiproliferative activity of the TzC derivatives. They selectively inhibited the proliferation of pancreatic cell lines, which express a high level of phosphorylated STAT3 (Table 2; Figure 18). (Debnath *et al.* 2012)

Table 2. Antiproliferative activity of TZC salts against pancreatic, breast, brain, and colorectal cancer cell lines.

Composund	IC ₅₀ (μM) ^a			
	Mia PaCa-2	MDA-MB-231	U87MG	HCT116 p53 ^{+/+}
TZC4	7.6 ± 2.5	18.5 ± 4.6	23.4 ± 6.4	9.7 ± 0.4
TZC7	2.1 ± 0.3	3.5 ± 0.6	5.9 ± 1.7	4.3 ± 0.8
TZC8	3.1 ± 0.8	3.7 ± 0.9	5.6 ± 0.7	7.3 ± 0.5
TZC9	5.3 ± 0.4	5.9 ± 0.6	6.9 ± 0.8	5.1 ± 0.8
TZC10	1.2 ± 0.1	2.5 ± 0.4	3.9 ± 0.7	1.4 ± 0.3
TZC18	6.1 ± 2.8	17.0 ± 7.9	13.8 ± 2.6	6.3 ± 2.6
TZC19	3.7 ± 0.7	5.2 ± 0.8	9.1 ± 0.3	7.1 ± 1.9
TZC20	4.5 ± 1.0	7.4 ± 0.4	10.2 ± 1.6	5.9 ± 2.4
TZC21	4.4 ± 2.6	5.1 ± 0.9	6.9 ± 1.5	6.4 ± 1.9
Gemcitabine^b	2.0 ± 0.3	2.8 ± 0.9	3.9 ± 1.7	2.0 ± 0.6

^a IC₅₀ values were determined by MTT assay after 72 h treatment. The data are shown as the mean ± standard deviation (SD), n=3.

^b Gemcitabine was used as a positive control.

In order to investigate the involvement of STAT3 signaling pathway in the mechanism of action of the new TZC salts, they were tested against engineered cell lines, such as ovarian cancer cell lines (SKOV3 WT and STAT3 KO). Stattic was used as positive control.

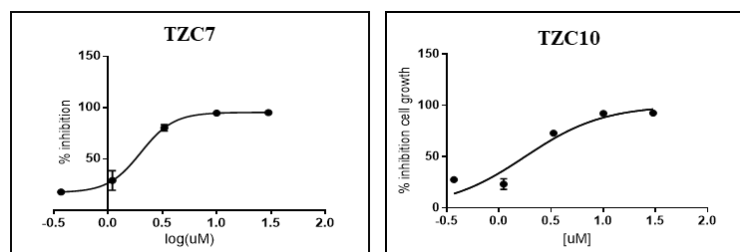


Figure 18. Dose-response curves of the best TZC salts in pancreatic cancer cells.

If the compounds are able to block cell proliferation inhibiting STAT3 signal directly or indirectly, they should exhibit different cytotoxicity against the two cell lines. As reported in Table 3, the TZC salts showed a similar cytotoxic effect against both cell lines, except for **TZC10**, which was more cytotoxic in the wild-type cell line, suggesting that it may inhibit cancer cell proliferation by inhibiting STAT3 signaling pathway.

Table 3. Antiproliferative activity of TZC salts against engineered ovarian cancer cell lines.

Compound	IC ₅₀ (μM) ^a	
	SKOV3 WT	SKOV3 STAT3 KO
TZC7	7.5 ± 0.5	8.9 ± 0.8
TZC8	22.3 ± 0.7	21.8 ± 0.4
TZC9	21.6 ± 0.6	23.3 ± 1.3
TZC10	6.0 ± 0.3	9.2 ± 0.2
TZC18	22.1 ± 0.5	13.7 ± 0.7
TZC19	18.2 ± 0.3	16.1 ± 0.6
TZC20	17.7 ± 0.8	18.4 ± 0.4
TZC21	10.6 ± 0.2	7.7 ± 1.2
Stattic ^b	5.1 ± 0.4	9.8 ± 0.9

^a IC₅₀ values were determined by MTT assay after 72 h treatment. The data are shown as the mean ± standard deviation (SD), n=3.

^b Stattic was used as a positive control.

The ability of the best TZC salts to inhibit colony formation was also evaluated in a panel of cancer cell lines, using three different concentrations (10μM, 5μM and 1μM). All the tested derivatives inhibited colony formation at 10μM, while **TCZ10** was active even at lower concentrations (Figure 19).

The most potent TZC salts were also able to inhibit cell migration of pancreatic cancer cells, probably because of inhibiting STAT3 signaling pathway (Figure 20).

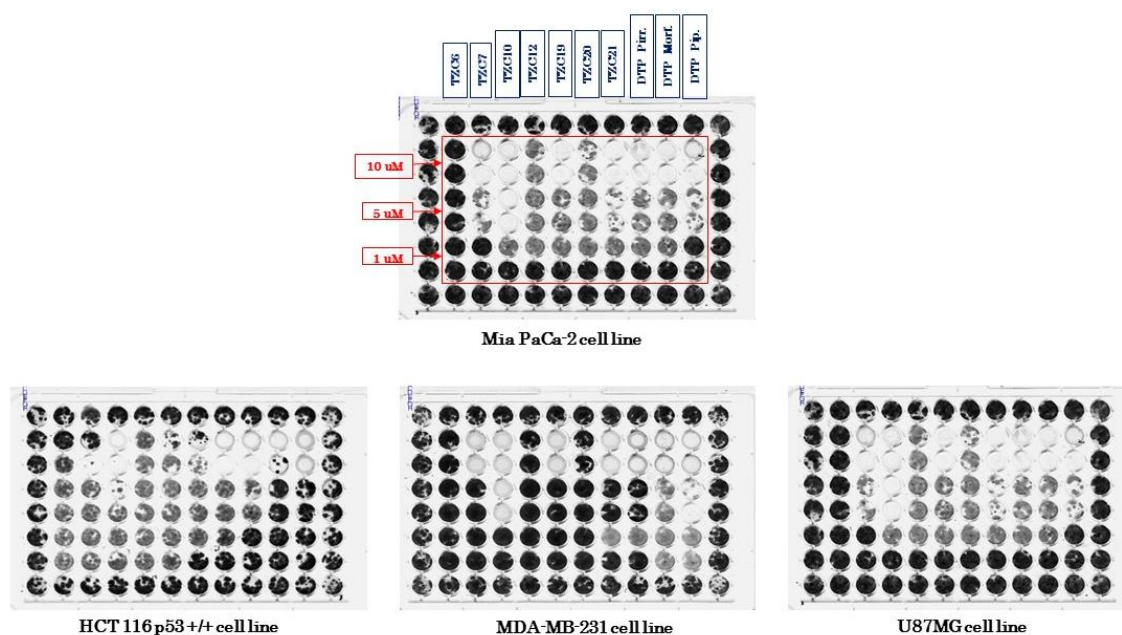


Figure 19. Colony formation assay using different cancer cell lines.

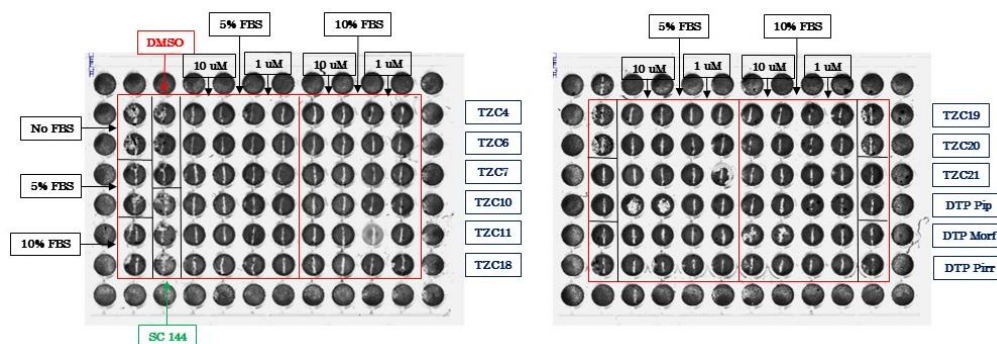


Figure 20. Wound healing (scratch) assay using pancreatic cancer cells.

3.3.2 Evaluation of the direct inhibition of STAT3

To determine whether TZC salts inhibit STAT3 signaling pathway by directly targeting its SH2 domain, FP assay using purified STAT3 was performed, at 37°C. Stattic was used as positive control. With this assay, the ability of compounds to displace the tracer from the SH2 domain is evaluated and calculated as percentage of inhibition of the binding tracer-STAT3. Compounds were initially tested at two different concentrations (50µM and 10µM) and the IC₅₀ values were then determined. In a primary screening, most of the tested compounds were not able to bind to the SH2 domain of the protein at the tested concentrations. Some compounds (**TZC1**, **TZC6**, and **TZC11**) were fluorescent, so their obtained results might be unreliable since they interfere with the assay. As expected based on the cytotoxic activity, **TZC10** was the best compound. It binds to the SH2 domain of STAT3 in a similar way of Stattic (Table 4).

Table 4. Binding of TZC salts to the SH2 domain of STAT3, using FP assay.

Compound	% inhibition (50 µM)	% inhibition (10 µM)	IC ₅₀ (µM)
Stattic	68.5	23.7	28.0
TZC1	48.1	39.2	fluorescent
TZC2	61.1	62.2	>100
TZC3	14.8	4.6	>100
TZC6	52.0	37.2	fluorescent
TZC10	65.5	33.7	27.0
TZC11	23.2	17.3	fluorescent

3.3.3 Western blot analysis of compound **TZC10**

In general, small molecules targeting the SH2 domain of STAT3 suppress the phosphorylation and the activation of the protein. (Xiong *et al.* 2014)

The inhibition of STAT3 phosphorylation was investigated using Western blot analysis, as shown in Figure 21A and B. Compound **TZC10** was selected based on its cytotoxic activity, in particular against the pancreatic cancer cell line, and its ability to bind to the SH2 domain of STAT3. The positive control Stattic was tested at a single concentration (10 μ M), while **TZC10** was tested at three different concentrations (1 μ M, 5 μ M and 10 μ M).

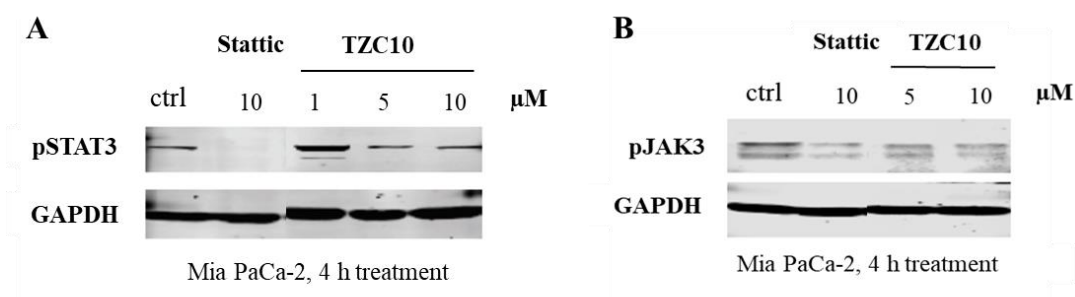


Figure 21. The effect of TZC10 on the expression of pSTAT3 in pancreatic cancer cells.

Cells were treated with the indicated concentrations for 4 h, and the proteins expression were determined by Western blot assay using antibodies against pSTAT3 (Y705) and pJAK3. GAPDH was used as a loading control.

Results suggest that **TZC10** suppresses the level of phosphorylated STAT3 at the Y705 residue in a dose-dependent manner. In contrast, it does not inhibit JAK3 kinase, confirming that **TZC10** act as a direct inhibitor of STAT3.

3.3.4 Induction of ROS generation and combination study

The mechanism of action of the TZC salts was further investigate determining the induction of ROS production in pancreatic cancer cell line, using hydrogen peroxide (H₂O₂) as positive control. Compounds were tested at a single concentration (10 μ M).

Salts with the free amino group and bearing electron-attracting substituent (**TZC7-TZC9**) induce ROS production in a time-dependent way, similarly to the positive control (Figure 22). Samples containing TZC compounds without the dye did not show any change in the fluorescent signal, confirming no endogenous fluorescence interfering the assay.

The mechanisms by which antitumor drugs induce death of cancer cells are different and include apoptosis, autophagy, necrosis and the non-apoptotic cell death ferroptosis.

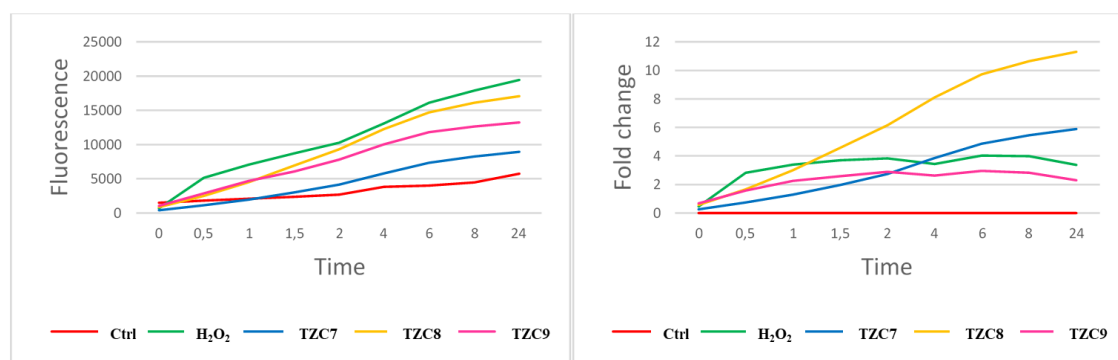


Figure 22. TZC salts induce ROS production in pancreatic cancer cells.

Therefore, an understanding of these mechanisms might be helpful to discover more convenient therapeutic strategies. To determine the cell death mechanism induced by treatment with TZC salts, a combination study was also performed, using the MTT assay. Cells were treated with **TZC7** and **TZC10** alone and in combination with an irreversible caspase inhibitor (z-VAD), a necroptosis inhibitor (Necrostatin-1), and the iron-chelator deferoxamine (DFO). As shown in Table 5, TZC derivatives might induce apoptosis, since in the presence of z-VAD, the antiproliferative activity of **TZC7** and **TZC10** is less potent than when used alone.

Table 5. Combination study. Determination of IC₅₀ values of **TZC7** and **TZC10** in combination with inhibitors of apoptosis, autophagy, and ferroptosis.

	TZC7	+ z-VAD (5μM)	+ z-VAD (10μM)	+ Nocr (10μM)	+ DFO (10μM)
IC₅₀ (μM)	4.7	6.4	9.1	5.0	8.6
	TZC24	+ z-VAD (5μM)	+ z-VAD (10μM)	+ Nocr (10μM)	+ DFO (10μM)
IC₅₀ (μM)	5.1	7.0	9.5	5.2	8.7

^a IC₅₀ values were determined by MTT assay after 72 h treatment.

3.4 Conclusion

In summary, TZC nucleus was identified as a scaffold for the development of potential STAT3 inhibitors, through rational functionalization. A small library of derivatives was built and their antiproliferative activity as well as the involvement of STAT3 signaling pathway in the mechanism of action were investigated. TZC salts with the free amino group, in particular **TCZ10**, exhibited excellent cytotoxicity against different cancer cell lines. It showed the best antiproliferative activity against pancreatic cancer cells, which expressed constitutively, activated STAT3. **TCZ10** blocks cell proliferation through direct inhibition of STAT3, targeting its SH2 domain and inhibiting phosphorylation at Y705 residue. Compounds **TCZ7**, **TCZ8** and **TCZ9** also induces ROS production in pancreatic cancer cells, suggesting the possible mechanism by which these derivatives exhibit their antiproliferative activity. Results from the combination assay suggest that TZC salts might induce apoptosis of cancer cells. Further investigations are still ongoing to confirm the mechanism of action of these new derivatives. Taken together, these results support the therapeutic potential of TZC salts for further development as promising direct STAT3 inhibitors for pancreatic cancer.

3.5 Experimental section

Chemistry

3.5.1 General experimental methods

All chemicals and reagents were purchased from Fisher or Sigma Aldrich and they were used without further purification. Reactions were monitored by thin-layer chromatography, performed on plates of silica gel (Merck 60F254, 0.2mm), and visualized under UV light at 254 and 366nm of wavelength. Reaction solutions were concentrated in a rotary evaporator (Büchi Rotavapor) under reduced pressure.

Purifications were performed by crystallization and chromatographic column on silica gel (Merck, 60, 230-400 mesh, 0.040-0.063 mm). Melting points were determined with a Gallenkamp 21374 apparatus. ¹H-NMR and ¹³C-NMR spectra were recorded on a Bruker AV-300 instrument, using deuterated solvents (DMSO-*d*₆ and CDCl₃) with tetramethylsilane (TMS) as internal standard. Chemical shift (δ) are reported in ppm. The multiplicities are denoted as follows: s, singlet; d, doublet; t, triplet; q, quartet; m, multiplet; bs, broad singlet. Multiplicities, coupling constants, reported as a *J* value in hertz, and number of protons are indicated parenthetically. Mass spectra data were determined after electron impact ionization (EI) at 70 eV with HP 5973MS spectrometer. Yields refer to purified products and are not optimized.

3.5.2 Synthesis

5,7-Diphenyl-[1,2,4]triazolo[1,5-a]pyrimidin-2-amine (**TZC1**). A solution of 2,5-diamino-triazole **1** (1.000 g; 10.09 mmol) and *trans*-chalcone **2** (2.017 g; 9.69 mmol) in *N,N*-dimethylformamide (DMF) (2 ml) was stirred and refluxed at 150-160°C, for 30 min. Then, the reaction was cooled at room temperature (rt). The solid was filtered under vacuum, using a Gooch filter, collected and washed with a mixture of methanol/acetone (1:1). The solid was further purified by recrystallization from methanol/acetone (1:1) to give the title compound as a light-yellow solid (2.343 g; 84%). **m.p.** 199.0-199.5°C. **¹H-NMR (CDCl₃) δ:** 8.22-8.17 (m, 2H); 8.09-8.04 (m, 2H); 7.60 (m, 3H); 7.51 (m, 3H); 7.44 (s, 1H); 4.91 (s, 2H). **¹³C-NMR (CDCl₃) δ:** 167.1, 159.6, 146.0, 136.7 (x2C), 129.1 (x2C), 128.9 (x2C), 127.4 (x2C), 105.0. **MS (EI):** *m/z* 287 [M]⁺.

N,N-Dimethyl-5,7-diphenyl-[1,2,4]triazolo[1,5-a]pyrimidin-2-amine (**TZC2**). A Solution of **TZC1** (40 mg; 0.139 mmol) and methyl iodide **3** (8.66 μl; 0.139 mmol) in tetrahydrofuran (THF) (2 ml) was stirred at rt for 1 h. Then, potassium carbonate **4** (17.32

mg; 0.125 mmol) was added to the solution and the reaction was kept at rt, overnight. The solution was diluted with dichloromethane, and the formed solid was filtered under vacuum, using a Gooch filter, collected and purified by chromatographic column (eluent: dichloromethane/methanol/ammonium hydroxide, 90:10:1). The pure compound was isolated as dark yellow needles (3.46 mg; 7.5%). **m.p.** 201-205.7°C (dec.). **¹H-NMR (Acetone-d₆)** δ : 8.55-8.48 (m, 3H); 8.33 (dd, 2H, J = 1.3-7.9 Hz); 7.78-7.60 (m, 6H); 4.25 (s, 3H); 3.38 (s, 3H). **MS (EI):** m/z 315 [M]⁺.

N-(5,7-diphenyl-[1,2,4]triazolo[1,5-*a*]pyrimidin-2-yl)acetamide (**TZC3**). A solution of **TZC1** (20 mg; 0.0696 mmol) and acetic anhydride **5** (174 μ l; 1.84 mmol) was stirred and refluxed at 140°C for 1.5 h. Then, the solvent was vacuum-evaporated and the residue was dissolved in distilled water (0.347 ml). The reaction mixture was stirred at rt, for 24 h. The formed solid was collected and purified by column chromatography (eluent: n-hexane/ethyl acetate, 1:1). The pure compound was isolated as white solid (6.78 mg; 26.2%). **m.p.** 119.0-119.5°C. **¹H-NMR (CDCl₃)** δ : 8.32-8.24 (m, 2H); 8.15-8.08 (m, 2H); 7.77 (s, 1H); 7.63 (dd, 3H, J = 1.7-16.7 Hz); 7.61 (dd, 3H, J = 2.5-17.2 Hz); 3.52 (s, 3H); 2.18 (s, 3H). **¹³C-NMR (CDCl₃)** δ : 171.9, 171.0, 162.3, 160.3, 155.5, 147.4, 136.0, 130.9, 129.6, 129.3, 129.2, 129.1, 128.7, 128.4, 128.3, 128.2, 127.9, 127.0, 106.6, 26.2, 25.3. **MS (EI):** m/z 329 [M]⁺.

1-Acetophenone-2-amino-5,7-diphenyl-[1,2,4]triazolo[1,5-*a*]pyrimidinium bromide (**TZC4**). A solution of **TZC1** (34 mg; 0.118 mmol) and 2-bromoacetophenone **6** (28 mg; 0.1419 mmol) in DMF (385 μ l) was stirred and refluxed at 120°C, for 1.5 h. Then, the reaction was cooled to rt and, subsequently, placed on ice (0°C) for 30 min. The solvent was evaporated under vacuum and the residue was washed with dichloromethane. The solid was further purified by recrystallization from dichloromethane, to give the titled compound as a yellow solid (48.5 g; 84.7%). **m.p.** 200-214°C (dec.). **¹H-NMR (DMSO)**

δ : 8.39 (s, 1H); 8.34 (d, 3H, J = 6.99 Hz); 8.22 (dd, 3H, J = 1.21-7.58 Hz); 8.16 (d, 3H, J = 7.74 Hz); 7.85-7.52 (m, 6H); 6.15 (s, 2H); 5.62 (s, 2H). $^{13}\text{C-NMR}$ (CDCl_3) δ : 189.9, 162.8, 156.7, 149.1, 147.3, 134.5, 134.2, 133.8, 132.6, 132.5, 130.0, 129.0, 128.9, 128.6, 128.3, 128.1, 127.9, 110.4, 49.8. **MS (EI)**: m/z 405 $[\text{M}]^+$.

1-Acetophenone-2-acetamide-5,7-diphenyl-[1,2,4]triazolo[1,5-a]pyrimidinium bromide (TZC5). A solution of **TZC4** (26 mg; 0.0536 mmol) and **5** (134 μl ; 1.415 mmol) was put in reaction following the synthetic method described for **TZC3**. Then, the solvent was vacuum-evaporated and the residue was dissolved in distilled water (268 μl). The obtained orange solid was collected and purified by column chromatography (eluent: n-hexane/ethyl acetate, 1:1). The pure compound was isolated as orange solid (11 mg; 38.8%). $^1\text{H-NMR}$ (DMSO) δ : 8.54-8.48 (m, 2H); 8.36-8.28 (m, 2H); 8.17 (s, 1H); 7.82-7.59 (m, 4H); 7.52- 7.31 (m, 6H); 6.84 (s, 2H); 2.09 (s, 3H).

5,7-Bis(4-methoxyphenyl)-[1,2,4]triazolo[1,5-a]pyrimidin-2-amine (TZC6). A solution of **1** (1 g; 10.09 mmol) and 4,4'-dimethoxy chalcone **7** (2.599 g; 9.69 mmol) in DMF (2 ml) was put in reaction following the synthetic method described for **TZC1**. The pure compound was isolated as yellow solid (1.37 g; 40.7%). **m.p.** 232.0-232.5°C. $^1\text{H-NMR}$ (DMSO) δ : 8.28 (dd, 4H, J = 8.93-17.4 Hz); 7.70 (s, 1H); 7.10 (dd, 4H, J = 8.94-20.49 Hz); 6.42 (s, 2H); 3.85 (d, 6H, J = 8.73 Hz). $^{13}\text{C-NMR}$ (DMSO) δ : 162.0, 161.6, 160.7, 156.7, 148.5, 128.7, 127.9, 127.9, 127.5, 123.1, 114.8, 114.8, 114.6, 114.4, 102.9, 58.8, 56.0. **MS (EI)**: m/z 348 $[\text{M}]^+$.

1-Acetophenone-2-amino-5,7-bis(4-methoxyphenyl)-[1,2,4]triazolo[1,5-a]pyrimidinium bromide (TZC7). A solution of **TZC6** (100 mg; 0.288 mmol) and **6** (68.5 mg; 0.3443 mmol) in DMF (939 μl) was put in reaction following the synthetic method described for **TZC4**. The pure compound was isolated as yellow solid (125.85 mg; 80%). **m.p.** 233-240°C (carbonize). $^1\text{H-NMR}$ (DMSO) δ : 8.55-8.16 (m, 5H); 7.82 (m, 1H); 7.69 (d, 2H,

$J=7.37$ Hz); 7.25 (d, 2H, $J=8.85$ Hz); 7.09 (d, 2H, $J=9.0$ Hz); 6.12 (s, 2H); 3.96 (s, 3H), 3.85 (s, 3H). $^{13}\text{C-NMR}$ (DMSO) δ : 190.9, 163.4, 163.2, 161.1, 156.3, 148.3, 147.3, 135.1, 134.1, 132.9, 130.7, 129.5, 129.1, 126.9, 120.5, 115.1, 114.7, 109.2, 56.2, 56.1, 49.6. **MS (EI)**: m/z 466 $[\text{M}]^+$.

1-(4-fluoroacetophenone)-2-amino-5,7-bis(4-methoxyphenyl)-[1,2,4]triazolo[1,5-a]pyrimidinium bromide (TZC8). A solution of **TZC6** (100 mg; 0.288 mmol) and 2-bromo-4'-fluoro-acetophenone **8** (74.7 mg; 0.344 mmol) in DMF (939 μl) was put in reaction following the synthetic method described for **TZC4**. The pure compound was isolated as a yellow solid (159 mg; 98%). **m.p.** 195.0-195.5°C. $^1\text{H-NMR}$ (DMSO) δ : 8.46-8.40 (m, 2H); 8.39-8.33 (m, 2H); 8.32-8.23 (m, 4H); 8.20 (s, 1H); 7.58-7.48 (m, 2H); 7.30-7.20 (m, 2H); 7.15-7.07 (m, 2H); 6.06 (s, 2H); 5.97 (bs, 2H); 3.93 (s, 3H); 3.87 (s, 3H). **MS (EI)**: m/z 484 $[\text{M}]^+$.

1-(4-chloroacetophenone)-2-amino-5,7-bis(4-methoxyphenyl)-[1,2,4]triazolo[1,5-a]pyrimidinium bromide (TZC9). A solution of **TZC6** (100 mg; 0.288 mmol) and 2-bromo-4'-chloro-acetophenone **9** (80.3 mg; 0.344 mmol) in DMF (939 μl) was put in reaction following the synthetic method described for **TZC4**. The pure compound was isolated as a yellow-orange solid (51 mg; 30.5%). **m.p.** 215.5-216.1°C. $^1\text{H-NMR}$ (DMSO) δ : 8.42-8.32 (m, 4H); 8.24-8.15 (m, 3H); 7.82-7.73 (m, 2H); 7.27 (d, 2H); 7.17-7.09 (m, 2H); 7.01 (d, 2H); 6.15 (s, 2H); 5.90 (bs, 2H); 3.87 (s, 6H). **MS (EI)**: m/z 501 $[\text{M}]^+$.

1-(4-methylacetophenone)-2-amino-5,7-bis(4-methoxyphenyl)-[1,2,4]triazolo[1,5-a]pyrimidinium bromide (TZC10). A solution of **TZC6** (100 mg; 0.288 mmol) and 2-bromo-4'-methyl-acetophenone **10** (73.3 mg; 0.344 mmol) in DMF (939 μl) was put in reaction following the synthetic method described for **TZC4**. The pure compound was isolated as a yellow-orange solid (32 mg; 20%). **m.p.** 252.5-253.0°C. $^1\text{H-NMR}$ (DMSO)

δ : 8.44-8.33 (m, 6H); 8.22 (s, 1H); 8.09 (d, 2H); 7.50 (d, 2H); 7.26 (d, 2H); 7.11 (d, 2H); 6.02 (s, 2H); 5.94 (bs, 2H); 3.95 (s, 3H); 3.86 (s, 3H). **MS (EI)**: m/z 480 [M]⁺.

1-Acetophenone-2-acetamide-5,7-bis(4-methoxyphenyl)-[1,2,4]triazolo[1,5-a]pyrimidinium bromide (TZC11). A solution of **TZC7** (50 mg; 0.0915 mmol) and **5** (228 μ l; 2.416 mmol) was put in reaction following the synthetic method described for **TZC3**. Then, the solvent was vacuum-evaporated and the residue was dissolved in distilled water (457 μ l). The obtained yellow solid was collected and purified by column chromatography (eluent: dichloromethane/methanol 9:1). The pure compound was isolated as yellow solid (41 mg; 76.1%). **¹H-NMR (DMSO) δ** : 8.53 (d, 2H, J = 8.94 Hz); 8.37 (d, 1H, J = 9.07 Hz); 8.28 (s, 1H); 8.21 (d, 2H, J = 7.63 Hz); 7.73-7.62 (m, 4H); 7.27 (d, 2H, J = 8.92 Hz); 7.11 (d, 2H, J = 8.89 Hz), 5.81 (s, 2H), 5.78 (s, 1H), 3.96 (s, 3H), 3.88 (s, 3H), 2.0 (s, 3H). **¹³C-NMR (DMSO) δ** : 191.0, 162.0, 146.0, 134.3, 133.2, 131.9, 130.8, 129.5, 129.0, 128.4, 128.4 (x2C), 127.9, 127.3, 126.1, 114.6, 113.5 (x2C), 55.6, 55.5, 54.5 (x2C), 54.4, 25.7.

1-Acetophenone-2-benzamide-5,7-diphenyl-[1,2,4]triazolo[1,5-a]pyrimidinium bromide (TZC12). A solution of **TZC4** (45 mg; 0.093 mmol), benzoyl chloride **11** (8.97 μ l; 0.077 mmol) and triethylamine **12** (21.4 μ l; 0.155 mmol) in dry THF (1 ml) was stirred at rt, under argon atmosphere, overnight. Then, the solvent was vacuum-evaporated and the yellow residue was purified by column chromatography (eluent: dichloromethane/methanol 9:1). The titled compound was isolated as a yellow solid (17 mg; 37.1%). **¹H-NMR (CDCl₃) δ** : 8.37-8.31 (m, 2H); 8.16-8.06 (m, 6H); 7.81 (s, 1H); 7.72-7.46 (m, 10H); 7.37- 7.30 (m, 2H); 7.28-7.21 (m, 2H); 5.85 (s, 1H). **¹³C-NMR (DMSO) δ** : 191.0, 164.0, 157.0, 147.0, 134.3 (x2C), 132.8 (x2C), 130.0 (x2C), 129.2 (x2C), 129.1 (x2C), 128.4 (x4C), 127.8 (x2C), 127.6 (x2C), 54.0 **MS (EI)**: m/z 510 [M]⁺.

1-Acetophenone-2-benzamide-5,7-bis(4-methoxyphenyl)-[1,2,4]triazolo[1,5-a]

pyrimidinium bromide (**TZC13**). A solution of **TZC7** (42 mg; 0.0769 mmol), **11** (7.43 μ l; 0.064 mmol) and **12** (17.7 μ l; 0.128 mmol) in dry THF (1 ml) was put in reaction following the synthetic method described for **TZC12**. The yellow residue was purified by column chromatography (eluent: dichloromethane/methanol 9:1). The titled compound was isolated as a yellow solid (30%). ¹H-NMR (CDCl₃) δ : 8.37-8.31 (m, 2H); 8.16-8.06 (m, 6H); 7.81 (s, 1H); 7.72-7.46 (m, 10H); 7.37- 7.30 (m, 2H); 7.28-7.21 (m, 2H); 5.85 (s, 1H), 3.73 (s, 6H).

1-Acetophenone-2-[N-(2-methoxybenzyl)amino]-5,7-diphenyl-[1,2,4]triazolo[1,5-a]pyrimidinium bromide (**TZC14**). A solution of **TZC4** (65 mg; 0.134 mmol) and potassium *tert*-butoxide **13** (15 mg; 0.134 mmol) in dry THF (2 ml), was stirred at 0°C, under argon atmosphere. A solution of 2-methoxy-benzyl chloride **14** (18.7 μ l; 0.134 mmol) was added, drop by drop, to the reaction mixture and stirred at rt, overnight. Then, the solvent was evaporated under vacuum and the dark red oily residue was purified by column chromatography (eluent: n-hexane/ethyl acetate 1:1). The pure compound was isolated as a red solid (31 mg; 38.2%). ¹H-NMR (CDCl₃) δ : 8.38-8.33 (m, 2H); 8.02-7.95 (m, 3H); 7.94 (s, 1H); 7.81 (s, 1H); 7.70-7.63 (m, 4H); 7.53 (d, 2H, *J*= 3.34 Hz); 7.50 (d, 1H, *J*= 2.2 Hz), 7.49-7.42 (m, 3H), 7.39-7.35 (m, 1H), 7.28- 7.20 (m, 1H), 7.19-7.15 (m, 1H), 7.05-7.0 (d, 1H, *J*= 8.3 Hz), 6.85-6.78 (m, 1H), 4.82 (s, 2H), 4.0 (s, 3H). ¹³C-NMR (CDCl₃) δ : 191.0, 167.0, 156.0, 155.0, 146.0, 136.0, 135.0, 133.0, 129.0 (x2C), 128.7 (x2C), 128.2 (x2C), 128.1 (x2C), 127.6, 127.2, 126.7, 126.2, 120.0, 114.0, 111.5, 104.0, 55.0, 52.0, 36.0.

1-Acetophenone-2-[N-(2-methoxybenzyl)amino]-5,7-bis(4-methoxyphenyl)-[1,2,4]triazolo[1,5-a]pyrimidinium bromide (**TZC15**). A solution of **TZC7** (65 mg; 0.119 mmol) and **13** (13.3 mg; 0.119 mmol) in dry THF (1 ml) was put in reaction following the synthetic method described for **TZC14**. Then **14** (16.6 μ l; 0.119 mmol) was added to

the reaction mixture. The orange oily residue was purified by column chromatography (eluent: n-hexane/ethyl acetate 1:1). The pure compound was isolated as an orange solid (26 mg; 32.3%). **¹H-NMR (CDCl₃) δ:** 8.44-8.38 (m, 2H); 8.29-7.90 (m, 4H); 7.68 (s, 1H); 7.51-7.41 (m, 3H); 7.20- 7.11 (m, 4H); 7.05-6.97 (t, 3H, *J*= 7.89 Hz); 6.87-6.78 (m, 1H), 4.80 (s, 2H), 4.01-3.90 (m, 9H). **¹³C-NMR (CDCl₃) δ:** 191.0, 167.0, 160.0 (x2C), 156.0, 146.0, 136.0, 133.0, 131.4 (x2C), 130.5 (x2C), 128.6, 128.4, 128.0 (x2C), 125.0, 119.8, 114.9, 55.5 (x2C), 52.0, 35.5.

1-Acetophenone-2-[N-(3-chlorobenzyl)amino]-5,7-diphenyl-[1,2,4]triazolo[1,5-a]pyrimidinium bromide (TZC16). A solution of **TZC4** (60 mg; 0.124 mmol) and **13** (13.9 mg; 0.124 mmol) in dry THF (1 ml) was put in reaction following the synthetic method described for **TZC14**. Then, 3-chloro-benzyl chloride **15** (15.7 μl; 0.124 mmol) was added to the reaction mixture. The oily residue was purified by column chromatography (eluent: n-hexane/ethyl acetate 1:1). The pure compound was isolated as a yellow solid (12 mg; 16%). **¹H-NMR (CDCl₃) δ:** 8.32-8.26 (m, 2H); 8.20-8.15 (m, 2H); 7.97 (d, 2H, *J*=7.29 Hz); 7.91 (s, 1H); 7.80 (s, 1H); 7.62-7.57 (m, 3H); 7.54-7.48 (m, 3H), 7.46-7.40 (m, 2H), 7.37 (d, 2H, *J*=7.95 Hz), 7.28 (d, 2H, *J*=7.32 Hz), 7.21-7.18 (m, 5H), 4.71 (bs, 1H).

1-Acetophenone-2-[N-(3-chlorobenzyl)amino]-5,7-bis(4-methoxyphenyl)-[1,2,4]triazolo[1,5-a]pyrimidinium bromide (TZC17). A solution of **TZC7** (64 mg; 0.117 mmol) and **13** (13.1 mg; 0.117 mmol) in dry THF (1 ml) was put in reaction following the synthetic method described for **TZC14**. Then, **15** (14.9 μl; 0.117 mmol) was added to the reaction mixture. The oily residue was purified by column chromatography (eluent: n-hexane/ethyl acetate 1:1). The pure compound was isolated as a brown solid (24 mg; 30.1 %). **¹H-NMR (CDCl₃) δ:** 8.45-8.29 (m, 1H); 8.26-8.16 (m, 2H); 8.14-8.08 (m, 1H); 8.06-7.99 (m, 1H); 7.65-7.57 (m, 1H); 7.55-7.40 (m, 3H); 7.37 (s, 1H), 7.32-7.27 (m, 5H),

7.18-7.01 (m, 5H), 4.78- 4.60 (m, 2H), 4.0-3.81 (s, 6H). ¹³C-NMR (CDCl₃) δ: 195.6, 169.2 (x2C), 168.3 (x2C), 157.0, 146.0, 142.2, 141.3, 135.1, 134.2, 126.1 (x2C), 125.2 (x2C), 122.7, 122.0, 121.8, 121.1 (x2C), 105.5, 56.0 (x2C), 52.0, 45.0.

1-Acetophenone-2-[N-(acetophenone)amino]-5,7-diphenyl-[1,2,4]triazolo[1,5-a]pyrimidinium bromide (TZC18). A solution of **TZC1** (100 mg; 0.348 mmol) and **6** (173.2 mg; 0.87 mmol) in DMF (2.4 ml) was put in reaction following the synthetic method described for **TZC4**. The pure compound was isolated as a yellow solid (25 mg; 12%). ¹H-NMR (DMSO) δ: 8.62 (s, 1H); 8.25-8.58 (m, 8H); 7.65-9.75 (m, 12H); 6.24 (s, 2H); 5.85 (s, 2H). MS (EI): *m/z* 406 [M]⁺.

1-Acetophenone-2-[N-(acetophenone)amino]-5,7-bis(4-methoxyphenyl)-[1,2,4]triazolo[1,5-a]pyrimidinium bromide (TZC19). A solution of **TZC6** (100 mg; 0.288 mmol) and **6** (143.3 mg; 0.719 mmol) in DMF (2.0 ml) was put in reaction following the synthetic method described for **TZC4**. The pure compound was isolated as a yellow solid (25 mg; 13%). ¹H-NMR (DMSO) δ: 8.40-8.52 (m, 8H); 8.23-8.35 (m, 3H); 7.95-7.87 (m, 2H); 7.82-7.73 (m, 2H); 7.35 (d, 2H); 7.19 (d, 2H); 6.18 (s, 2H); 5.82 (s, 2H); 3.25 (s, 6H). MS (EI): *m/z* 466 [M]⁺.

1-(4-Methylacetophenone)-2-[N-(4-methylacetophenone)amino]-5,7-diphenyl-[1,2,4]triazolo[1,5-a]pyrimidinium bromide (TZC20). A solution of **TZC1** (100 mg; 0.348 mmol) and **2 10** (185.4 mg; 0.87 mmol) in DMF (2.4 ml) was put in reaction following the synthetic method described for **TZC4**. The pure compound was isolated as a yellow-orange solid (20 mg; 9%). ¹H-NMR (DMSO) δ: 8.39-8.26 (m, 4H); 8.13 (d, 2H); 8.0 (s, 1H); 7.89 (d, 2H); 7.95-7.67 (m, 3H); 7.64-7.55 (m, 3H); 7.48 (d, 2H); 7.37 (d, 2H); 6.05 (s, 2H); 5.56 (s, 2H); 2.50 (s, 3H); 2.48 (s, 3H). MS (EI): *m/z* 420 [M]⁺.

1-(4-Methylacetophenone)-2-[N-(4-methylacetophenone)amino]-5,7-bis(4-methoxyphenyl)-[1,2,4]triazolo[1,5-a]pyrimidinium bromide (TZC21). A solution of **TZC6** (100

mg; 0.288 mmol) and **10** (153.3 mg; 0.719 mmol) in DMF (2.0 ml) was put in reaction following the synthetic method described for **TZC4**. The pure compound was isolated as a yellow solid (20 mg; 10%). **¹H-NMR (DMSO) δ** : 8.38 (d, 2H); 8.30 (d, 2H); 8.18 (s, 1H); 8.13 (d, 2H); 8.03-7.77 (m, 6H); 7.49 (d, 2H); 7.22 (d, 2H); 7.07 (d, 2H); 6.03 (s, 2H); 3.98 (s, 3H); 3.85 (s, 3H); 2.68 (s, 3H); 2.50 (s, 3H). **MS (EI)**: m/z 480 [M]⁺.

Biology

3.5.3 Cell culture. Different cancer cell lines (Mia PaCa-2, MDA MB-231, U87G, HCT116 p53^{+/+}, SKOV3 WT and SKOV3 STAT3 KO) were used. All cell lines were grown at 37°C in a humidified incubator with 5% CO₂, and maintained in RPMI-1640 medium supplemented with 10% FBS. For subculture and counting, cells were washed with DPBS (Gibco) without calcium or magnesium and incubated with 0.25% trypsin-EDTA solution (Gibco) for 2-5 min. Then they were neutralized with full medium, centrifuged, re-suspended with culture medium and counted by Countess II FL.

Cells were regularly checked for *Mycoplasma* contamination.

3.5.4 Growth inhibition assay. Growth inhibition assay was assessed by MTT assay. Cells were seeded in 180 μ L medium in 96-well plates. After overnight attachment at 37°C in 5% CO₂, 20 μ L of medium containing sequential dilutions of compounds, ranging from 30 to 0.12 μ M, were added to the wells, in duplicate. DMSO was used as negative control. Cells were incubated in the presence of compounds for 72h. 20 μ L of MTT solution in DPBS (3mg/mL) was added and cells were incubated for further 3-4h. Mitochondrial reductase enzymes in viable cells reduce the yellow tetrazolium MTT in its formazan, which has a purple color when dissolved in DMSO. Media was finally replaced with 125 μ L of DMSO and cell viability was determined by measuring absorbance of the colored well at 570 nm, using a spectrophotometer. Percent cell growth inhibition was expressed

as $(1-A/C) \times 100\%$ (A and C are the absorbance values from experimental and control cells, respectively). IC₅₀ values were determined from nonlinear regression analysis of log (drug concentration) vs. percentage of cell growth inhibition, using Prism 7.0 SD was calculated based on the IC₅₀ values from three independent experiments.

3.5.5 Colony formation assay. Cells were seeded in 180 μ L medium in 96-well plates and allowed to attach overnight. 20 μ L of medium containing compounds were then added in duplicate. DMSO was used as negative control. After 24h treatment, compound-containing medium was carefully removed and replaced with 200 μ L of fresh medium 10% FBS. Cells were kept in culture until visible colonies were formed in control wells. Then, medium was removed and colonies were stained with 50 μ L of crystal violet solution for 30min at rt. Finally, colonies were washed 3 times with 100 μ L of distilled water to remove excessive stain and let dry overnight under hood. Colonies were imaged by Odyssey® CLx Imaging System (LI-COR Biosciences, Lincoln, NE).

3.5.6 Wound healing (scratch) assay. Cells were seeded in 96-well plates, at a high density to have 70-80% confluency after overnight attachment, and then starved for 24h. Using 200 μ L tip, every well was gently and slowly scratched and washed twice. Fresh medium, containing compounds, was added and cells were grown at least 24h, until the wound in control wells was closed. Finally, medium was removed and cells were stained with 50 μ L of crystal violet solution for 30min at rt. Finally, colonies were washed 3 times with 100 μ L of distilled water to remove excessive stain and let dry overnight under hood. Cells were imaged by Odyssey® CLx Imaging System (LI-COR Biosciences, Lincoln, NE).

3.5.7 Fluorescence polarization assay. FP assay analyzes binding of small molecules to the SH2 domain of STAT3. The final concentration of buffer components was 10mM HEPES (pH 7.5), 1mM EDTA, 0.1% Nonidet P-40, 50mM NaCl, and 10% DMSO. The

sequence of peptide was: STAT3, 5-carboxyfluorescein-GY(PO₃H₂)LPQTV-NH₂. Purified STAT3 was used at 150 nM. STAT3 was incubated with tested compounds in 384-well plates for 30 min at rt; the final volume per well was 20µL. Polarization measurements were conducted at 37°C using a microplate reader with the fluorescence polarization module.

3.5.8. Western blot. Mia PaCa-2 cells were seeded into 6-well plates and allowed to attach overnight before the addition of the proper dilution of compound. After 4h treatment, cells were washed with DPBS and lysated with RIPA lysis buffer, in the presence of protease and phosphatase inhibitors. Cell lysates were sonicated and centrifuged for 10min at 4°C. The supernatant was collected and the protein concentration of whole-cell lysate was determined by BCA protein assay kit (Thermo Scientific). Proteins were resolved in 10% SDS/PAGE and electroblotted onto transfer nitrocellulose membrane (Immobilon®-FL). After blocking with TBS blocking buffer (Thermo Scientific), membranes were probed with pSTAT3 primary antibody (Signaling; 1:1000) in 5% BSA (EMD Millipore corporation) in TBST (Tris-buffered saline, 0.1% Tween 20) at 4°C overnight. Then, the membrane was washed and incubated with secondary antibody. The membrane was imaged by Odyssey® CLx Imaging System (LI-COR Biosciences, Lincoln, NE).

3.5.9 ROS detection assay. DCFDA-Cellular Reactive Oxygen Species Detection Assay Kit uses the cell permeant reagent 2',7'-dichlorofluorescein diacetate (DCFDA), a fluorogenic dye able to measure ROS activity within the cell. After diffusion into the cell, DCFDA is deacetylated by cellular esterases to a non-fluorescent compound, which is later oxidized by ROS into 2',7'-dichlorofluorescein (DCF). DCF is a highly fluorescent compound which can be detected by fluorescence spectroscopy with maximum excitation and emission spectra of 495 nm and 529 nm respectively.

Cells were detached with 0.05% trypsin-EDTA, neutralized, centrifuged and resuspended in RPMI-1640 media without phenol red. The cell suspension was treated with 20 μ M DCFDA and incubated for 30-45 min at 37°C in the dark. Then, cells were centrifuged again and washed with cell culture media to remove excess probe. After washing, cells were seeded in clear bottom-black wall-384-well microplate and incubated for 30-45 min at 37°C in the dark and treated with compounds at designed concentrations. The fluorescent signals were read at 493 nm/523 nm for ROS detection on a fluorescence plate reader at regular time points.

3.5.10 Combination assay. Combination assay was assessed by MTT assay as stated before. Cells were seeded in 180 μ L medium in 96-well plates and incubated at 37°C and 5% CO₂ overnight. For the combination therapies, cells were pre-treated with z-VAD and Necrostatin-1 to designed concentrations 1 h prior to the selected compounds. On the contrary, DFO was added to the cells immediately before the selected compounds. They were added to the well in sequential dilutions of compounds, ranging from 30 to 0.12 μ M, in duplicate. DMSO was used as negative control. Cells were incubated in the presence of compounds for 72h at 37°C and 5% CO₂. The MTT assay was performed as stated above.

CHAPTER 4:

**Design, synthesis, and experimental validation of 4-methyl
substituted 2,6-di-*tert*-butylphenol derivatives**

4.1 Design and synthesis of DTP derivatives

Another promising scaffold, selected for the development of inhibitors of STAT3 signal, is the DTP framework. As shown in Figure 23, derivatives containing various heterocyclic moieties were designed and synthesized.

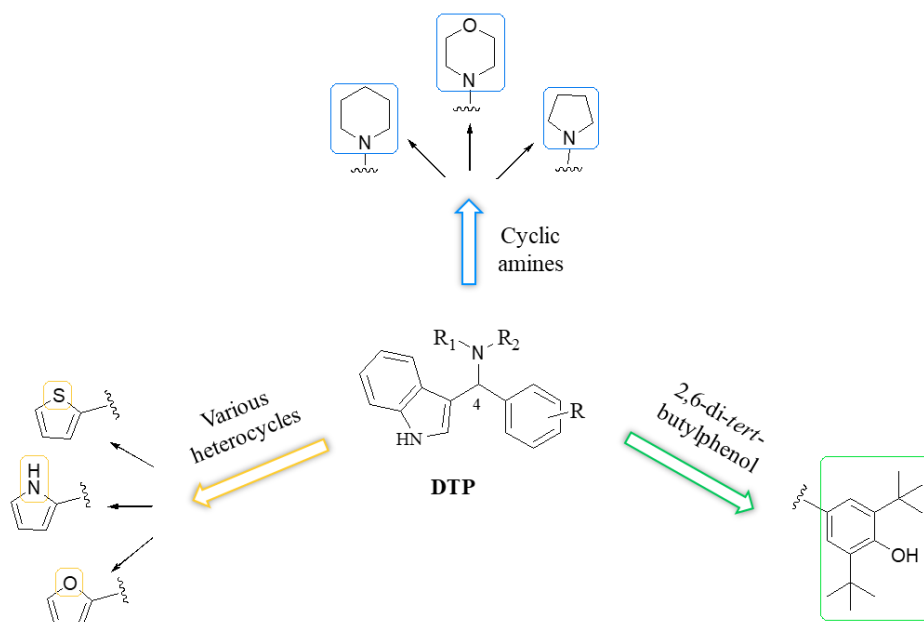
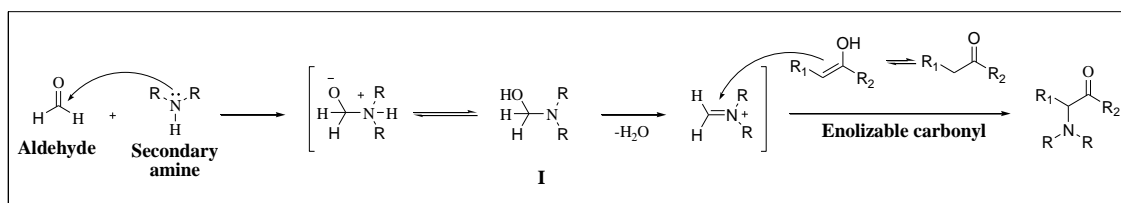


Figure 23. Design of DTP derivatives.

4.2 Chemistry

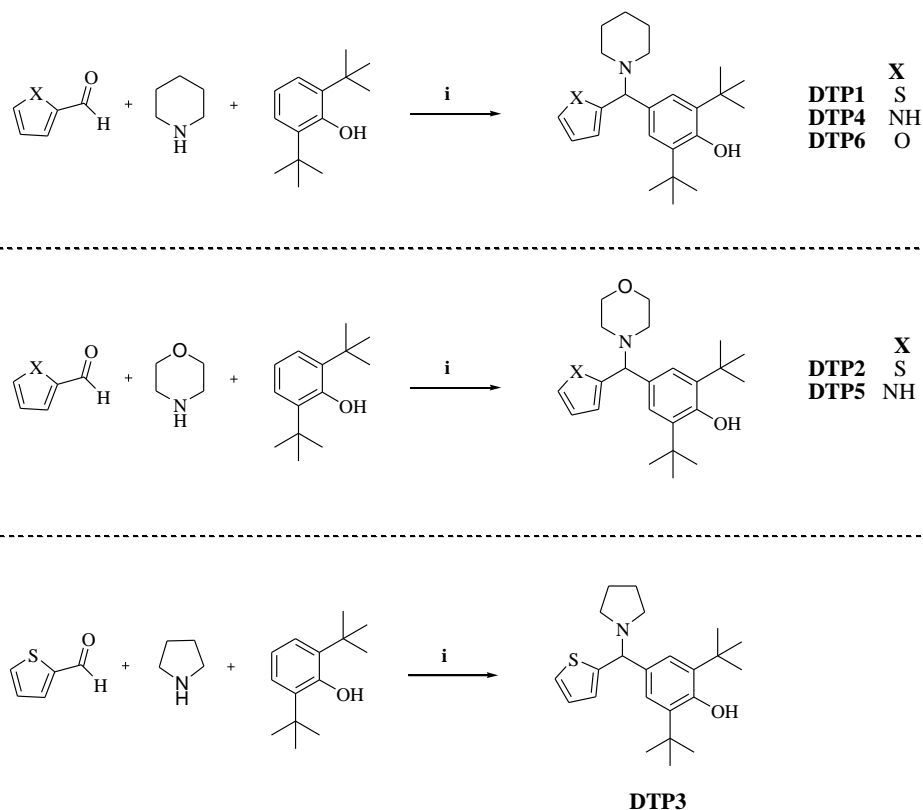
The chemical approach to synthesize DTP derivatives was a catalyst-free Mannich-type reaction in mild conditions (Box 3).



Box 3. Mechanism of Mannich reaction.

The mechanism involves a reaction between an aldehyde with a secondary amine and an enolizable carbonyl compound.

According to Scheme 5, the DTP derivatives were obtained through a three-component reaction of heterocyclic aldehydes with various aliphatic cyclic amines and 2,6-di-*tert*-butylphenol, in dry THF as solvent. The presence of various aliphatic cyclic amines did not interfere with the reaction, while the use of thiophene-2-carbaldehyde led to less by-products, compared to the use of 1*H*-pyrrole-2-carbaldehyde and furan-2-carbaldehyde.



Scheme 5. Reagents and conditions.

i) heterocyclic aldehyde (1.05 eq.), aliphatic cyclic amine (2.31 eq.), 2,6-di-*tert*-butylphenol (1 eq.), dry THF, 110°C, inert atmosphere.

4.3 Biological evaluation

4.3.1 Antiproliferative activity of DTP derivatives

The *in vitro* antiproliferative activity of the DTP derivatives was determined against different human cancer cell lines, including pancreatic (Mia PaCa-2), breast (MDA-MB0-

231), brain (U87G), colorectal (HCT116 p53^{+/+}), and ovarian (OVCAR-8) cancers, by MTT assay, using gemcitabine as positive control.

Based on the MTT results a SAR study was started (Figure 24).

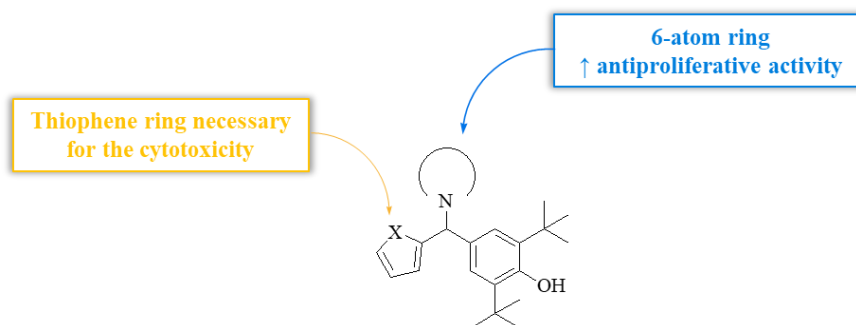


Figure 24. Structure-activity for DTP derivatives.

Derivatives with furan and pyrrole substituents did not inhibit the proliferation of cancer cells. On the contrary, all derivatives containing the thiophene substituent ring (**DTP1-3**) showed moderate antiproliferative activity, with IC₅₀ values in the micromolar range (Table 6).

Table 6. Antiproliferative activity of DTP derivatives against pancreatic, breast, brain, and colorectal cancer cell lines.

Composund	IC ₅₀ (μM) ^a				
	Mia PaCa-2	MDA-MB-231	U87MG	HCT116 p53 ^{+/+}	OVCAR-8
DTP1	5.0 ± 0.3	8.7 ± 0.1	8.5 ± 0.3	11.1 ± 0.5	3.4 ± 0.4
DTP2	5.1 ± 0.2	9.7 ± 0.3	8.8 ± 0.3	13.3 ± 0.6	3.8 ± 0.6
DTP3	7.0 ± 0.9	9.7 ± 0.3	18.3 ± 0.8	19.3 ± 0.6	6.9 ± 0.9
DTP4	> 30	> 30	> 30	> 30	> 30
DTP5	> 30	> 30	> 30	> 30	> 30
DTP6	> 30	> 30	> 30	> 30	> 30
Gemcitabine^b	2.0 ± 0.3	2.8 ± 0.9	3.9 ± 1.7	2.0 ± 0.6	2.4 ± 0.3

^a IC₅₀ values were determined by MTT assay after 72 h treatment. The data are shown as the mean ± standard deviation (SD), n=3.

^b Gemcitabine was used as a positive control.

It is important to note that **DTP1-3** exhibited the best antiproliferative activity against the pancreatic and ovarian cancer cell line, which expresses increased levels of both STAT3 and PDI, supporting cell survival and proliferation. (Xu et al. 2014)

To investigate whether STAT3 signaling pathway is involved in the mechanism of action of DTP derivatives, they were tested against engineered cell lines SKOV3 WT and SKOV3 STAT3 KO, and the results are shown in Table 7. Again, thiophene derivatives were the only active compounds, in particular against the wild-type cell line, suggesting that they may inhibit cell proliferation by inhibiting STAT3 signaling pathway.

DTP1-3 derivatives also inhibited the colony formation and migration of pancreatic cancer cells (Figure 19 and 20).

Table 7. Antiproliferative activity of DTP derivatives against engineered ovarian cancer cell lines.

Compound	IC ₅₀ (μM)	
	SKOV3 WT	SKOV3 STAT3 KO
DTP1	29.2	44.2
DTP2	28.1	35.8
DTP3	40.9	39.2
Stattic ^b	5.1 ± 0.4	9.8 ± 0.9

^a IC₅₀ values were determined by MTT assay after 72 h treatment.

^b Stattic was used as a positive control.

4.3.2 Direct inhibition of STAT3 signal

All the designed DTP derivatives were tested in the FP assay to evaluate their binding to the SH2 domain of STAT3. The assay was performed at 37°C, using Stattic as positive control. Compounds were initially tested at two different concentrations (50μM and 10μM) and the IC₅₀ values were then determined.

As shown in Table 8, some derivatives did not bind to the protein, whereas others showed endogenous fluorescence. **DTP1** slightly bind to the SH2 domain of STAT3 compared to the positive control. Although **DTP1** showed a weak binding to the SH2 domain of STAT, this protein may not be its main target.

Table 8. Binding of DTP derivatives to the SH2 domain of STAT3, using FP assay.

Compound	% inhibition (50 μ M)	% inhibition (10 μ M)	IC ₅₀ (μ M)
Stattic	68.5	23.7	28.0
DTP1	37.5	9.2	67.0
DTP2	35.3	14.1	>100
DTP3	24.8	9.7	>100
DTP4	8.8	6.1	fluorescente
DTP5	37.9	23.6	fluorescente
DTP6	23.6	16.5	>100

4.3.3 Inhibition of the reductase activity of PDI

Like STAT3, increasing evidences indicate that protein disulfide isomerase (PDI) is involved in both physiology and pathophysiology of cells and it is involved in the survival and proliferation of cancer cells. Therefore, PDI is another attracting target in the development of anticancer drugs. It is a member of the thioredoxin superfamily of redox enzymes (Figure 25). PDI is a multifunctional protein, acting as a protein folding catalyst and as a chaperone in the endoplasmic reticulum. The modulation of PDI activity with function-specific molecules may have a therapeutic effect in various diseases, including cancer. A wide range of drugs, such as antibiotics, estrogen, polyphenols, and heterocyclic compounds, have been found to modulate PDI activity.

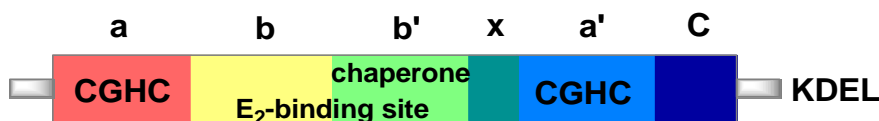


Figure 25. Domain structure of PDI.

PDI is a soluble 55-kDa protein with four tandem thioredoxin-like domains, namely **a**, **b**, **b'**, **a'**. The homologous **a** and **a'** domains contain the catalytically active site of PDI, that consists of a CGHC (Cys-Gly-His-Cys) motif. The cysteines can either exist in an intramolecular disulfide (oxidized PDI) or in the dithiol form (reduced PDI). The **b** and **b'** domains link the active site domains and assist in the binding of protein substrates. Between the **b'** and the **a'** domains there is a short x-linker interdomain region, responsible for the U-shape structure of PDI. The acidic C-terminus of PDI is followed by an endoplasmic reticulum (ER) retrieval signal, KDEL.

Recent studies have suggested that PDI can bind small molecules containing, for example, a phenolic structure, including endogenous hormones like estrogen (E_2). In particular, E_2 forms a H-bond with the imidazole ring of a histidine residue (H256) in the E_2 -binding site of PDI, located to a hydrophobic pocket between the **b** and the **b'** domains of the protein. On the other hand, propionic acid carbamoyl methyl amide-31 (PACMA-31), bearing specific substituents in critical positions, showed anticancer activity in human ovarian cancer, both *in vitro* and *in vivo*, through irreversible inhibition of PDI, by forming a covalent bond (C-S) with the cysteine residues in the active site. (Xu *et al.* 2014)

As shown in Figure 26, DTP derivatives present structural similarity with the known PDI modulators E_2 and PACMA-31. Based on the MTT and FP assays results, the ability of the best DTP derivatives to inhibit the reductase activity of PDI was investigated, using the insulin turbidimetry assay. In the presence of dithiothreitol (DTT), PDI catalyzes the reduction of insulin, which aggregates and turbidimetry is monitored using a spectrophotometer. Reductase activity of PDI was then assayed by measuring the reduction of insulin, in the presence of DTP derivatives. PACMA-31 was used as positive control.

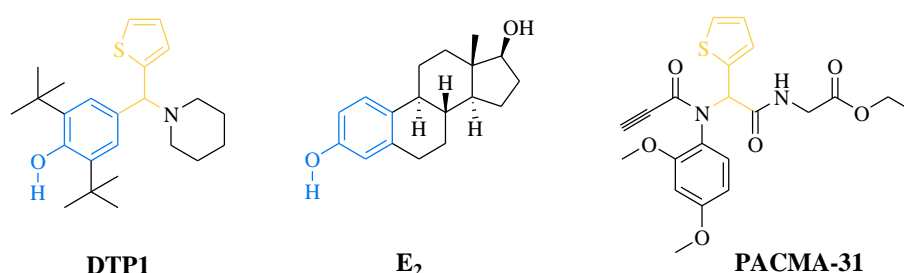


Figure 26. Chemical structures of DTP derivatives and known PDI modulators.

As reported in Table 9, in a primary screening, all the compounds were tested at a single concentration (100 μ M), showing a good inhibition of PDI reductase activity (inhibition

> 80%). Subsequently, dose-response curves and IC₅₀ values were calculated. DTP derivatives inhibited PDI in a dose-dependent manner; in particular, piperidine and morpholine derivatives were the most potent, with IC₅₀ lower than 2 μM (Figure 27).

Table 9. Inhibition of PDI reductase activity (expressed in %) by DTP derivatives.

Compound	% inhibition (100 μM)	IC ₅₀ (μM)
PACMA-31	80.5	10.0 ± 0.10
DTP1	98.5	1.51 ± 0.09
DTP2	97.5	1.69 ± 0.22
DTP3	82.3	4.17 ± 0.40

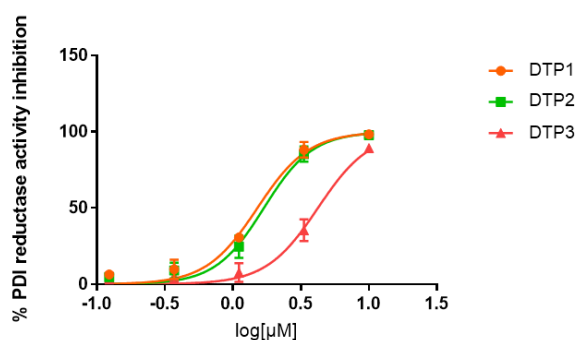


Figure 27. Dose-response curves of DTP derivatives.

4.4 Conclusion

Drugs commonly exhibit a therapeutic effect by targeting a specific molecular mechanism. In drug discovery, it is important a complete knowledge of the specific disease to treat. The first step is to identify single molecular targets and validate their relevance to the human disease, followed by the identification of specific chemical-based small molecule modulators or inhibitors of the central target. The main goal of using a target-specific drug is to inhibit a molecular target, mostly receptors or enzymes, which plays an essential role in the disease mechanism of interest. Theoretically, targeting a single molecular mechanism should be sufficient to achieve a significant therapeutic

effect; but single-target drugs often have a poor therapeutic impact, because of the tangle of molecular mechanisms involved in the development of the disease. Then, they may not be completely efficacious in treating complex diseases like cancers. Recently, drug discovery is moving from the design of single-target to multi-target drugs. Drugs targeting multiple targets at the same time might be more efficacious and less suitable to resistance. Therefore, the multi-target approach can be particularly beneficial in treating cancers. (*Sestito et al. 2017*)

DTP was identified as potential scaffold for the development of STAT3 inhibitors. A small library of derivatives was built through rational functionalization. The antiproliferative activity of the new DTP derivatives was evaluated in a panel of human cancer cell lines. The involvement of STAT3 signaling pathway in their mechanism of action were investigated. Thiophene derivatives (**DTP1-3**) mainly inhibited the proliferation of human ovarian cancer cells, which express high levels of both STAT3 and PDI. Although **DTP1** slightly binds to the SH2 domain of STAT3 protein, it may not be its main target. Using the insulin turbidimetry assay, **DTP1-3** have been found to significantly inhibit the reductase activity of PDI. DTP derivatives might show antiproliferative activity by inhibition of PDI as their preferred target.

Taken together these results suggest that DTP derivatives might be promising multi-target agents to treat cancer.

4.5 Experimental section

Chemistry

4.5.1 General experimental methods

All reagents were purchased from Sigma-Aldrich and used without further purification. Solvents were distilled according to conventional procedures. Reactions were carried out

under nitrogen (N₂) atmosphere, monitored by thin layer chromatography (TLC) on silica gel plates (Merck 60F254, 0.2mm) and visualized by UV light at 254 and 366nm of wavelength. Reaction solutions were evaporated on a rotary evaporator under reduced pressure. Final compounds were purified by crystallization and flash chromatography columns, on silica gel (Merck, 60, 230–400mesh, 0.040–0.063 mm). Melting points were obtained by a Gallenkamp 21374 apparatus and were uncorrected. ¹H-NMR spectra were recorded on a Bruker 300MHz spectrometer. Chemical shift (δ) was reported in ppm, using tetramethylsilane (TMS) as the internal reference standard. Multiplicities, coupling constants reported as a J value in Hertz (Hz), and number of protons are indicated parenthetically. MS spectrometry data were obtained using Shimadzu LCMS 20-20 instrument, with electro spray ionization (ESI) mode. Yields refer to purified products and are not optimized.

4.5.2 Synthesis

2,6-Di-tert-butyl-4-(piperidin-1-yl(thiophen-2-yl)methyl)phenol (DTPI). A stirred solution of thiophene-2-carbaldehyde **1** (475μL; 5.1mmol) and piperidine **2** (1.1mL; 11.2mmol) in dry toluene (4mL) was heated to reflux at 110 °C, under a N₂ atmosphere, for 4 h. Then, the reaction mixture was cooled down to 90 °C and a solution of 2,6-di-*tert*-butylphenol **3** (1.0g; 4.85mmol) in dry toluene (2mL) was added, drop by drop. The reaction mixture was heated to reflux again, under N₂ atmosphere, overnight. The solvent was evaporated under vacuum; methanol was added to the reaction residue and was stirred and heated at 60°C, for 30 minutes. The obtained solid was collected by filtration and purified by crystallization from methanol. The pure compound was isolated as yellow solid (33% yield). **m.p.** 133–134°C. ¹H-NMR (DMSO) δ: 7.39–7.36 (m, 1H); 7.14 (s, 2H); 6.92–6.87 (m, 2H); 6.85 (bs, 1H); 4.55 (s, 1H); 2.25 (s, 4H); 1.52 (s, 6H); 1.35 (s,

18H). **¹³C-NMR (CDCl₃) δ**: 152.6, 148.6, 148.5, 135.2, 131.4, 126.0, 125.1 (x2C), 124.9, 124.4, 71.3, 52.3 (x2C), 34.3 (x2C), 30.3 (x6C), 26.3 (x2C), 24.7. **LC-MS (ESI): *m/z*** 384 [M-H]⁻, 301 [M-piperidiny]⁻.

2,6-Di-tert-butyl-4-(morpholino(thiophen-2-yl)methyl)phenol (DTP2). A solution of **1** (143μL; 1.5mmol) and morpholine **4** (290μL; 3.4mmol) in dry toluene (4mL) was put in reaction following by addition of a solution of **3** (300mg; 1.4mmol), based on the synthetic method described for **DTP1**. The final compound was purified by column chromatography on silica gel (n-hexane/ethyl acetate, 9:1, as eluent) and isolated as reddish orange oil (46% yield). **¹H-NMR (DMSO) δ**: 7.99 (d, 1H, *J* = 3.0Hz); 7.85 (s, 1H); 7.68 (s, 1H); 7.58 (d, 1H, *J* = 3.0Hz); 7.28–7.24 (m, 1H); 7.18–7.15 (m, 1H); 6.87 (s, 1H); 4.01–3.98 (m, 4H); 2.10–1.98 (m, 4H); 1.30 (s, 9H); 1.24 (s, 9H). **¹³C-NMR (CDCl₃) δ**: 152.6, 148.6, 148.5, 136.1, 128.0, 127.0, 126.8, 125.5, 125.0 (x2C), 71.7, 67.0 (x2C), 52.1 (x2C), 34.7 (x2C), 31.6 (x6C). **LC-MS (ESI): *m/z*** 301 [M-morpholino]⁻.

2,6-Di-tert-butyl-4-(pyrrolidin-1-yl(thiophen-2-yl)methyl)phenol (DTP3). A solution of **1** (143μL; 1.5mmol) and pyrrolidine **5** (290μL; 3.4mmol) in dry toluene (4mL) was put in reaction following by addition of a solution of **3** (300mg; 1.4mmol), based on the synthetic method described for **DTP1**. The final compound was purified by column chromatography on silica gel (n-hexane/ethyl acetate, 3:1, as eluent) and isolated as brown oil (46% yield). **¹H-NMR (DMSO) δ**: 8.0 (d, 1H, *J* = 3.0Hz); 7.84 (s, 1H); 7.67 (s, 1H); 7.57 (d, 1H *J* = 3.0Hz); 7.29–7.24 (m, 1H); 7.20–7.16 (m, 1H); 7.13 (s, 1H); 1.48 (s, 8H); 1.30 (s, 9H); 1.24 (s, 9H). **LC-MS (ESI): *m/z*** 372 [M+H]⁺.

2,6-Di-tert-butyl-4-(piperidin-1-yl(1H-pyrrol-2-yl)methyl)phenol (DTP4). A solution of pyrrole-2-carbaldehyde **6** (145mg; 1.5mmol) and **2** (333μL; 3.4mmol) in dry toluene (4mL) was put in reaction following by addition of a solution of **3** (300mg; 1.4mmol), based on the synthetic method described for **DTP1**. The final compound was purified by

chromatographic column on silica gel (n-hexane/ethyl acetate, 3:1, as eluent) and isolated as brown oil (30%). ¹H-NMR (DMSO) δ: 7.4–7.36 (m, 1H); 7.15 (s, 2H); 6.90–6.85 (m, 2H); 6.80 (bs, 1H); 6.0 (bs, 1H); 4.55 (s, 1H); 2.25 (s, 4H); 1.52 (s, 6H); 1.35 (s, 18H).

2,6-Di-tert-butyl-4-(morpholino(1H-pyrrol-2-yl)methyl)phenol (DTP5). A solution of **6** (145mg; 1.5mmol) and **2** (290μL; 3.4mmol) in dry toluene (4mL) was put in reaction following by addition of a solution of **3** (300mg; 1.4mmol), based on the synthetic method described for **DTP1**. The final compound was purified by column chromatography on silica gel (n-hexane/ethyl acetate, 3:1, as eluent) and isolated as brown oil (34%). ¹H-NMR (DMSO) δ: 8.0 (d, 1H, *J* = 3.0Hz); 7.82 (s, 1H); 7.70 (s, 1H); 7.60 (d, 1H, *J* = 3.0Hz); 7.30–7.25 (m, 1H); 7.20–7.15 (m, 1H); 6.80 (s, 1H); 6.0 (bs, 1H); 4.01–3.98 (m, 4H); 2.10–1.98 (m, 4H); 1.30 (s, 9H); 1.24 (s, 9H).

2,6-Di-tert-butyl-4-(piperidin-1-yl(furan-2-yl)methyl)phenol (DTP6). A solution of furan-2-carbaldehyde **7** (127mg; 1.5mmol) and **2** (333μL; 3.4mmol) in dry toluene (4mL) was put in reaction following by addition of a solution of **3** (300mg; 1.4mmol), based on the synthetic method described for **DTP1**. The final compound was purified by column chromatography on silica gel (n-hexane/ethyl acetate, 3:1, as eluent) and isolated as brown oil (37%). ¹H-NMR (DMSO) δ: 7.39–7.36 (m, 1H); 7.14 (s, 2H); 6.92–6.87 (m, 2H); 6.85 (bs, 1H); 4.55 (s, 1H); 2.25 (s, 4H); 1.52 (s, 6H); 1.35 (s, 18H).

Biology

4.5.3 Insulin turbidimetry assay. Reductase activity was assayed by measuring the PDI-catalyzed reduction of insulin in the presence of the selected compounds. They were added in serial concentrations, ranging from 30μM to 0.33μM, in duplicate, to the recombinant PDI protein (0.4 μM) and incubated at 37° for 1 h, in sodium phosphate buffer containing sodium phosphate (100 mM), EDTA (2 mM), and DTT (8 μM) at pH

7.0. Then a mixture of sodium buffer, DTT ($0.5 \mu\text{M}$), and bovine insulin ($130 \mu\text{M}$) was added to the incubated PDI protein. PDI catalyzed the reaction at room temperature and the resulting aggregation of reduced insulin B chains was measured spectrophotometrically at 620nm. The IC_{50} values were determined using GraphPad Prism and expressed as average of three independent experiments \pm standard deviation value.

CHAPTER 5:

**Design and synthesis of novel 2,3-dihydroquinazolin-4-(1*H*)-
one derivatives with remarkable antiproliferative activity**

5.1.1 Design and synthesis of DHP, QZ and DHQ derivatives

In order to investigate a deep SAR of DHQ framework, series of DHP, QZ and DHQ derivatives were designed and synthesized. As shown in Figure 28, the synthetic strategies included different modifications such as replacement of the benzene ring of the scaffold with a pyridine one, oxidation of the bond N1-C2, introduction of a fluorine atom at C6, and substitution with indole moieties on C2.

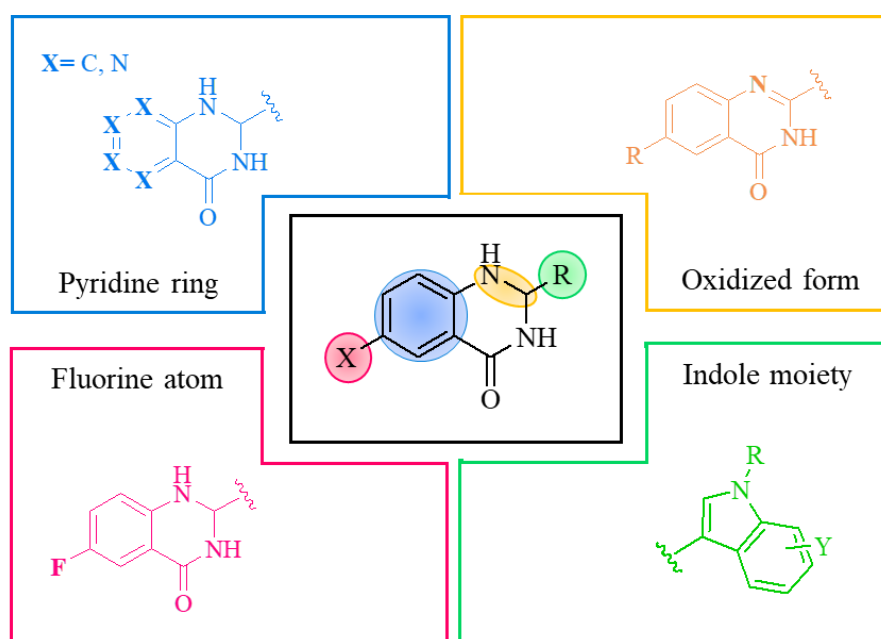
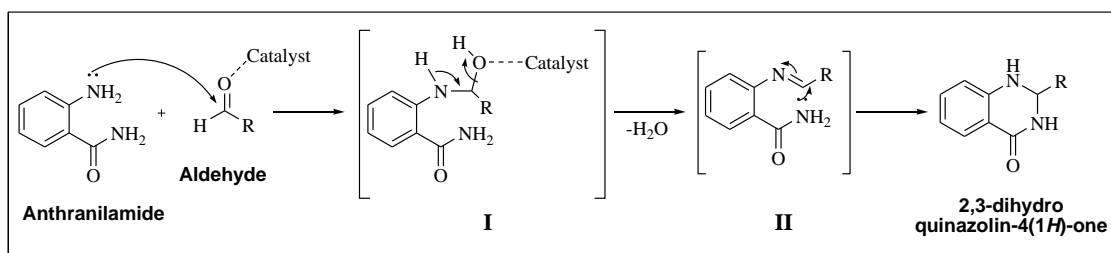


Figure 28. Lead optimization of the DHQ core structure.

5.2 Chemistry

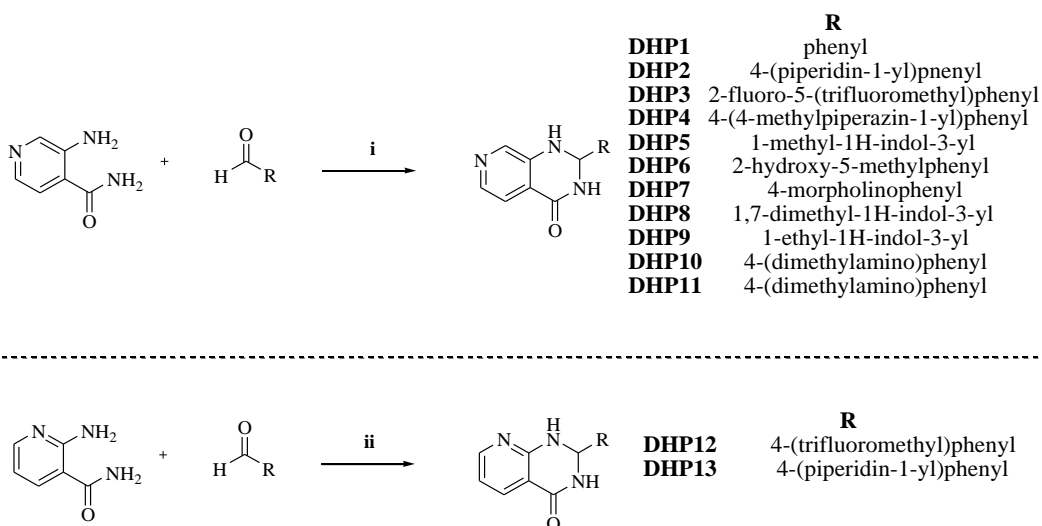
The DHQ framework is a privileged scaffold in drug design; in particular, 2-substituted DHQ derivatives showed several important pharmacological properties (*Badolato et al.* 2018). Because of their importance, their synthesis has attracted much attention and different synthetic strategies have been developed. The most common and simple synthetic route for the preparation of DHQs is the direct cyclocondensation of anthranilamide and an aldehyde, in the presence of a catalyst.

The presumed mechanism of reaction is shown in Box 4.



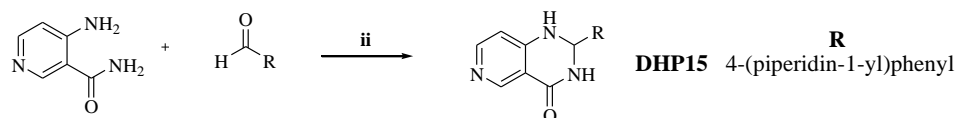
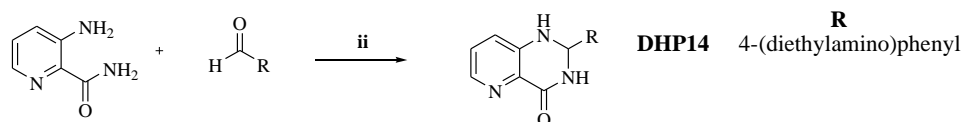
Box 4. Presumed mechanism of the cyclocondensation of anthranilamide and aldehyde. The first step involves the nucleophilic attack of the nitrogen of the amino group of the anthranilamide on the carbonyl carbon of the aldehyde, promoted by the catalyst, resulting in the formation of hydroxyl intermediate **I**. Next, the catalyst promotes the formation of the Schiff base (**II**) from **I** through the removal of a water molecule. Finally, the imine undergoes intramolecular cyclization by nucleophilic attack of the nitrogen of the amide group on the imine carbon, to furnish the corresponding 2,3-dihydroquinazolin-4(1*H*)-one.

DHP derivatives were obtained through cyclocondensation of an aldehyde with a pyridine ring bearing an amino and an amide group on two adjacent carbons, in the presence of Lewis acid as catalyst, as represented in Scheme 6.



Scheme 6. Reagents and conditions.

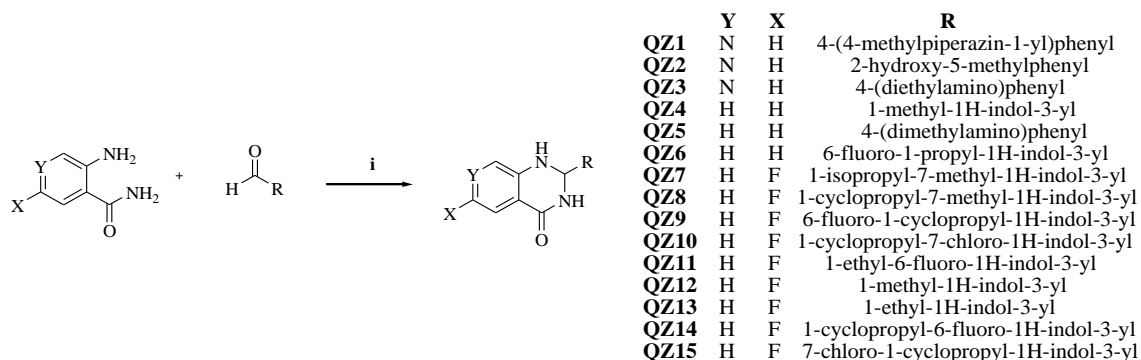
i) amide (1 eq.), aldehyde (1 eq.), MES (20 mol%), aq. Ethanol (50%), reflux. ii) amide (1 eq.), aldehyde (1 eq.), ZnCl₂ (10 mol%), diglyme, 110°C.



Scheme 6. Reagents and conditions.

i) amide (1 eq.), aldehyde (1 eq.), MES (20 mol%), aq. Ethanol (50%), reflux. ii) amide (1 eq.), aldehyde (1 eq.), ZnCl₂ (10 mol%), diglyme, 110°C.

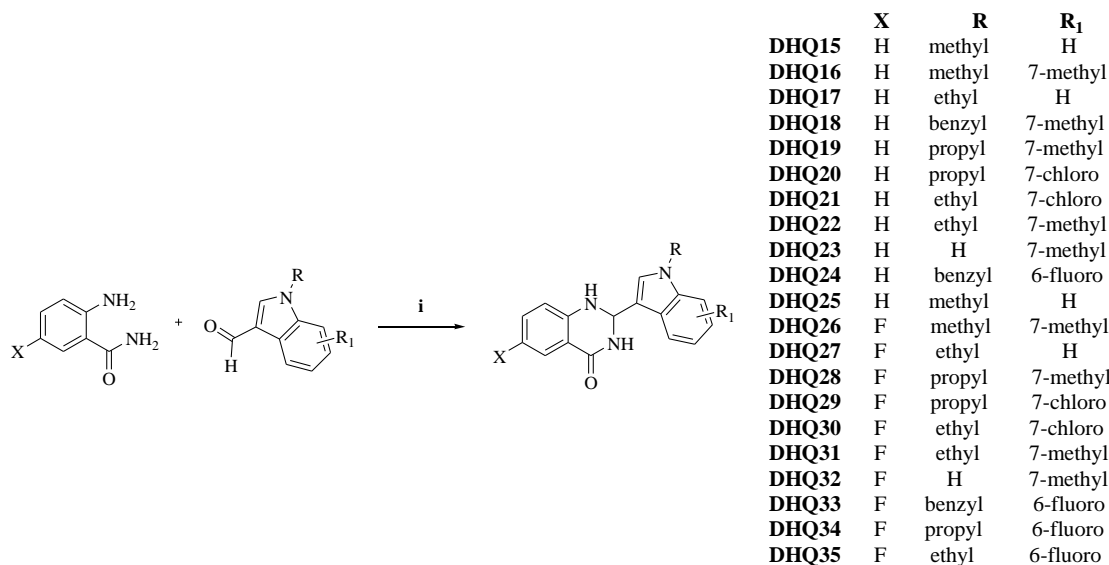
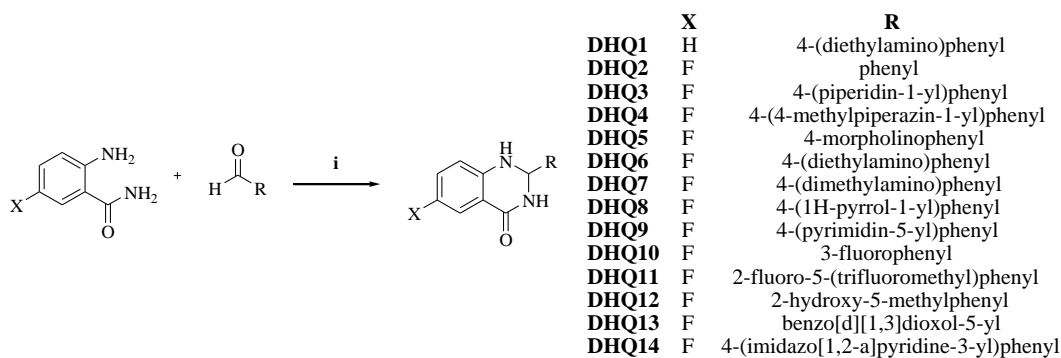
The cyclocondensation of 4-aminonicotine, 2-aminobenzamide or 2-amino-6-fluorobenzamide with an aldehyde under microwave irradiation gave the oxidized QZ derivatives (Scheme 7).



Scheme 7. Reagents and conditions.

i) 4-aminonicotine or anthranilamide or 2-amino-6-fluorobenzamide (1 eq.), aldehyde (0.96 eq.), NaHSO₃ (1.03 eq.), DMA, 180°C, MW.

The 2-aryl and 2-indole substituted DHQ derivatives were synthesized according to green chemistry strategy by cyclocondensation of anthranilamide and an aldehyde (Scheme 8).



Scheme 8. Reagents and conditions.

i) anthranilamide or 2-amino-6-fluorobenzamide (1 eq.), benzaldehyde or indole-3-carbaldehyde (1 eq.), MES (5-10 mol%), aq. Ethanol (50%), reflux or MW.

5.3 Cytotoxic profile of the new DHQ derivatives

The *in vitro* antiproliferative activity of all new synthesized derivatives was assessed by MTT assay, in a panel of human cancer cell lines, including pancreatic, ovarian, breast and brain cancer. As shown in Figure 29, a SAR study was started.

5.3.1 The benzene ring of DHQs is necessary for their cytotoxicity

The *in vitro* cytotoxicity of compounds **DHP1-15** was determined by MTT assay in different tumor cell lines. As reported in Table 9, both 2-aryl and 2-indole substituted

DHP derivatives were not able to inhibit the proliferation of the used pancreatic (Mia PaCa-2 and Panc-1) and ovarian (SKOV3 WT) cancer cell lines ($IC_{50} > 30\mu M$). Even the presence of various substituents on the phenyl or indole moiety at position 2 and the presence of nitrogen atom in different position of the benzene ring of DHP derivatives did not change their cytotoxicity.

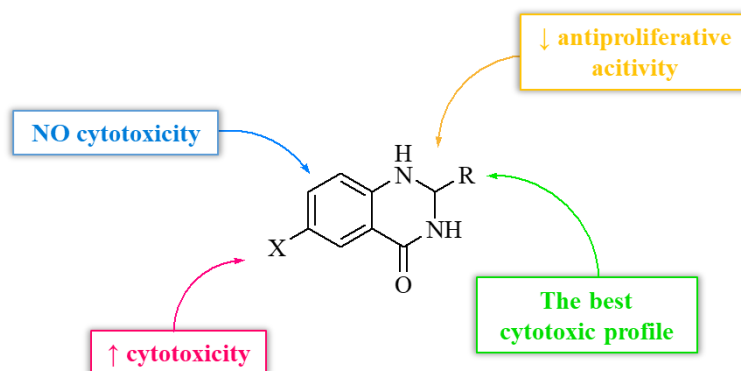


Figure 29. Structure-activity relationship of the new synthesized derivatives.

Table 9. Antiproliferative activity of DHP derivatives in different cancer cell lines.

Cmpnd	IC_{50} (μM) ^a		
	Mia PaCa-2	Panc-1	SKOV3 WT
DHP1	>30	>30	>30
DHP2	>30	>30	>30
DHP3	>30	>30	>30
DHP4	>30	>30	>30
DHP5	>30	>30	>30
DHP6	>30	>30	>30
DHP7	>30	>30	>30
DHP8	>30	>30	>30
DHP9	>30	>30	>30
DHP10	>30	>30	>30
DHP11	>30	>30	>30
DHP12	27.9	>30	26.7
DHP13	>30	>30	31.8
DHP14	>30	>30	>30
DHP15	>30	>30	>30

^a IC_{50} values were determined by MTT assay after 72 h treatment.

5.3.2 The oxidized form of DHQ has a lower cytotoxicity against cancer cell lines

Results of the *in vitro* antiproliferative activity in several cancer cell lines (Table 10) confirm that the presence of nitrogen atom at position 6 of the benzene ring of DHQ core

structure does not improve the cytotoxicity of compounds **QZ1-3**. On the contrary, most of 2-indole substituted QZ derivatives showed moderate capacity to inhibit the cell proliferation. The presence of fluorine atom at position 6 does not significantly change the cytotoxicity of compounds, except for compound **QZ12**. Compared to the analog **QZ4**, it showed a good cytotoxicity against most of cancer cell lines tested ($IC_{50} < 10\mu M$). Compound **QZ8** exhibits the best cytotoxicity against Mia PaCa-2 cell line ($IC_{50}=2\mu M$), suggesting that the simultaneous presence of cyclopropyl and methyl substituents at position 1 and 7 of the indole moiety is important, while compound bearing halogen like chlorine and fluorine at position 7 and 6 of the indole showed only moderate cytotoxicity. Hence, DHP derivatives do not show cytotoxic effect, while QZ derivatives can mildly inhibit cancer cell proliferation. Among them, 2-indole substituted compounds showed a better cytotoxicity.

Table 10. Antiproliferative activity of QZ derivatives in different cancer cell lines.

Cmpnd	IC_{50} (μM) ^a					
	Mia PaCa-2	BxPc3	Panc-1	HCT116 p53 ^{+/+}	OVCAR-8	SKOV3 WT
QZ1	>30	>30	>30	>30	>30	>30
QZ2	27.1	>30	>30	>30	>30	>30
QZ3	5.1	>30	>30	>30	>30	>30
QZ4	14.5±0.4	10.8±0.3	>30	2.5	2.5	>30
QZ5	>100	NT	NT	NT	NT	NT
QZ6	>30	>30	>30	NT	NT	NT
QZ7	9.2; 10.7	>10	>30	>30	NT	>30
QZ8	2.0±0.29	3.4±0.47	7.7±0.7	9.4	NT	10.2
QZ9	11.7	15.2	>30	5.0	NT	>30
QZ10	14.5	5.8	>30	17.4	NT	15.7
QZ11	4.9±0.83	4.5±0.8	1.6	3.7	NT	12.6
QZ12	3.1±0.66	5.1	6.8	5.6±0.9	4.7	8.85
QZ13	18.6; 5.4	8.8	10.4	NT	NT	15.5
QZ14	13.4±0.6	9.8	18.5	5.0	NT	16.9
QZ15	28.0±0.9	13.9	>30	15.2	NT	>30

^a IC_{50} values were determined by MTT assay after 72 h treatment. The data are shown as the mean ± standard deviation (SD), n=3.

5.3.3 The cytotoxicity of 2-aryl DHQs depends on the feature and the position of different substituents of the phenyl ring

The *in vitro* cytotoxic activity of 2-aryl DHQ derivatives is reported in Table 11. 2-phenyl

substituted derivative (**DHQ2**) showed a good capacity to inhibit cell proliferation of most tested cancer cell lines, with IC₅₀ values in the micromolar range. The presence of heterocycles in *para* on the phenyl ring as well as imidazo[1,2-*a*]pyridine substituent at position 2 of DHQ core structure leads to the loss of cytotoxicity in compounds **DHQ3-5**, **DHQ8-9**, and **DHQ14**. Electron-withdrawing substituents (**DHQ11**) are also responsible of the loss of the antiproliferation effect, although compound **DHQ10** bearing a fluorine atom in *meta* on the phenyl ring showed a good effect in some cancer cell lines. Compound **DHQ12**, with two electron-donating groups on the phenyl ring, and compound **DHQ13**, bearing benzo[*d*][1,3]dioxole at position 2, showed only a moderate cytotoxic effect against pancreatic cancer cells. The presence of dimethylamino group in *para* (**DHQ7**) does not improve the antiproliferative activity while diethylamino group (**DHQ1** and **DHQ6**) leads to a good cytotoxicity.

Table 11. Antiproliferative activity of 2-aryl substituted DHQ derivatives in different cancer cell lines.

Cmpnd	IC ₅₀ (μM) ^a					
	Mia PaCa-2	BxPc3	Panc-1	HCT116 p53 ^{+/+}	OVCAR-8	SKOV3 WT
DHQ1	1.3±0.2	2.1±0.9	15.4±0.9	NT	2.3±0.9	>30
DHQ2	3.5±0.8	2.0±0.5	23.2±1.9	4.6±0.4	2.9±0.3	>30
DHQ3	>30	NT	>30	NT	NT	>30
DHQ4	>30	NT	>30	NT	NT	>30
DHQ5	>30	NT	>30	NT	NT	>30
DHQ6	6.4	5.3	>30	11.5	3.4	18.7
DHQ7	34.4	NT	>30	NT	NT	>30
DHQ8	>30	NT	>30	NT	NT	>30
DHQ9	>30	NT	NT	>30	>30	>30
DHQ10	5.9	NT	NT	4.7	4.2	29.1
DHQ11	>30	NT	>30	NT	NT	>30
DHQ12	9.1	NT	NT	>30	>30	>30
DHQ13	14.7	NT	NT	14.1	27.4	>30
DHQ14	>30	NT	>30	NT	NT	>30

^aIC₅₀ values were determined by MTT assay after 72 h treatment. The data are shown as the mean ± standard deviation (SD), n=3.

5.3.4 2-Indole substituted DHQs are selectively cytotoxic against pancreatic cancer cells but not against normal ones

Table 12 reports the results of *in vitro* cytotoxicity of all 2-indole DHQ derivatives, which

showed selectivity against pancreatic cancer cells (Mia PaCa-2, BxPc-3, Panc-1).

Table 12. Antiproliferative activity of 2-indole substituted DHQ derivatives in different cancer cell lines.

Cmpnd	IC ₅₀ (μM) ^a					
	Mia PaCa-2	BxPc3	Panc-1	HCT116 p53 ^{+/+}	OVCAR-8	SKOV3 WT
DHQ15	0.77±0.18	1.78±0.13	6.05±0.11	2.5±0.4	3.2±0.22	16.5
DHQ16	0.71±0.11	0.97±0.18	6.65±0.43	0.97	4.36	4.28±1.39
DHQ17	0.33±0.16	0.41±0.14	4.89±1.32	0.85±0.35	1.67	15.5
DHQ18	26.6	11.35	>30	>30	>30	>30
DHQ19	6.38±1.83	6.6±0.15	13.6±2.4	8.5±0.7	NT	17.06
DHQ20	4.03±1.4	2.9±0.65	16.7±0.9	12.85±0.45	NT	21.3
DHQ21	0.56±0.15	0.42±0.12	2.3	0.69	NT	1.45±0.65
DHQ22	0.29±0.07	0.69±0.22	2.45±0.35	NT	NT	3.25±0.26
DHQ23	27.0	22.0	>30	NT	NT	>30
DHQ24	9.8	2.3	>30	11.1	NT	12.3
DHQ25	1.84±0.71	1.98±0.42	10.65±0.9	6.40±0.65	5.15±0.71	8.2±0.53
DHQ26	0.71±0.18	0.44±0.13	2.1±0.28	4.1±0.73	1.55±0.63	1.2±0.24
DHQ27	0.15±0.03	0.43±0.09	4.45±0.65	0.32±0.11	0.55±0.21	4.6±0.36
DHQ28	1.16±0.33	1.06±0.60	2.75±0.15	2.10±0.05	1.9±0.15	8.7±0.95
DHQ29	1.5±0.49	1.70±0.34	12.3±0.69	5.4±0.41	NT	>30
DHQ30	0.36±0.14	0.24±0.05	1.1±0.26	NT	NT	1.22±0.19
DHQ31	0.17±0.09	0.20±0.06	0.83±0.13	NT	NT	2.0±0.16
DHQ32	11.8	13.1	28.4	NT	NT	29.7
DHQ33	11.5	2.8	>30	3.8	NT	16.3
DHQ34	>30	>30	>30	NT	NT	NT
DHQ35	2.8±0.25	2.8±0.95	4.5	6.8	NT	10.35±0.35

^aIC₅₀ values were determined by MTT assay after 72 h treatment. The data are shown as the mean ± standard deviation (SD), n=3.

In general, 6-fluoro substituted derivatives inhibit the cell proliferation better than their unsubstituted analogs. The absence of substituents on the nitrogen of the indole moiety (DHQ23 and DHQ32) leads to the decrease of the cytotoxicity, while compounds DHQ18, DHQ24 and DHQ33, bearing a benzyl substituent, have a moderate antiproliferative effect (10μM<IC₅₀<30μM). The best cytotoxic effect is given by short alkyl substituents, in particular methyl and ethyl, with IC₅₀ values in the nanomolar range. Compounds with a second substituent on the benzene ring of the indole moiety showed different cytotoxicity, in dependence of its chemical feature and position. In fact, substituted position 6 of the indole structure is less important than position 7, whereas the presence of electro-donating group in position 7 is better than electro-withdrawing group.

Most of the 2-indole substituted DHQs showed nanomolar potency against many tumor cell lines, in particular against pancreatic one (Mia PaCa-2). Interestingly, human pancreatic normal cells (HPNE) are less sensitive to the cytotoxic activity of these compounds, supporting the potential applications of 2-indole substituted DHQs for cancer treatment (Table 13).

Table 13. Antiproliferative activity of 2-indole substituted DHQ derivatives against cancer and normal pancreatic cell lines.

Cmpnd	IC ₅₀ (μM)	
	Mia PaCa-2	HPNE
DHQ15	0.77±0.18	18.0±0.9
DHQ16	0.71±0.11	9.0±0.5
DHQ17	0.33±0.16	10.6±0.7
DHQ18	26.6	NT
DHQ19	6.38±1.83	16.6±0.5
DHQ20	4.03±1.4	10.8±0.2
DHQ21	0.56±0.15	7.8±0.6
DHQ22	0.29±0.07	6.3±0.3
DHQ23	27.0	>30
DHQ24	9.8	NT
DHQ25	1.84±0.71	10.9±0.5
DHQ26	0.71±0.18	1.9±0.1
DHQ27	0.15±0.03	5.2±0.7
DHQ28	1.16±0.33	3.5±0.4
DHQ29	1.5±0.49	6.1±0.9
DHQ30	0.36±0.14	5.2±0.2
DHQ31	0.17±0.09	6.2±0.6
DHQ32	11.8	>30
DHQ33	11.5	NT
DHQ34	>30	NT
DHQ35	2.8±0.25	NT

^aIC₅₀ values were determined by MTT assay after 72 h treatment. The data are shown as the mean ± standard deviation (SD), n=3.

5.3.5 Direct inhibition of STAT3

All the designed DHQ derivatives were tested in the FP assay to evaluate their binding to the SH2 domain of STAT3. The assay was performed at 37°C, using Stattic as positive control. Compounds were initially tested at two different concentrations (50μM and 10μM) and none of them was able to bind to the protein at the tested concentrations. Therefore, DHQ derivatives do not act as direct inhibitors of STAT3.

5.3.6 Western blot analysis of compounds **DHQ27-28** and **DHQ30-31**

Since DHQ framework was initially identified as scaffold for the development of potential STAT3 inhibitors, the inhibition of STAT3 phosphorylation was investigated using Western blot analysis, as shown in Figure 30. Based on the MTT results against the pancreatic cancer cell lines (Mia PaCa-2, BxPc3, Panc-1), compounds **DHQ27-28** and **DHQ30-31** were selected and the levels of phosphorylated STAT3 were evaluated in Mia PaCa-2 cells, after 4 h treatment. Stattic was used as positive control. All the compounds were tested at a single concentration (10 μ M).

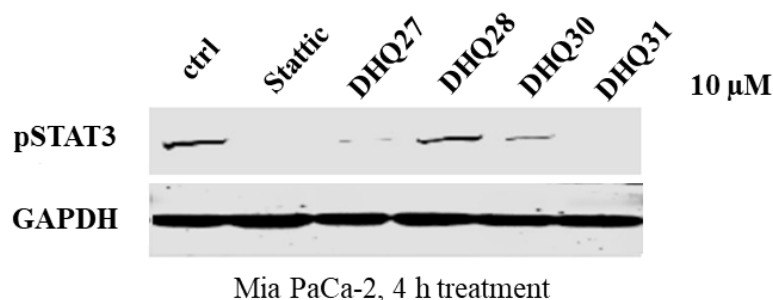


Figure 30. The effect of TZC10 on the expression of pSTAT3 in pancreatic cancer cells.

Cells were treated with the indicated concentrations for 4 h, and the protein expression were determined by Western blot assay using antibody against pSTAT3 (Tyr705). GAPDH was used as a loading control.

Results suggest that DHQ derivatives significantly suppress the level of phosphorylated STAT3. If DHQ derivatives do not directly bind the SH2 domain of STAT3 protein, they could inhibit some upstream signals in its signaling pathway, such as kinases.

The mechanism of action of DHQ derivatives is still being investigated in order to explain their potent antiproliferative activity.

5.4 Conclusion

In summary, DHQ was identified as potential scaffold for the development of

antiproliferative agents. Different classes of DHP, QZ and DHQ derivatives were designed and synthesized with the aim to perform a SAR study. The lead optimization led to the discovery of novel 2-indole DHQ derivatives with remarkable antiproliferative activity, selectively against pancreatic cancer cells. Interestingly, 2-indole DHQ derivatives are quite well safe against normal cells. This property could make them promising drug candidates for chemotherapy. Although DHQ derivatives do not directly bind to the SH2 domain of STAT3 protein, they significantly reduce the level of phosphorylated STAT3 in Mia PaCa-2 cancer cells. They might inhibit upstream kinases in STAT3 signaling pathway.

Further studies are ongoing to understand the mechanisms involved in their antiproliferative activity. These promising results make us more interested to continue in this direction, trying to find a potential candidate to apply for the cancer treatment.

5.5 Experimental section

Chemistry

5.5.1 General experimental methods.

Reagents were purchased from Fisher or Sigma and they were used without further purification. The intermediate aldehydes were obtained from variously substituted indole-3-carbaldehyde by alkylation and Suzuki coupling. Reactions were monitored by thin layer chromatography (TLC). Microwave irradiation was performed using Biotage Initiator+ in 2-5 and 10-20 ml capped flasks at constant Temperature. ¹H-NMR spectra were obtained on a Bruker 300 or 400 MHz spectrometer and measured on compounds in solution in DMSO-*d*₆, methanol-*d*₄, or CDCl₃. Chemical shift (δ), reported in ppm, were recorded with tetramethylsilane (TMS) as the internal reference standard. Multiplicities, coupling constants reported as a *J* value in Hertz (Hz), and number of

protons are indicated parenthetically. MS spectrometry data were obtained using Shimadzu LCMS 20-20 instrument, with electro spray ionization (ESI) mode. The HPLC traces were obtained using the Shimadzu Test Kit C18 column (3mm, 4.6x50mm), under two different gradient conditions: from 10% to 95% acetonitrile in water with 0.01% formic acid (mobile phase A); and from 10% to 95% methanol in water with 0.01% formic acid (mobile phase B). The flow rate was 0.6 mL/min. The purity of compounds was based on the HPLC chromatograph by integration of the areas of major peaks detected at 254 nm. Yields refer to purified products and are not optimized.

5.5.2 Synthesis of 2-substituted 2,3-dihydropyridopyrimidin-4-(1H)-one derivatives (DHP1-11). To a stirred solution of 2-(N-morpholino)ethanesulfonic acid (MES) (20 mol%) in Ethanol:water (50:50), aldehyde (1 equiv.) and 3-aminoisonicotinamide (1 equiv.) were added. The reaction was heated to reflux and stirred for 8-12h. The consumption of starting materials was followed by TLC. The mixture was cooled to room temperature and the obtained solid was collected by filtration and recrystallized from ethanol. The final product was dried in vacuum.

2-phenyl-2,3-dihydropyrido[3,4-d]pyrimidin-4(1H)-one (DHP1). ¹H NMR (300 MHz, Methanol-*d*₄) δ 8.14 (s, 1H), 7.98 (d, *J* = 5.1 Hz, 1H), 7.65 (dd, *J* = 0.8, 5.1 Hz, 1H), 7.59 (dd, *J* = 2.2, 7.5 Hz, 2H), 7.50 – 7.40 (m, 3H), 5.95 (s, 1H). LC-MS (ESI): *m/z* 226 [M+H]⁺; HPLC (mobile phase A): purity 99%.

2-(4-(piperidin-1-yl)phenyl)-2,3-dihydropyrido[3,4-d]pyrimidin-4(1H)-one (DHP2). ¹H NMR (300 MHz, Methanol-*d*₄) δ 8.12 (d, *J* = 0.8 Hz, 1H), 7.97 (d, *J* = 5.1 Hz, 1H), 7.64 (dd, *J* = 0.8, 5.1 Hz, 1H), 7.44 (d, *J* = 8.7 Hz, 2H), 7.06 – 6.99 (m, 2H), 5.85 (s, 1H), 3.24 – 3.17 (m, 4H), 1.71 (d, *J* = 4.9 Hz, 6H). LC-MS (ESI): *m/z* 306.9 [M-H]⁻; HPLC (mobile phase A): purity 100%.

2-(2-fluoro-5-(trifluoromethyl)phenyl)-2,3-dihydropyrido[3,4-d]pyrimidin-4(1H)-one (**DHP3**). ¹H NMR (300 MHz, Methanol-*d*₄) δ 8.17 (dd, *J* = 2.5, 6.6 Hz, 2H), 7.94 (dd, *J* = 2.4, 6.6 Hz, 1H), 7.87 – 7.76 (m, 2H), 7.68 (d, *J* = 4.9 Hz, 1H), 7.47 – 7.26 (m, 2H), 6.36 (s, 1H). LC-MS (ESI): *m/z* 311.9 [M+H]⁺; HPLC (mobile phase A): purity 98%.

2-(4-(4-methylpiperazin-1-yl)phenyl)-2,3-dihydropyrido[3,4-d]pyrimidin-4(1H)-one (**DHP4**). ¹H NMR (300 MHz, Methanol-*d*₄) δ 8.12 (d, *J* = 0.8 Hz, 1H), 7.97 (d, *J* = 5.0 Hz, 1H), 7.64 (dd, *J* = 0.8, 5.0 Hz, 1H), 7.46 (d, *J* = 8.7 Hz, 2H), 7.03 (d, *J* = 8.8 Hz, 2H), 5.86 (s, 1H), 3.29 – 3.22 (m, 4H), 2.66 – 2.59 (m, 4H), 2.36 (s, 3H). LC-MS (ESI): *m/z* 324.0 [M+H]⁺; HPLC (mobile phase A): purity 92%.

2-(1-methyl-1H-indol-3-yl)-2,3-dihydropyrido[3,4-d]pyrimidin-4(1H)-one (**DHP5**). ¹H NMR (300 MHz, Methanol-*d*₄) δ 8.15 (d, *J* = 0.8 Hz, 1H), 7.99 (d, *J* = 5.1 Hz, 1H), 7.82 (d, *J* = 8.0 Hz, 1H), 7.69 (d, *J* = 5.2 Hz, 1H), 7.42 (d, *J* = 8.4 Hz, 1H), 7.38 (s, 1H), 7.24 (t, *J* = 7.7 Hz, 1H), 7.12 (d, *J* = 7.1 Hz, 1H), 6.24 (s, 1H), 3.83 (s, 3H). LC-MS (ESI): *m/z* 279.0 [M+H]⁺; HPLC (mobile phase A): purity 87%.

2-(2-hydroxy-5-methylphenyl)-2,3-dihydropyrido[3,4-d]pyrimidin-4(1H)-one (**DHP6**). ¹H NMR (300 MHz, Methanol-*d*₄) δ 8.14 (s, 1H), 7.94 (d, *J* = 5.1 Hz, 1H), 7.63 (dd, *J* = 0.8, 5.1 Hz, 1H), 7.23 (d, *J* = 2.2 Hz, 1H), 7.01 (dd, *J* = 0.8, 2.3, 8.2 Hz, 1H), 6.76 (d, *J* = 8.2 Hz, 1H), 6.24 (s, 1H), 2.24 (d, *J* = 0.7 Hz, 3H). LC-MS (ESI): *m/z* 255.9 [M+H]⁺; 253.9 [M-H]⁻; HPLC (mobile phase A): purity 100%.

2-(4-morpholinophenyl)-2,3-dihydropyrido[3,4-d]pyrimidin-4(1H)-one (**DHP7**). ¹H NMR (300 MHz, Methanol-*d*₄) δ 8.13 (d, *J* = 0.8 Hz, 1H), 7.97 (d, *J* = 5.0 Hz, 1H), 7.64 (dd, *J* = 0.8, 5.1 Hz, 1H), 7.47 (d, *J* = 8.7 Hz, 2H), 7.03 (d, *J* = 8.8 Hz, 2H), 5.87 (s, 1H), 3.90 – 3.77 (m, 4H), 3.23 – 3.12 (m, 4H). LC-MS (ESI): *m/z* 311.0 [M+H]⁺; HPLC (mobile phase A): purity 98%.

2-(1,7-dimethyl-1H-indol-3-yl)-2,3-dihydropyrido[3,4-d]pyrimidin-4(1H)-one (**DHP8**). ¹H NMR (300 MHz, Chloroform-*d*) δ 8.35 (s, 1H), 8.17 (d, *J* = 5.0 Hz, 1H), 7.84 (d, *J* = 5.1 Hz, 1H), 7.68 (d, *J* = 7.6 Hz, 1H), 7.17 (s, 1H), 7.09 – 6.96 (m, 2H), 6.25 (s, 1H), 6.07 (s, 1H), 5.14 (s, 1H), 4.09 (s, 3H), 2.80 (s, 3H). LC-MS (ESI): *m/z* 293.0 [M+H]⁺; HPLC (mobile phase A): purity 96%.

2-(1-ethyl-1H-indol-3-yl)-2,3-dihydropyrido[3,4-d]pyrimidin-4(1H)-one (**DHP9**). ¹H NMR (300 MHz, Chloroform-*d*) δ 9.25 (s, 1H), 8.62 (d, *J* = 5.3 Hz, 1H), 8.32 (d, *J* = 3.1 Hz, 1H), 8.23 – 8.11 (m, 1H), 7.86 (dd, *J* = 6.5, 12.4 Hz, 1H), 7.42 (d, *J* = 8.1 Hz, 1H), 7.35 (s, 1H), 7.21 (d, *J* = 7.6 Hz, 1H), 6.29 (s, 1H), 6.19 (s, 1H), 5.00 (s, 1H), 4.42 – 4.13 (m, 2H), 1.73 – 1.47 (m, 3H). LC-MS (ESI): *m/z* 292.95 [M+H]⁺; 290.90 [M-H]⁻; HPLC (mobile phase A): purity 83%.

2-(4-(diethylamino)phenyl)-2,3-dihydropyrido[3,4-d]pyrimidin-4(1H)-one (**DHP10**). ¹H NMR (300 MHz, Methanol-*d*₄) δ 8.12 (d, *J* = 0.8 Hz, 2H), 7.96 (d, *J* = 5.1 Hz, 1H), 7.64 (d, *J* = 5.0 Hz, 1H), 7.38 (d, *J* = 8.8 Hz, 2H), 6.75 (d, *J* = 8.8 Hz, 2H), 5.81 (s, 1H), 5.51 (s, 1H), 3.41 (d, *J* = 7.0 Hz, 4H), 1.16 (t, *J* = 7.0 Hz, 6H). LC-MS (ESI): *m/z* 296.90 [M+H]⁺; HPLC (mobile phase A): purity 97%.

2-(4-(dimethylamino)phenyl)-2,3-dihydropyrido[3,4-d]pyrimidin-4(1H)-one (**DHP11**). ¹H NMR (300 MHz, Methanol-*d*₄) δ 8.12 (d, *J* = 0.8 Hz, 1H), 7.96 (d, *J* = 5.1 Hz, 1H), 7.64 (dd, *J* = 0.8, 5.1 Hz, 1H), 7.41 (d, *J* = 8.8 Hz, 2H), 6.81 (d, *J* = 8.9 Hz, 2H), 5.83 (s, 1H), 2.97 (s, 6H). LC-MS (ESI): *m/z* 269.0 [M+H]⁺; HPLC (mobile phase A): purity 100%.

5.5.3 *Synthesis of 2-substituted 2,3-dihydropyridopyrimidin-4-(1H)-one derivatives (DHP12-15)*. A solution of 2-aminonicotinamide (**DHP12-13**), 3-aminopicolinamide (**DHP14**), 4-aminonicotinamide (**DHP15**) (1 equiv.), aldehyde (1.76 equiv.) and ZnCl₂ (10 mol%) in diglyme was heated at 110°C overnight. The consumption of starting

materials was followed by TLC. The mixture was cooled to room temperature and washed with methanol. **DHP12** was collected by recrystallization from methanol. For the other compounds, the obtained solid was filtered off and the final product was purified from the filtering solution by chromatographic column on silica gel (DCM:MeOH 9:1).

2-(4-trifluoromethyl)phenyl)-2,3-dihydropyrido[3,4-d]pyrimidin-4(1H)-one (**DHP12**). **¹H NMR (300 MHz, DMSO-*d*₆)** δ 8.68 (s, 1H), 8.17 (d, *J* = 4.9 Hz, 1H), 8.09 (s, 1H), 7.91 (d, *J* = 7.5 Hz, 1H), 7.78 (d, *J* = 8.0 Hz, 2H), 7.66 (d, *J* = 8.1 Hz, 2H), 6.80 – 6.68 (m, 1H), 5.93 (s, 1H). **LC-MS (ESI):** *m/z* 294 [M+H]⁺; **HPLC (mobile phase A):** purity 91%.

2-(4-(piperidin-1-yl)phenyl)-2,3-dihydropyrido[3,4-d]pyrimidin-4(1H)-one (**DHP13**). **¹H NMR (300 MHz, DMSO-*d*₆)** δ 8.42 (s, 1H), 8.13 (d, *J* = 4.8 Hz, 1H), 7.88 (d, *J* = 7.6 Hz, 1H), 7.81 (s, 1H), 7.24 (d, *J* = 8.5 Hz, 2H), 6.90 (d, *J* = 8.4 Hz, 2H), 6.73 – 6.58 (m, 1H), 5.71 (s, 1H), 3.14 (d, *J* = 8.6 Hz, 4H), 1.57 (s, 6H). **LC-MS (ESI):** *m/z* 309 [M+H]⁺; **HPLC (mobile phase A):** purity 90%.

2-(4-(diethylamino)phenyl)-2,3-dihydropyrido[3,2-d]pyrimidin-4(1H)-one (**DHP14**). **¹H NMR (300 MHz, Methanol-*d*₄)** δ 7.96 (d, *J* = 8.7 Hz, 1H), 7.55 (d, *J* = 8.6 Hz, 1H), 7.41 (d, *J* = 8.7 Hz, 1H), 7.35 (d, *J* = 8.5 Hz, 1H), 7.22 (d, *J* = 8.3 Hz, 1H), 6.76 (dd, *J* = 5.9, 8.5 Hz, 2H), 6.69 (dd, *J* = 4.3, 8.6 Hz, 2H), 5.81 (s, 1H), 4.18 (q, *J* = 6.8 Hz, 4H), 1.40 (d, *J* = 6.7 Hz, 6H). **LC-MS (ESI):** *m/z* 297 [M+H]⁺.

2-(4-(piperidin-1-yl)phenyl)-2,3-dihydropyrido[4,3-d]pyrimidin-4(1H)-one (**DHP15**). **¹H NMR (300 MHz, DMSO-*d*₆)** δ 8.53 (s, 1H), 8.31 (s, 1H), 8.11 (d, *J* = 6.6 Hz, 1H), 7.74 (d, *J* = 8.3 Hz, 1H), 7.27 (d, *J* = 8.4 Hz, 2H), 6.93 (d, *J* = 8.4 Hz, 2H), 6.61 (d, *J* = 5.6 Hz, 1H), 5.78 (s, 1H), 3.14 (d, *J* = 6.8 Hz, 4H), 1.58 (s, 6H). **LC-MS (ESI):** *m/z* 307 [M-H]⁻.

5.5.4 Synthesis of 2-substituted quinazolin-4(3H)-one derivatives (**QZ1-15**). A solution of 2-aminobenzamide (**QZ1-3**), 2-amino-6-fluorobenzamide (**QZ4-15**) (1 equiv.), aldehyde (1 equiv.) and NaHSO₃ (1.03 equiv.) in DMA, contained in 2-5 ml capped flask, was subjected to microwave irradiation at 180°C for 30-45min. The mixture was cooled to room temperature and the obtained solid was collected by filtration and recrystallized from methanol. The final product was dried in vacuum.

2-(4-(4-methylpiperazin-1-yl)phenyl)pyrido[4,3-d]pyrimidin-4(1H)-one (**QZ1**). ¹H NMR (300 MHz, DMSO-*d*₆) δ 12.52 (s, 1H), 9.23 (s, 1H), 8.76 (d, *J* = 5.7 Hz, 1H), 8.16 (d, *J* = 8.6 Hz, 2H), 7.54 (d, *J* = 5.7 Hz, 1H), 7.06 (d, *J* = 8.8 Hz, 2H), 2.46 (t, *J* = 5.2 Hz, 8H), 2.24 (s, 3H). LC-MS (ESI): *m/z* 363 [M+AcCN]⁺; HPLC (mobile phase A): purity 100%.

2-(2-hydroxy-5-methylphenyl)pyrido[4,3-d]pyrimidin-4(1H)-one (**QZ2**). ¹H NMR (300 MHz, DMSO-*d*₆) δ 12.92 (s, 1H), 12.71 (s, 1H), 9.28 (s, 1H), 8.84 (d, *J* = 5.7 Hz, 1H), 8.09 (s, 1H), 7.70 (d, *J* = 5.7 Hz, 1H), 7.33 (d, *J* = 8.3 Hz, 1H), 6.94 (d, *J* = 8.4 Hz, 1H), 2.30 (s, 3H). LC-MS (ESI): *m/z* 254 [M+H]⁺; HPLC (mobile phase A): purity 100%.

2-(4-(dimethylamino)phenyl)pyrido[4,3-d]pyrimidin-4(1H)-one (**QZ3**). ¹H NMR (300 MHz, DMSO-*d*₆) δ 12.40 (s, 1H), 9.19 (s, 1H), 8.72 (d, *J* = 5.7 Hz, 1H), 8.14 (d, *J* = 8.8 Hz, 2H), 7.49 (d, *J* = 5.6 Hz, 1H), 6.77 (d, *J* = 8.8 Hz, 2H), 3.45 (d, *J* = 7.2 Hz, 4H), 1.14 (t, *J* = 6.9 Hz, 6H). LC-MS (ESI): *m/z* 295 [M+H]⁺; HPLC (mobile phase A): purity 100%.

2-(1-methyl-1H-indol-3-yl)quinazolin-4(3H)-one (**QZ4**). ¹H NMR (300 MHz, DMSO-*d*₆) δ 12.14 (s, 1H), 8.71 (d, *J* = 7.6 Hz, 1H), 8.52 (s, 1H), 8.11 (d, *J* = 7.6 Hz, 1H), 7.77 (dt, *J* = 8.0, 16.2 Hz, 2H), 7.57 (d, *J* = 7.8 Hz, 1H), 7.42 (t, *J* = 7.4 Hz, 1H), 7.30 (p, *J* = 7.0 Hz, 2H), 3.89 (s, 3H). LC-MS (ESI): *m/z* 276 [M+H]⁺; 274 [M-H]⁻; HPLC (mobile phase A): purity 96%.

2-(4-(diethylamino)phenyl)quinazolin-4(3H)-one (QZ5). ¹H NMR (300 MHz, DMSO-*d*₆) δ 12.16 (s, 1H), 8.69 (dd, *J* = 5.7, 8.6 Hz, 1H), 8.59 (d, *J* = 1.7 Hz, 1H), 8.11 (d, *J* = 7.8 Hz, 1H), 7.77 (dt, *J* = 8.0, 17.0 Hz, 2H), 7.55 (d, *J* = 10.1 Hz, 1H), 7.43 (t, *J* = 7.5 Hz, 1H), 7.12 (t, *J* = 9.3 Hz, 1H), 4.19 (t, *J* = 7.0 Hz, 2H), 1.85 (q, *J* = 7.2 Hz, 2H), 1.20 (d, *J* = 16.5 Hz, 1H), 0.90 (t, *J* = 7.1 Hz, 3H). LC-MS (ESI): *m/z* 292.15 [M-H]⁻.

2-(6-fluoro-1-propyl-1H-indol-3-yl)quinazolin-4(3H)-one (QZ6). ¹H NMR (300 MHz, Methanol-*d*₄) δ 7.80 (d, *J* = 12.0 Hz, 1H), 7.69 (d, *J* = 6.0 Hz, 1H), 7.33 (d, *J* = 6.0 Hz, 2H), 6.95 (d, *J* = 6.0 Hz, 2H), 6.80 (t, *J* = 9.0 Hz, 2H), 6.12 (s, 1H), 4.33 (t, *J* = 9.0 Hz, 2H), 1.81 (q, 2H), 0.95 (t, *J* = 9.0 Hz, 3H). LC-MS (ESI): *m/z* 322.10 [M+H]⁺; HPLC (mobile phase A): purity 97%.

2-(1-isopropyl-7-methyl-1H-indol-3-yl)quinazolin-4(3H)-one (QZ7). ¹H NMR (300 MHz, DMSO-*d*₆) δ 12.06 (s, 1H), 8.78 (s, 1H), 8.66 (d, *J* = 7.8 Hz, 1H), 8.10 (d, *J* = 7.8 Hz, 1H), 7.79 (t, *J* = 7.6 Hz, 1H), 7.72 (d, *J* = 8.1 Hz, 1H), 7.42 (t, *J* = 7.5 Hz, 1H), 7.12 (t, *J* = 7.5 Hz, 1H), 7.02 (d, *J* = 7.2 Hz, 1H), 5.27 – 5.15 (m, 1H), 2.75 (s, 3H), 1.54 (d, *J* = 6.4 Hz, 6H). LC-MS (ESI): *m/z* 318.30 [M+H]⁺; HPLC (mobile phase A): purity 100%.

2-(1-cyclopropyl-7-methyl-1H-indol-3-yl)quinazolin-4(3H)-one (QZ8). ¹H NMR (300 MHz, DMSO-*d*₆) δ 12.02 (s, 1H), 8.59 (d, *J* = 10.6 Hz, 2H), 8.10 (d, *J* = 7.9 Hz, 1H), 7.78 (t, *J* = 7.6 Hz, 1H), 7.71 (d, *J* = 8.1 Hz, 1H), 7.42 (t, *J* = 7.4 Hz, 1H), 7.13 (t, *J* = 7.6 Hz, 1H), 7.04 (d, *J* = 7.1 Hz, 1H), 3.96 (s, 1H), 2.89 (s, 3H), 1.19 (t, *J* = 6.5 Hz, 4H). LC-MS (ESI): *m/z* 316.20 [M+H]⁺; HPLC (mobile phase A): purity 100%.

2-(1-cyclopropyl-6-fluoro-1H-indol-3-yl)quinazolin-4(3H)-one (QZ9). ¹H NMR (300 MHz, DMSO-*d*₆) δ 12.10 (s, 1H), 8.70 (d, *J* = 7.4 Hz, 1H), 8.62 (s, 1H), 8.11 (d, *J* = 8.3 Hz, 1H), 7.85 – 7.70 (m, 2H), 7.55 – 7.40 (m, 2H), 7.15 (dd, *J* = 8.1, 10.4 Hz, 1H), 3.60

(s, 1H), 1.30 – 1.11 (m, 4H). **LC-MS (ESI):** m/z 320.10 [M+H]⁺; **HPLC (mobile phase A):** purity 95%

2-(7-chloro-1-cyclopropyl-1H-indol-3-yl)quinazolin-4(3H)-one (QZ10). **¹H NMR (300 MHz, DMSO-*d*₆)** δ 12.23 (s, 1H), 8.73 – 8.61 (m, 2H), 8.12 (d, $J = 8.0$ Hz, 1H), 7.84 – 7.73 (m, 2H), 7.45 (t, $J = 7.4$ Hz, 1H), 7.34 (d, $J = 7.6$ Hz, 1H), 7.24 (t, $J = 7.9$ Hz, 1H), 3.55 (s, 1H), 1.12 – 1.01 (m, 4H). **LC-MS (ESI):** m/z 337.05 [M+H]⁺.

2-(1-ethyl-6-fluoro-1H-indol-3-yl)quinazolin-4(3H)-one (QZ11). **¹H NMR (300 MHz, DMSO-*d*₆)** δ 8.10 (d, $J = 9.7$ Hz, 1H), 7.77 (dt, $J = 4.3, 8.4$ Hz, 1H), 7.66 (d, $J = 7.7$ Hz, 1H), 7.50 (s, 1H), 7.45 – 7.36 (m, 1H), 7.25 (t, $J = 7.7$ Hz, 1H), 6.92 (d, $J = 5.4$ Hz, 1H), 6.78 – 6.66 (m, 1H), 6.01 (s, 1H), 4.16 (q, $J = 7.2$ Hz, 2H), 1.33 (t, $J = 7.1$ Hz, 3H). **LC-MS (ESI):** m/z 308.15 [M+H]⁺; 306.15 [M-H]⁻; **HPLC (mobile phase A):** purity 98%.

6-fluoro-2-(1-methyl-1H-indol-3-yl)quinazolin-4(3H)-one (QZ12). **¹H NMR (300 MHz, DMSO-*d*₆)** δ 12.28 (s, 1H), 8.69 (d, $J = 7.6$ Hz, 1H), 8.51 (s, 1H), 7.87 – 7.74 (m, 2H), 7.73 – 7.62 (m, 1H), 7.57 (d, $J = 7.8$ Hz, 1H), 7.29 (p, $J = 7.1$ Hz, 2H), 3.89 (s, 3H). **LC-MS (ESI):** m/z 293.75 [M+H]⁺; 291.45 [M-H]⁻; **HPLC (mobile phase B):** purity 75%.

2-(1-ethyl-1H-indol-3-yl)-6-fluoroquinazolin-4(3H)-one (QZ13). **¹H NMR (300 MHz, DMSO-*d*₆)** δ 12.25 (s, 1H), 8.69 (d, $J = 7.6$ Hz, 1H), 8.63 (s, 1H), 7.88 – 7.74 (m, 2H), 7.70 (d, $J = 9.5$ Hz, 1H), 7.65 – 7.58 (m, 1H), 7.28 (p, $J = 7.1$ Hz, 2H), 4.29 (q, $J = 7.3$ Hz, 2H), 1.48 (t, $J = 7.2$ Hz, 3H). **LC-MS (ESI):** m/z 308.15 [M+H]⁺; 306.15 [M-H]⁻; **HPLC (mobile phase A):** purity 100%.

2-(1-cyclopropyl-6-fluoro-1H-indol-3-yl)-6-fluoroquinazolin-4(3H)-one (QZ14). **¹H NMR (300 MHz, DMSO-*d*₆)** δ 7.76 (s, 1H), 7.40 – 7.28 (m, 2H), 7.21 (s, 1H), 7.15 – 6.95 (m, 2H), 6.73 – 6.60 (m, 1H), 6.45 (s, 2H), 4.37 (s, 1H), 1.09 (t, $J = 7.2$ Hz, 4H). **LC-MS (ESI):** m/z 338.30 [M+H]⁺; **HPLC (mobile phase A):** purity 63%.

2-(7-chloro-1-cyclopropyl-1H-indol-3-yl)-6-fluoroquinazolin-4(3H)-one (**QZ15**). ¹H NMR (300 MHz, DMSO-*d*₆) δ 12.30 (s, 1H), 8.64 (s, 2H), 7.77 (s, 2H), 7.74 (d, *J* = 37.1 Hz, 1H), 7.29 (dd, *J* = 7.8, 27.6 Hz, 2H), 4.35 (s, 1H), 1.07 (d, *J* = 7.2 Hz, 4H). LC-MS (ESI): *m/z* 355.05 [M+H]⁺; HPLC (mobile phase A): purity 100%.

5.5.5 Synthesis of 2-aryl substituted 2,3-dihydroquinazolin-4(1H)-one derivatives (DHQ1-14). To a stirred solution of 2-(N-morpholino)ethanesulfonic acid (MES) (5-10 mol%) in ethanol:water (50:50), 2-aminobenzamide (**DHQ1**) and 2-amino-6-fluorobenzamide (**DHQ2-14**) (1 equiv.) and aldehyde (1 equiv.) were added. Some reactions were heated to 70°C and stirred for 4-12h. In order to decrease the time of reaction and obtain a better purity of final compounds, some reactions were performed with unconventional conditions, using microwave irradiation (T=90°C, P=1-2bar) of 15-60 min. The consumption of starting materials was followed by TLC. The mixture was cooled to room temperature and the obtained solid was collected by filtration and recrystallized from ethanol. The final product was dried in vacuum.

2-(4-(diethylamino)phenyl)-2,3-dihydroquinazolin-4(1H)-one (**DHQ1**). ¹H NMR (300 MHz, DMSO-*d*₆) δ 8.01 (s, 1H), 7.61 (d, *J* = 7.7 Hz, 1H), 7.27 (d, *J* = 8.6 Hz, 2H), 7.21 (d, *J* = 8.0 Hz, 1H), 6.88 (s, 1H), 6.76 – 6.67 (m, 1H), 6.65 (d, *J* = 8.1 Hz, 3H), 5.60 (s, 1H), 1.07 (t, *J* = 6.9 Hz, 6H). LC-MS (ESI): *m/z* 296.10 [M+H]⁺; HPLC (mobile phase A): purity 99%.

6-fluoro-2-phenyl-2,3-dihydroquinazolin-4(1H)-one (**DHQ2**). ¹H NMR (300 MHz, DMSO-*d*₆) δ 8.46 (s, 1H), 7.50 (d, *J* = 7.2 Hz, 2H), 7.39 (q, *J* = 6.5, 7.0 Hz, 3H), 7.32 (dd, *J* = 3.0, 9.2 Hz, 1H), 7.15 (td, *J* = 3.1, 8.8 Hz, 1H), 7.09 (s, 1H), 6.78 (dd, *J* = 4.5, 8.9 Hz, 1H), 5.75 (s, 1H). LC-MS (ESI): *m/z* 243.0 [M+H]⁺; HPLC (mobile phase B): purity 100%.

6-fluoro-2-(4-(piperidin-1-yl)phenyl)-2,3-dihydroquinazolin-4(1H)-one (**DHQ3**). ¹H NMR (300 MHz, DMSO-*d*₆) δ 8.28 (s, 1H), 7.31 (d, *J* = 8.4 Hz, 3H), 7.14 (t, *J* = 9.3 Hz, 1H), 6.92 (d, *J* = 7.2 Hz, 3H), 6.76 (dd, *J* = 4.5, 9.0 Hz, 1H), 5.63 (s, 1H), 3.14 (t, *J* = 4.8 Hz, 4H), 1.57 (s, 6H). LC-MS (ESI): *m/z* 325.0 [M+H]⁺; HPLC (mobile phase B): purity 93%.

6-fluoro-2-(4-(4-methylpiperazin-1-yl)phenyl)-2,3-dihydroquinazolin-4(1H)-one (**DHQ4**). ¹H NMR (300 MHz, DMSO-*d*₆) δ 8.30 (s, 1H), 7.32 (d, *J* = 8.2 Hz, 3H), 7.20 – 7.08 (m, 1H), 6.94 (d, *J* = 8.0 Hz, 3H), 6.76 (dd, *J* = 4.6, 8.8 Hz, 1H), 5.64 (s, 1H), 3.14 (d, *J* = 5.0 Hz, 4H), 2.44 (d, *J* = 5.3 Hz, 4H), 2.21 (s, 3H). LC-MS (ESI): *m/z* 340.60 [M+H]⁺; HPLC (mobile phase A): purity 100%.

6-fluoro-2-(4-morpholinophenyl)-2,3-dihydroquinazolin-4(1H)-one (**DHQ5**). ¹H NMR (300 MHz, DMSO-*d*₆) δ 8.32 (s, 1H), 7.34 (d, *J* = 8.6 Hz, 2H), 7.29 (d, *J* = 3.2 Hz, 1H), 7.14 (td, *J* = 3.1, 8.8 Hz, 1H), 6.95 (d, *J* = 8.3 Hz, 3H), 6.77 (dd, *J* = 4.5, 8.9 Hz, 1H), 5.65 (s, 1H), 3.73 (t, *J* = 4.8 Hz, 4H), 3.10 (t, *J* = 4.8 Hz, 4H). LC-MS (ESI): *m/z* 327.60 [M+H]⁺; HPLC (mobile phase B): 98%.

2-(4-(diethylamino)phenyl)-6-fluoro-2,3-dihydroquinazolin-4(1H)-one (**DHQ6**). ¹H NMR (300 MHz, DMSO-*d*₆) δ 8.40 (s, 1H), 8.20 (s, 1H), 7.72 (d, *J* = 8.6 Hz, 1H), 7.34 – 7.23 (m, 2H), 6.87 (s, 1H), 6.78 (t, *J* = 8.6 Hz, 2H), 6.65 (d, *J* = 8.4 Hz, 1H), 5.59 (s, 1H), 3.44 (t, *J* = 7.1 Hz, 4H), 1.07 (t, *J* = 6.9 Hz, 6H). LC-MS (ESI): *m/z* 314.45 [M+H]⁺; HPLC (mobile phase A): purity 100%.

2-(4-(dimethylamino)phenyl)-6-fluoro-2,3-dihydroquinazolin-4(1H)-one (**DHQ7**). ¹H NMR (300 MHz, DMSO-*d*₆) δ 8.25 (s, 1H), 7.30 (d, *J* = 8.2 Hz, 3H), 7.14 (td, *J* = 8.7, 3.1 Hz, 1H), 6.90 (s, 1H), 6.80 – 6.75 (m, 1H), 6.72 (d, *J* = 8.7 Hz, 2H), 5.62 (s, 1H), 2.89 (s, 6H). LC-MS (ESI): *m/z* 285.70 [M+H]⁺; HPLC (mobile phase B): purity 99%.

2-(4-(1H-pyrrol-1-yl)phenyl)-6-fluoro-2,3-dihydroquinazolin-4(1H)-one (DHQ8). ¹H NMR (300 MHz, DMSO-*d*₆) δ 8.64 (s, 1H), 8.41 (s, 1H), 8.03 (d, *J* = 8.3 Hz, 2H), 7.81 (d, *J* = 8.4 Hz, 3H), 7.67 (dd, *J* = 3.0, 9.8 Hz, 1H), 7.54 (s, 2H), 7.47 – 7.33 (m, 2H), 6.34 (s, 2H). LC-MS (ESI): *m/z* 308.15 [M+H]⁺; HPLC (mobile phase B): purity 74%.

6-fluoro-2-(4-(pyrimidin-5-yl)phenyl)-2,3-dihydroquinazolin-4(1H)-one (DHQ9). ¹H NMR (300 MHz, DMSO-*d*₆) δ 9.20 (s, 1H), 9.15 (s, 2H), 8.60 (s, 1H), 8.15 – 8.01 (m, 1H), 7.85 (d, *J* = 8.0 Hz, 2H), 7.63 (d, *J* = 8.0 Hz, 2H), 7.33 (dd, *J* = 3.1, 9.0 Hz, 1H), 7.20 (d, *J* = 7.3 Hz, 1H), 6.81 (dd, *J* = 4.4, 8.9 Hz, 1H), 5.83 (s, 1H). LC-MS (ESI): *m/z* 321.20 [M+H]⁺; 319.15 [M-H]⁻; HPLC (mobile phase B): purity 80%.

6-fluoro-2-(3-fluorophenyl)-2,3-dihydroquinazolin-4(1H)-one (DHQ10). ¹H NMR (300 MHz, DMSO-*d*₆) δ 8.56 (s, 1H), 7.44 (q, *J* = 7.5 Hz, 1H), 7.35 – 7.25 (m, 3H), 7.17 (d, *J* = 6.4 Hz, 3H), 6.80 (dd, *J* = 4.5, 9.0 Hz, 1H), 5.78 (s, 1H). LC-MS (ESI): *m/z* 261.10 [M+H]⁺; HPLC (mobile phase A): purity 97%.

6-fluoro-2-(2-fluoro-5-(trifluoromethyl)phenyl)-2,3-dihydroquinazolin-4(1H)-one (DHQ11). ¹H NMR (300 MHz, DMSO-*d*₆) δ 8.52 (s, 1H), 7.88 (d, *J* = 6.1 Hz, 2H), 7.53 (t, *J* = 9.4 Hz, 1H), 7.36 (d, *J* = 9.2 Hz, 1H), 7.20 (s, 1H), 7.12 (s, 1H), 6.80 (dd, *J* = 4.6, 8.9 Hz, 1H), 6.13 (s, 1H). LC-MS (ESI): *m/z* 328.55 [M+H]⁺; HPLC (mobile phase A): purity 93%.

6-fluoro-2-(2-hydroxy-5-methylphenyl)-2,3-dihydroquinazolin-4(1H)-one (DHQ12). ¹H NMR (300 MHz, DMSO-*d*₆) δ 9.60 (s, 1H), 8.07 (s, 1H), 7.33 (dd, *J* = 3.1, 9.2 Hz, 1H), 7.16 (d, *J* = 7.3 Hz, 1H), 7.11 (dd, *J* = 3.2, 8.7 Hz, 1H), 6.97 (d, *J* = 8.3 Hz, 1H), 6.85 – 6.79 (m, 1H), 6.76 (d, *J* = 8.3 Hz, 1H), 6.70 (s, 1H), 5.97 (s, 1H), 2.18 (s, 3H). LC-MS (ESI): *m/z* 273.10 [M+H]⁺; 271.05 [M-H]⁻; HPLC (mobile phase A): purity 96%.

*2-(benzo[*d*][1,3]dioxol-5-yl)-6-fluoro-2,3-dihydroquinazolin-4(1H)-one (DHQ13)*. ¹H NMR (300 MHz, DMSO-*d*₆) δ 8.39 (s, 1H), 7.31 (dd, *J* = 3.1, 9.2 Hz, 1H), 7.20 – 7.10

(m, 1H), 7.03 (d, $J = 6.4$ Hz, 2H), 6.92 (t, $J = 6.7$ Hz, 2H), 6.78 (dd, $J = 4.4, 8.9$ Hz, 1H), 6.02 (s, 2H), 5.67 (s, 1H). **LC-MS (ESI):** m/z 286.60 $[M+H]^+$; **HPLC (mobile phase B):** purity 100%.

6-fluoro-2-(4-(imidazo[1,2-a]pyridine-3-yl)phenyl)-2,3-dihydroquinazolin-4(1H)-one (DHQ14). **1H NMR (300 MHz, DMSO- d_6)** δ 9.74 (d, $J = 6.9$ Hz, 1H), 8.85 (s, 1H), 8.31 (s, 1H), 7.98 (s, 1H), 7.84 (d, $J = 9.0$ Hz, 1H), 7.70 (s, 1H), 7.60 (t, $J = 7.9$ Hz, 1H), 7.46 (d, $J = 8.9$ Hz, 1H), 7.38 (d, $J = 6.0$ Hz, 2H), 7.24 (t, $J = 6.9$ Hz, 1H). **LC-MS (ESI):** m/z 283.15 $[M+H]^+$; **HPLC (mobile phase A):** purity 96%.

5.5.6 Synthesis of 2-indole substituted 2,3-dihydroquinazolin-4(1H)-one derivatives (DHQ15-35). To a stirred solution of 2-(N-morpholino)ethanesulfonic acid (MES) (5-10 mol%) in Ethanol:water (50:50), 2-aminobenzamide (**DHQ15-25**) and 2-amino-6-fluorobenzamide (**DHQ26-35**) (1 equiv.) and variously substituted 1H-indole-3-carboxaldehyde (1 equiv.) were added. The final products were obtained following the same work-up procedure of General Procedure D.

2-(1-methyl-1H-indol-3-yl)-2,3-dihydroquinazolin-4(1H)-one (DHQ15). **1H NMR (300 MHz, DMSO- d_6)** δ 8.09 (s, 1H), 7.78 (d, $J = 7.9$ Hz, 1H), 7.66 (d, $J = 7.7$ Hz, 1H), 7.44 (d, $J = 8.3$ Hz, 1H), 7.40 (s, 1H), 7.21 (dt, $J = 7.8, 15.7$ Hz, 2H), 7.05 (t, $J = 7.5$ Hz, 1H), 6.92 (s, 1H), 6.71 (dd, $J = 7.9, 18.0$ Hz, 2H), 6.03 (s, 1H), 3.77 (s, 3H). **LC-MS (ESI):** m/z 278.15 $[M+H]^+$; **HPLC (mobile phase A):** purity 93%.

2-(1,7-dimethyl-1H-indol-3-yl)-2,3-dihydroquinazolin-4(1H)-one (DHQ16). **1H NMR (300 MHz, DMSO- d_6)** δ 8.04 (s, 1H), 7.65 (d, $J = 7.8$ Hz, 1H), 7.62 – 7.57 (m, 1H), 7.27 (s, 1H), 7.22 (d, $J = 7.7$ Hz, 1H), 6.88 (d, $J = 7.2$ Hz, 3H), 6.76 – 6.64 (m, 2H), 5.99 (s, 1H), 4.01 (s, 3H), 2.71 (s, 3H). **LC-MS (ESI):** m/z 292.10 $[M+H]^+$; **HPLC (mobile phase A):** purity 97%.

2-(1-ethyl-1H-indol-3-yl)-2,3-dihydroquinazolin-4(1H)-one (**DHQ17**). ¹H NMR (300 MHz, DMSO-*d*₆) δ 8.06 (s, 1H), 7.77 (d, *J* = 8.2 Hz, 1H), 7.66 (d, *J* = 7.8 Hz, 1H), 7.49 (d, *J* = 6.3 Hz, 2H), 7.21 (dt, *J* = 7.7, 20.9 Hz, 2H), 7.04 (t, *J* = 7.5 Hz, 1H), 6.92 (s, 1H), 6.72 (dd, *J* = 7.8, 19.0 Hz, 2H), 6.03 (s, 1H), 4.20 (q, *J* = 7.2 Hz, 2H), 1.35 (t, *J* = 7.2 Hz, 3H). LC-MS (ESI): *m/z* 292.20 [M+H]⁺; HPLC (mobile phase A): purity 98%.

2-(1-benzyl-7-methyl-1H-indol-3-yl)-2,3-dihydroquinazolin-4(1H)-one (**DHQ18**). ¹H NMR (300 MHz, DMSO-*d*₆) δ 8.15 (s, 1H), 7.72 – 7.63 (m, 2H), 7.49 (s, 1H), 7.27 (d, *J* = 7.5 Hz, 4H), 6.92 (d, *J* = 9.1 Hz, 5H), 6.80 (dd, *J* = 7.6, 14.3 Hz, 2H), 6.71 (t, *J* = 7.6 Hz, 1H), 6.07 (s, 1H), 5.62 (s, 2H), 2.44 (d, *J* = 6.2 Hz, 3H). LC-MS (ESI): *m/z* 368.25 [M+H]⁺; HPLC (mobile phase B): purity 98%.

2-(7-methyl-1-propyl-1H-indol-3-yl)-2,3-dihydroquinazolin-4(1H)-one (**DHQ19**). ¹H NMR (300 MHz, DMSO-*d*₆) δ 8.52 (s, 1H), 8.07 (s, 1H), 7.65 (d, *J* = 7.2 Hz, 2H), 7.37 (s, 1H), 6.89 (s, 3H), 6.78 – 6.61 (m, 2H), 6.01 (s, 1H), 4.26 (t, *J* = 7.2 Hz, 2H), 2.66 (s, 3H), 1.77 – 1.58 (m, 2H), 0.88 (t, *J* = 7.4 Hz, 3H). LC-MS (ESI): *m/z* 320.25 [M+H]⁺; HPLC (mobile phase A): purity 73%.

2-(7-chloro-1-propyl-1H-indol-3-yl)-2,3-dihydroquinazolin-4(1H)-one (**DHQ20**). ¹H NMR (300 MHz, DMSO-*d*₆) δ 8.13 (s, 1H), 7.79 (d, *J* = 7.9 Hz, 1H), 7.66 (d, *J* = 7.7 Hz, 1H), 7.52 (d, *J* = 1.5 Hz, 1H), 7.23 (dd, *J* = 7.7, 20.1 Hz, 2H), 7.03 (td, *J* = 1.6, 7.7 Hz, 1H), 6.94 (s, 1H), 6.78 – 6.67 (m, 2H), 6.04 (s, 1H), 4.42 (q, *J* = 6.6 Hz, 2H), 1.77 (q, *J* = 7.3 Hz, 2H), 0.91 – 0.79 (m, 3H). LC-MS (ESI): *m/z* 340.50 [M+H]⁺; HPLC (mobile phase A): purity 96%.

2-(7-chloro-1-ethyl-1H-indol-3-yl)-2,3-dihydroquinazolin-4(1H)-one (**DHQ21**). ¹H NMR (300 MHz, DMSO-*d*₆) δ 8.11 (s, 1H), 7.79 (d, *J* = 8.0 Hz, 1H), 7.66 (d, *J* = 7.7 Hz, 1H), 7.56 (s, 1H), 7.24 (dd, *J* = 7.9, 17.5 Hz, 2H), 7.04 (t, *J* = 7.6 Hz, 1H), 6.94 (s, 1H),

6.78 – 6.67 (m, 2H), 6.04 (s, 1H), 4.54 (q, $J = 6.5$ Hz, 2H), 1.36 (t, $J = 7.1$ Hz, 3H). **LC-MS (ESI):** m/z 326.15 $[M+H]^+$; **HPLC (mobile phase A):** purity 100%.

2-(1-ethyl-7-methyl-1H-indol-3-yl)-2,3-dihydroquinazolin-4(1H)-one (**DHQ22**). ^1H **NMR (300 MHz, DMSO- d_6)** δ 8.04 (s, 1H), 7.70 – 7.61 (m, 2H), 7.41 (s, 1H), 7.24 (t, $J = 7.7$ Hz, 1H), 6.90 (q, $J = 2.8, 4.0$ Hz, 3H), 6.79 – 6.66 (m, 2H), 6.02 (s, 1H), 4.37 (q, $J = 7.2$ Hz, 2H), 2.68 (s, 3H), 1.33 (t, $J = 7.1$ Hz, 3H). **LC-MS (ESI):** m/z 306.20 $[M+H]^+$; **HPLC (mobile phase A):** purity 100%.

2-(7-methyl-1H-indol-3-yl)-2,3-dihydroquinazolin-4(1H)-one (**DHQ23**). ^1H **NMR (300 MHz, DMSO- d_6)** δ 11.06 (s, 1H), 8.07 (s, 1H), 7.65 (d, $J = 6.4$ Hz, 1H), 7.63 – 7.56 (m, 1H), 7.37 (d, $J = 2.6$ Hz, 1H), 7.28 – 7.20 (m, 1H), 6.92 (d, $J = 5.6$ Hz, 3H), 6.80 – 6.65 (m, 2H), 6.03 (s, 0H), 2.45 (s, 3H). **LC-MS (ESI):** m/z 276.15 $[M-H]^-$; **HPLC (mobile phase A):** purity 100%.

2-(1-benzyl-6-fluoro-1H-indol-3-yl)-2,3-dihydroquinazolin-4(1H)-one (**DHQ24**). ^1H **NMR (300 MHz, DMSO- d_6)** δ 8.49 (d, $J = 1.9$ Hz, 1H), 8.15 (s, 1H), 7.77 (t, $J = 7.3$ Hz, 1H), 7.66 (d, $J = 7.7$ Hz, 1H), 7.60 (s, 1H), 7.54 (d, $J = 10.3$ Hz, 1H), 7.32 (dd, $J = 7.7, 21.4$ Hz, 5H), 7.14 (d, $J = 9.2$ Hz, 1H), 6.93 (d, $J = 10.1$ Hz, 1H), 6.78 – 6.67 (m, 1H), 6.03 (s, 1H), 5.52 (d, $J = 1.6$ Hz, 1H), 5.38 (s, 2H). **LC-MS (ESI):** m/z 372.20 $[M+H]^+$; **HPLC (mobile phase A):** purity 94%.

6-fluoro-2-(1-methyl-1H-indol-3-yl)-2,3-dihydroquinazolin-4(1H)-one (**DHQ25**). ^1H **NMR (300 MHz, DMSO- d_6)** δ 9.03 (s, 1H), 8.68 (s, 1H), 8.22 (d, $J = 7.8$ Hz, 1H), 8.14 (s, 1H), 7.88 (s, 1H), 7.74 (dd, $J = 3.0, 9.9$ Hz, 1H), 7.61 (d, $J = 8.1$ Hz, 1H), 7.46 – 7.23 (m, 3H), 5.76 (s, 1H), 3.91 (s, 3H). **LC-MS (ESI):** m/z 296.15 $[M+H]^+$; **HPLC (mobile phase A):** purity 88%.

2-(1,7-dimethyl-1H-indol-3-yl)-6-fluoro-2,3-dihydroquinazolin-4(1H)-one (**DHQ26**). ^1H **NMR (300 MHz, DMSO- d_6)** δ 8.25 (s, 1H), 7.38 – 7.32 (m, 1H), 7.29 (s, 1H), 7.11 (t, J

= 7.2 Hz, 2H), 7.02 (d, $J = 7.5$ Hz, 1H), 6.87 (s, 2H), 6.80 – 6.74 (m, 1H), 5.98 (s, 1H), 4.02 (s, 3H), 2.73 (d, $J = 6.9$ Hz, 3H). **LC-MS (ESI):** m/z 310.0 $[M+H]^+$; **HPLC (mobile phase A):** purity 93%.

2-(1-ethyl-1H-indol-3-yl)-6-fluoro-2,3-dihydroquinazolin-4(1H)-one (**DHQ27**). **1H NMR (300 MHz, DMSO- d_6)** δ 8.20 (s, 1H), 7.35 – 7.23 (m, 3H), 7.13 (td, $J = 3.0, 8.7$ Hz, 1H), 6.87 (s, 1H), 6.76 (dd, $J = 4.5, 8.9$ Hz, 1H), 6.65 (d, $J = 8.6$ Hz, 2H), 5.59 (s, 1H), 2.09 (s, 2H), 1.07 (t, $J = 6.9$ Hz, 3H). **LC-MS (ESI):** m/z 310.10 $[M+H]^+$; **HPLC (mobile phase B):** purity 96%.

6-fluoro-2-(7-methyl-1-propyl-1H-indol-3-yl)-2,3-dihydroquinazolin-4(1H)-one (**DHQ28**). **1H NMR (300 MHz, DMSO- d_6)** δ 8.27 (s, 1H), 7.63 (d, $J = 7.4$ Hz, 1H), 7.40 – 7.31 (m, 2H), 7.19 – 7.08 (m, 1H), 6.91 (d, $J = 7.3$ Hz, 3H), 6.78 (dd, $J = 4.5, 8.9$ Hz, 1H), 5.99 (s, 1H), 4.27 (t, $J = 7.3$ Hz, 2H), 2.66 (s, 3H), 1.70 (d, $J = 7.2$ Hz, 2H), 0.87 (t, $J = 7.4$ Hz, 3H). **LC-MS (ESI):** m/z 338.30 $[M+H]^+$; **HPLC (mobile phase A):** purity 96%.

2-(7-chloro-1-propyl-1H-indol-3-yl)-6-fluoro-2,3-dihydroquinazolin-4(1H)-one (**DHQ29**). **1H NMR (300 MHz, DMSO- d_6)** δ 8.33 (s, 1H), 7.79 (d, $J = 7.8$ Hz, 1H), 7.53 (s, 1H), 7.40 – 7.35 (m, 1H), 7.23 – 7.12 (m, 2H), 7.04 (t, $J = 7.7$ Hz, 1H), 6.93 (s, 1H), 6.79 (dd, $J = 4.5, 9.1$ Hz, 1H), 6.03 (s, 1H), 4.42 (q, $J = 6.2, 6.8$ Hz, 2H), 1.76 (q, $J = 7.3$ Hz, 2H), 0.86 (t, $J = 7.4$ Hz, 3H). **LC-MS (ESI):** m/z 358.05 $[M+H]^+$; **HPLC (mobile phase A):** purity 100%.

2-(7-chloro-1-ethyl-1H-indol-3-yl)-6-fluoro-2,3-dihydroquinazolin-4(1H)-one (**DHQ30**). **1H NMR (300 MHz, DMSO- d_6)** δ 8.30 (s, 1H), 7.78 (d, $J = 7.8$ Hz, 1H), 7.57 (s, 1H), 7.36 (dd, $J = 2.7, 9.1$ Hz, 1H), 7.24 – 7.12 (m, 2H), 7.04 (dd, $J = 7.0, 8.7$ Hz, 1H), 6.94 (s, 1H), 6.82 – 6.75 (m, 1H), 6.03 (s, 1H), 4.59 – 4.44 (m, 2H), 1.36 (t, $J = 7.1$ Hz, 3H). **LC-MS (ESI):** m/z 344.15 $[M+H]^+$; **HPLC (mobile phase A):** purity 100%.

2-(1-ethyl-7-methyl-1H-indol-3-yl)-6-fluoro-2,3-dihydroquinazolin-4(1H)-one

(DHQ31). ¹H NMR (300 MHz, DMSO-*d*₆) δ 8.23 (s, 1H), 7.62 (d, *J* = 7.2 Hz, 1H), 7.41 (s, 1H), 7.36 (dd, *J* = 2.7, 9.2 Hz, 1H), 7.19 – 7.10 (m, 1H), 6.94 – 6.87 (m, 3H), 6.78 (dd, *J* = 4.5, 8.9 Hz, 1H), 6.00 (s, 1H), 4.38 (q, *J* = 7.3 Hz, 2H), 2.68 (s, 3H), 1.33 (t, *J* = 7.1 Hz, 3H). **LC-MS (ESI):** *m/z* 324.20 [M+H]⁺; **HPLC (mobile phase A):** purity 96%.

6-fluoro-2-(7-methyl-1H-indol-3-yl)-2,3-dihydroquinazolin-4(1H)-one **(DHQ32).** ¹H NMR (300 MHz, DMSO-*d*₆) δ 8.69 (s, 1H), 8.15 (d, *J* = 3.0 Hz, 1H), 8.03 (d, *J* = 7.6 Hz, 1H), 7.89 (s, 1H), 7.75 (dd, *J* = 3.1, 10.0 Hz, 1H), 7.42 (td, *J* = 3.1, 8.4 Hz, 1H), 7.29 (dd, *J* = 5.0, 8.9 Hz, 1H), 7.10 (dd, *J* = 7.2, 12.4 Hz, 3H), 6.01 (s, 1H), 2.53 (s, 3H). **LC-MS (ESI):** *m/z* 296.15 [M+H]⁺; 294.15 [M-H]⁻; **HPLC (mobile phase A):** purity 81%.

2-(1-benzyl-6-fluoro-1H-indol-3-yl)-6-fluoro-2,3-dihydroquinazolin-4(1H)-one

(DHQ33). ¹H NMR (300 MHz, DMSO-*d*₆) δ 8.48 (s, 1H), 8.34 (s, 1H), 7.61 (s, 1H), 7.39 – 7.23 (m, 7H), 7.12 (s, 1H), 6.94 (s, 2H), 6.02 (s, 1H), 5.52 (s, 1H), 5.38 (s, 2H). **LC-MS (ESI):** *m/z* 390.20 [M+H]⁺; **HPLC (mobile phase B):** purity 98%.

6-fluoro-2-(6-fluoro-1-propyl-1H-indol-3-yl)-2,3-dihydroquinazolin-4(1H)-one

(DHQ34). ¹H NMR (300 MHz, Methanol-*d*₄) δ 8.09 (s, 1H), 8.05 (s, 1H), 7.68 (d, *J* = 7.4 Hz, 1H), 7.48 (d, *J* = 9.0 Hz, 1H), 7.33 (s, 1H), 7.20 – 7.04 (m, 2H), 6.95 (d, *J* = 8.3 Hz, 1H), 6.79 (q, *J* = 6.8, 9.2 Hz, 1H), 6.09 (s, 1H), 4.43 (t, *J* = 7.4 Hz, 2H), 1.89 (q, *J* = 7.4 Hz, 2H), 0.99 (t, *J* = 7.3 Hz, 3H). **LC-MS (ESI):** *m/z* 342.20 [M+H]⁺; **HPLC (mobile phase A):** purity 64%.

2-(1-ethyl-6-fluoro-1H-indol-3-yl)-6-fluoro-2,3-dihydroquinazolin-4(1H)-one **(DHQ35).**

¹H NMR (300 MHz, DMSO-*d*₆) δ 8.28 (s, 1H), 7.76 (dd, *J* = 5.7, 8.7 Hz, 1H), 7.51 (s, 1H), 7.38 (td, *J* = 2.5, 9.0, 9.6 Hz, 2H), 7.15 (td, *J* = 3.0, 8.7 Hz, 1H), 6.94 (d, *J* = 8.8 Hz, 2H), 6.78 (dd, *J* = 4.5, 8.9 Hz, 1H), 6.00 (s, 1H), 4.17 (q, *J* = 7.2 Hz, 2H), 1.33 (t, *J* = 7.2 Hz, 3H). **LC-MS (ESI):** *m/z* 328.25 [M+H]⁺; **HPLC (mobile phase A):** purity 97%.

References

Badolato M, Aiello F, Neamati N. 2,3-Dihydroquinazolin-4(1H)-one as a Privileged Scaffold in Drug Design. Submitted to *RSC Advance* (2018).

Becerra C, Stephenson J, Jonker DJ, Cohn AL, Asmis TR, Bekaii-Saab TS, Conkling PR, Garbo LE, Lenz HJ, Richards DA, Spira AI, Mikhail S, Goodwin RA, Yoon HH, Hume S, Hitron M, Li C. Phase Ib/II study of cancer stem cell (CSC) inhibitor BBI608 combined with paclitaxel in advanced gastric and gastroesophageal junction (GEJ) adenocarcinoma. *J Clin Oncol*. 2015; 33.

Becker S, Groner B, Müller CW. Three-dimensional structure of the Stat3 β homodimer bound to DNA. *Nature*. 1998; 394:145-151.

Beerenwickel N, Antal T, Dingli D, Traulsen A, Kinzler KW, Velculescu VE, Vogelstein B, Nowak MA. Genetic progression and the waiting time to cancer. *PLoS Comput Biol* 2007; 3:e225.

Bendell JC, Hong D, Burris HA, Naing A, Jones SF, Falchook G, Bricmont P, Elekes A, Rock EP, Kurzrock R. Phase 1, open-label, dose-escalation, and pharmacokinetic study of STAT3 inhibitor OPB-31121 in subjects with advanced solid tumors. *Cancer Chemother Pharmacol*. 2014; 74:125-130.

Bild AH, Potti A, Nevins JR. Linking oncogenic pathways with therapeutic opportunities. *Nat Rev Cancer*. 2006; 6:735-741.

Bishop BC, Marley H, Preston PN, Wright SHB. Synthesis and reactions of [1,2,4]triazolo[1,5-a]pyrimidinium-2-amides. *J. Chem. Soc. Perkin Trans*. 1999; 1:1527-1532.

Brambilla L, Genini D, Laurini E, Merulla J, Perez L, Fermeglia M, Carbone GM, Prisci S, Catapano CV. Hitting the right spot: mechanism of action of OPB-31121, a novel and potent inhibitor of the Signal Transducer and Activator of Transcription 3 (STAT3). *Mol Oncol*. 2015; 9:1194-1206.

Cafferkey C, Chau I. Novel STAT3 inhibitors for treating gastric cancer. *Expert Opin Investig Drugs*. 2016.

Chinigo GM, Paige M, Grindrod S, Hamel E, Dakshanamurthy S, Chruszcz M, Minor W, Brown ML. Asymmetric Synthesis of 2,3-Dihydro-2-arylquinazolin-4-ones: Methodology and Application to a Potent Fluorescent Tubulin Inhibitor with Anticancer Activity. *J Med Chem.* 2008; 51:4620-4631.

Choi JY, Li WL, Kouri RE, Yu J, Kao FT, Ruano G. Assignment of the acute phase response factor (APRF) gene to 17q21 by microdissection clone sequencing and fluorescence *in situ* hybridization of a P1 clone. *Genetics.* 1996; 37:264-265.

Cimica V, Chen HC, Iyer JK, Reich NC. Dynamics of the STAT3 transcription factor: nuclear import dependent on Ran and importin- β 1. *PLoS One.* 2011; 6:e20188.

Copeland NG, Gilbert DJ, Schindler C, Zhong Z, Wen Z, Darnell JE Jr, Mui AL, Miyajima A, Quelle FW, Ihle JN, Jenkins NA. Distribution of the mammalian Stat gene family in mouse chromosomes. *Genomics.* 1995; 29:225-228.

Darnell JE Jr, Kerr IM, Stark GR. Jak-STAT pathways and transcriptional activation in response to IFNs and other extracellular signaling proteins. *Science* 1994; 264:1415-1421.

Debnath B, Xu S, Neamati N. Small molecule inhibitors of Signal transducer and activator of transcription (Stat3) protein. *J Med Chem.* 2012; 55:6645-6668.

Desenko SM, Kolos NN, Tuni M, Oriov VD. Cyclocondensation of chalcones with di- and tri-amino-1,2,4-triazoles. *Khim Geterotsikl Soedin.* 1990; 7:938-941.

Dimri S, Sukanya, De A. Approaching non-canonical STAT3 signaling to redefine cancer therapeutic strategy. *Integr Mol Med.* 2017; 4:4-10.

Gao P, Niu N, Wei T, Tozawa H, Chen X, Zhang C, Zhang J, Wada Y, Kapron CM, Liu J. The roles of signal transducer and activator of transcription factor 3 in tumor angiogenesis. *Oncotarget.* 2017; 8:69139-69161.

Groner B, Lucks P, Borghouts C. The function of Stat3 in tumor cells and their microenvironment. *Semin Cells Dev Biol.* 2008; 19:341-350.

Hamel E, Lin CM, Plowman J, Wang HJ, Lee KH, Paull KD. Antitumor 2,3-dihydro-2-(aryl)-4-(1*H*)-quinazolinone derivatives. Interaction with tubulin. *Biochem Pharm.* 1996;

51:53-59.

Heinrich PC, Behrmann I, Müller-Newen G, Schaper F, Graeve L. Interleukin-6-type cytokine signaling through the gp130/Jak/STAT pathway. *Biochem.* 1998; 334:297-314.

Hitron M, Stephenson J, Chi KN, Edenfield WJ, Leggett D, Li Y, Li W, Gada K, Li C. A phase Ib study of the cancer stem cell inhibitor BBI608 administered with paclitaxel in patients with advanced malignancies. *J Clin Oncol.* 2014; 325.

Hour MJ, Huang LJ, Kuo SC, Xia Y, Bastow K, Nakanisi Y, Hamel E, Lee KH. 6-alkylamino- and 2,3-dihydro-3'-methoxy-2-phenyl-4-quinazolinones and related compounds: their synthesis, cytotoxicity and inhibition of tubulin polymerization. *J Med Chem.* 2000, 43:4479-4487.

Kim MJ, Nam HJ, Kim HP, Han SW, Im SA, Kim TY, Oh, DY, Bang YJ. OPB-31121, a novel small molecular inhibitor, disrupts the JAK2/STAT3 pathway and exhibits an antitumor activity in gastric cancer cells. *Cancer Lett.* 2013b; 335:145-152.

Kolos NN, Orlov VD, Paponov BV, Shishkin OV, Baumer SV, Kyashnitskaya NA. Stable 1,2,4-triazolo[1,5- α]-pyrimidinium salts. *Chem Heterocycl Compd.* 1999; 35:708-715.

Langleben A, Supko J, Hotte SJ, Batist B, Hirte HW, Rogoff H, Li Y, Li W, Kerstein D, Leggett D, Hitron MJ, Li C. A dose escalation phase I study of a first in class cancer stemness inhibitors in patients with advanced malignancies. *J Clin Oncol.* 2013; 31.

Lavecchia A, Di Giovanni C, Novellino E. STAT-3 inhibitors: state of the art and new horizons for cancer treatment. *Curr Med Chem.* 2011; 18:2359-2375.

Leeson PD, Springthorpe B. The influence of drug-like concepts on decision-making in medicinal chemistry. *Nat Rev Drug Discov.* 2007; 6:881-890.

Levy DE, Darnell JE Jr. STATs: transcriptional control and biological impact. *Nat Rev Mol Cell Biol.* 2002; 3:651-662.

Levy ED, Lee CK. What does Stat3 do? *J Clin Invest.* 2002; 109:1143-1148.

Li Y, Rogoff H, Keates S, Gao Y, Murikipudi S, Mikule K, Leggett D, Li W, Pardee AB,

- Li CJ. Suppression of cancer relapse and metastasis by inhibiting cancer stemness. *PNAS* 2015; 112:1839-1844.
- Lim CP, Cao X. Structure, function, and regulation of STAT proteins. *Mol Biosyst.* 2006; 2:536-550.
- Lin WW, Karin M. A cytokine-mediated link between innate immunity, inflammation, and cancer. *J Clin Invest.* 2007; 117:1175-1183.
- Lütticken C, Wegenka UM, Yuan J, Buschmann J, Schindler C, Ziemiecki A, Harpur AG, Wilks AF, Yasukawa K, Taga T, Kishimoto T, Barbieri G, Pellegrini S, Sendtner M, Heinrich PC, Horn F. Association of transcription factor APRF and protein kinase Jak1 with the interleukin-6 signal transducer gp130. *Science.* 1994; 263:89-92.
- Maidannik AG, Chuiguk VA, Tolmachev AI. Mesoionic imidazo[2',1:3,4]-1,2,4-triazolo(1,5-a)pyrimidines. *Ukr. Khim. Zh. (Russ. Ed.)* 1986; 52:200. (*Chem. Abstr.* 1987; 106:119818w).
- Matsuda T, Nakamuri T, Nakao K, Arai T, Katsuki M, Heike T, Yokota T. STAT3 activation is sufficient to maintain an undifferentiated state of mouse embryonic stem cells. *EMBO J.* 1999; 18:4261-4269.
- Munoz J, Dhillon N, Janku F, Watowich SS, Hong DS. STAT3 inhibitors: finding a home in lymphoma and leukemia. *Oncologist.* 2014; 19:536-544.
- Niwa H, Burdon T, Chambers I, Smith A. Self-renewal of pluripotent embryonic stem cells is mediated via activation of STAT3. *Genes Dev.* 1998; 12:2048-2060.
- Ogura M, Uchida T, Terui Y, Hayakawa F, Kobayashi Y, Taniwaki M, Takamatsu Y, Naoe T, Tobinai K, Munakata W, Yamauchi T, Kageyama A, Yuasa M, Motoyama M, Tsunoda T, Hatake K. Phase I study of OPB-51602, an oral inhibitor of STAT3, in patients with relapsed/refractory hematological malignancies. *Cancer Sci.* 2015; 106:896-901.
- Park SJ, Nakagawa T, Kitamura H, Atsumi T, Kamon H, Sawa S, Kamimira D, Ueda N, Iwakura Y, Ishihara K, Murakami M, Hirano T. IL-6 regulates *in vivo* dendritic cell differentiation through STAT3 activation. *J Immunol.* 2004; 173:3844-3854.

Rane SG, Reddy EP. Janus kinases: components of multiple signaling pathways. *Oncogene*. 2000; 19:5662-5679.

Raz R, Durbin JE, Levy DE. Acute phase response factor and additional members of the interferon-stimulated gene factor 3 family integrate diverse signals from cytokines, interferons, and growth factors. *J Biol Chem*. 1994; 269:24394-24395.

Raz R, Lee CK, Cannizzaro LA, D'Eustachio P, Levy DE. Essential role of STAT3 for embryonic stem cell pluripotency. *Proc Natl Acad Sci USA*. 1999; 96:2846-2851.

Sestito S, Nesi G, Pi R, Macchia M, Rapposelli S. Hydrogen sulfide: a worthwhile tool in the design of new multitarget drugs. *Front Chem*. 2017; 5:72.

Shaha M, Muro K, Shitara KA, Tebbutt NC, Bang YJ, Lordick F, Borodyansky L, Li C. The brighter trial: a phase III randomized double-blind study of BBI608 + weekly paclitaxel versus placebo (PBO) + weekly paclitaxel in patients (pts) with pretreated advanced gastric and gastro-esophageal junction (GEJ) adenocarcinoma. *J Clin Oncol*. 2015; 33.

Siveen KS, Sikka S, Surana R, Dai X, Zhang J, Kumar AP, Tan BKH, Sethi G, Bishayee A. Targeting the STAT3 signaling pathway in cancer: role of synthetic and natural inhibitors. *Biochim Biophys Acta*. 2014; 1845:136-154.

Takeda K, Noguchi K, Shi W, Tanaka T, Matsumoto M, Yoshida N, Kishimoto T, Akira S. Targeted disruption of the mouse Stat3 gene leads to early embryonic lethality. *Proc Natl Acad Sci USA*. 1997; 94:3801-3804.

Thoma G, Drückes P, Zerwes HG. Selective inhibitors of the Janus kinase Jak3 – Are they effective? *Bioorg Med Chem Lett*. 2014; 24:4617-4621.

Wen Z, Zhong Z, Darnell JE Jr. Maximal activation of transcription by Stat1 and Stat3 requires both tyrosine and serine phosphorylation. *Cell*. 1995; 82:241-250.

Wong AL, Soo R, Tan D, Lee SC, Lim JS, Marban PC, Kong LR, Lee YJ, Wang LZ, Thuya WL, Soong R, Yee MQ, Chin TM, Cordero MT, Asuncion BR, Pang B, Pervaiz S, Hirpara JL, Sinha A, Xu WW, Yuasa M, Tsunoda T, Motoyama M, Yamauchi T, Goh BC. Phase I and biomarker study of OPB-51602, a novel signal transducer and activator

of transcription (STAT) 3 inhibitor, in patients with refractory solid malignancies. *Ann Oncol.* 2015; 26:998-1005.

Wu P, Nielsen TE, Clausen MH. FDA-approved small-molecule kinase inhibitors. *Trends Pharmacol Sci.* 2015; 36:422-439.

Xiong A, Yang Z, Shen Y, Zhou J, Shen Q. Transcription factor STAT3 as a novel molecular target for cancer prevention. *Cancers* 2014; 6:926-957.

Xu S, Sankar S, Neamati N. Protein disulfide isomerase: a promising target for cancer therapy. *Drug Discov Today.* 2014; 19:222-240.

Yale HL, Kalkstein M. Substituted 2,3-Dihydro-4-(1H)-quinazolinones. A New Class of Inhibitors of Cell Multiplication. *J Med Chem.* 1967; 10:334-336.

Yang XO, Panoloulos AD, Nurieva R, Chang SH, Wang D, Watowich SS, Dong C. STAT3 regulates cytokine-mediated generation of inflammatory helper T cells. *J Biol Chem.* 2007; 282:9358-9363.

Yuan Z, Guan Y, Chatterjee D, Chin YE. Stat3 dimerization regulated by reversible acetylation of a single lysine residue. *Science.* 2005; 307:269-273.

Zhang J, Yang PL, Gray NS. Targeting cancer with small molecule kinase inhibitors. *Nature Rev Cancer.* 2009; 9:28-39.